Future Flood Projections in Jakarta, Indonesia based on Urban Development and Urban Climate Change

Environmental Engineering, Graduate School of Engineering,
Toyama Prefectural University

March 2022

Bambang Adhi Priyambodho

Abstract

Floods in Indonesia are considered to be one of the major natural disasters. Jakarta City in Indonesia has experienced many floods in the past. The flood in February 2007 resulted in more than 80 deaths, and 40% of the area in Jakarta was inundated. Also, electrical system shutdowns in several districts in the city were reported. The flood event in 2013 caused the similar situation, which resulted in more than 40 deaths, 45,000 refugees, and terrible economic damage. According to the literature review, the factors contributing to floods in Jakarta are so complicated. In these factors, urban development and climate change could be main factors in the near future. Several previous studies had conducted climate change impact analyses in Jakarta, considering future climate and land use changes, land subsidence, and sea level rise. However, effects of urban development on the atmospheric environments of cities had not been taken into account in many previous climate change researches conducted in Jakarta or in urban cities across the world. Local urbanization is expected to affect the atmospheric environments of mega cities owing to the changing urban thermal environments, such as the heat island phenomena. In general, local urbanization was considered only for land use changes in runoff and flood inundation simulations. Also, previous studies only considered a land use change scenario (the worst case) toward the future. However, several land use change scenarios should be considered in the climate and land use change study in Jakarta in order to show how much CO_2 mitigation plans may work to reduce the flooding. The main objective of this study is to quantify the effects of both land use and climate change on future rainfall and flood inundation in Jakarta based on future urban growth and urban climate change scenarios including the heat island effects. Also, several counter measures not only structural but also nonstructural types such as a flood forecasting are proposed and evaluated in this study.

First, the four scenarios of future changes in land use in Jakarta based on the SLEUTH model: the worst-case, compact-growth, and controlled-growth-I and -II scenarios were evaluated based on the flood inundation simulations. The controlled-growth is a scenario to decrease the growth rate and delay the progress of urbanization compared to the compact-growth scenario. According to the analyses, the predicted changes in land use with the land subsidence in the worst-case and controlled-growth-II scenarios would cause flood inundation volumes in 2050 to be 35% and 25% larger than in 2013, respectively. Thus, even under the controlled-growth-II scenario, the modeled changes in land use with the land subsidence would significantly increase flood inundation.

Second, projected rainfall data of RCP2.6-SSP1 and RCP8.5-SSP3, based on the WRF simulation, were used as inputs for rainfall-runoff and flood inundation simulations in Jakarta. In addition, RCP2.6 and RCP8.5, without urban development scenarios, were investigated to specifically determine the effects of urbanization in Jakarta. Results showed that the rainfall intensity, peak discharge and flood inundation generally increased toward high RCP and SSP future scenarios. Significantly, the RCP2.6-SSP1 scenario showed a higher peak discharge value than RCP8.5 owing to the combination of land use change and increased rainfall. The effects of urban development on atmospheric and runoff processes should be considered for climate change studies in urban areas.

Finally, in order to reduce the flood damages in Jakarta, structural counter measures were evaluated based on the Expected Annual Damage Cost (EADC). Also, B/Cs were computed and compared with other counter measures proposed in previous studies. It was found that the structural counter measures will reduce the flood damage effectively but the implementation cost is too expensive, so that these counter measures are difficult to be implemented in Jakarta. So, nonstructural measures such as flood forecasting with the evacuation plans should be developed. Therefore, the GSMaP products (NRT and Gauge V7) were evaluated and compared with hourly observation data from five ground stations in the Ciliwung River Basin. In addition, a rainfall-runoff and flood inundation model was applied to the target basin. The results of the analysis showed that the GSMaP Gauge data were more accurate than the GSMaP NRT data. However, the GSMaP Gauge cannot be used to provide real-time rainfall data and is, therefore, inadequate for real-time flood forecasting. We conclude that the GSMaP Gauge is suitable for replicating past flood events, but it is challenging to use the GSMaP NRT for real-time flood forecasting in Jakarta.

Based on the analysis, conclusions of the study and recommendations for Jakarta were made at the end of this thesis.

TABLE OF CONTENT

4. Effects of Land Use/Cover Change and Land Subsidence

5. Effects of Climate Change

6. Evaluation of Counter Measures

7. Flood Forecasting as Nons-tructural Counter Measures

List of Abbreviation

ADI	Alternating Direction Implicit
ALOS	Advanced Land Observing Satellite
ARI	Acute Respiratory Infections
B/C	Benefit/Cost
BaU	Business as Usual
BP	Building Price
BPBD	Badan Penanggulangan Bencana Daerah
BPPT	Badan Pengkajian dan Penerapan Teknologi
BNPB	Badan Nasional Penanggulangan Bencana
BMKG	Badan Meteorologi, Klimatologi dan Geografi
CC	Correlation Coefficient
CDF	Cumulative Distribution Function
CM	Counter Measures
CMIP5	Coupled Model Intercomparison Project 5
DEM	Digital Elevation Model
DC	Damage Cost
DHI	Danish Hydraulic Institute
DR	Damage Rate
DS	Double Sweep
1D – 2D	1 Dimension – 2 Dimension
EADC	Expected Annual Damaged Cost
FAO	Food and Agriculture Organization of the United Nations
GCMs	Global Climate Models
GFDL-ESM2M	Geophysical Fluid Dynamics Laboratory Coupled Model
GI	Green Infrastructure
GSMaP	Global Satellite Mapping of Precipitation
GSMaP MVK	GSMaP Moving Kalman Filter
HadGEM2-ES	Hadley Centre Global Environment Model version 2
HC	Housing Content
ICHARM	International Centre for Water Hazard and Risk Management
IDR	Indonesia Rupiah

IPSL-CM5A-LR	A single version of the IPSL-CM5 model
IRIDes	International Research Institute of Disaster Science
JAXA	Japan Aerospace Exploration Agency: JAXA
JICA	Japan International Cooperation Agency
MIROC-ESM-CHEM	An atmospheric chemistry coupled version of MIROC-ESM
MLIT	Ministry of Land, Infrastructure, Transportation, and Tourism
NCEP-FNL	National Centers for Environmental Prediction Global Forecast System (GFS) final (FNL)
NRT	Near Real Time
NSE	the Nash–Sutcliffe Efficiency index
PU	Pekerjaan Umum
PGW	Philadelphia Gas Works
PMW	Passive MicroWave
PRISM	Panchromatic Remote-sensing Instrument for Stereo Mapping
RCP	Representative Concentration Pathways
RPP	Recharge and retention Ponds
RMSE	Root Mean Square Error
RWs	Recharge Wells
SLEUTH	Slope, Land use, Exclusion, Urban growth, Transportation, and Hillshade
SUMM	Simple Urban Energy Model for Mesoscale Simulation
SRTM	Shuttle Radar Topography Mission
SSP	Share Socioeconomic Pathways
SWP	Sea Wall Protection
TMI	TRMM Microwave Imager
TRMM	Tropical Rainfall Measuring Mission
WRF	Weather Research and Forecasting

Chapter 1

Introduction

1.1. Background

Floods are one of the natural hazards with a great impact to human activities and its frequency has been increasing during the last few years. Floods are often caused by heavy rainfall, rapid snowmelt or a storm surge from a tropical cyclone or tsunami in coastal areas. However, in tropical country including Indonesia, an opportunity of the snow fall is little, so that the snow can be ignored. Also, a storm surge is little possibility in Indonesia, so that heavy rainfall and tsunamis in coastal areas are usually often concerns in Indonesia. Especially, flood disasters are becoming more severe recent years because of climate change issues.

As such, floods in Indonesia are considered to be one of the major natural disasters. The Special Capital Region of Jakarta (referred to below as Jakarta) in Indonesia has experienced many floods in the past. The flood in February 2007 resulted in more than 80 deaths, and 40% of the area in Jakarta was inundated. Also, electrical system shutdowns in several districts in the city were reported. The flood event in 2013 caused the similar situation, which resulted in more than 40 deaths, 45,000 refugees, and terrible economic damage. Extreme flooding events might become more frequent in the future due to the impacts of land use change (urbanization) in the upstream region (e.g. Farid et al. 2011) and the climate change (e.g. Kure and Tebakari, 2012). Jakarta faces several infrastructural, social, and water- related problems, such as land subsidence in coastal areas and rapid land-use/cover changes in the upstream region, which have resulted in an increase in the high flood risk zones in Jakarta. The Indonesian economy has grown in the past three decades, leading to new and expanding urbanized areas in Jakarta and its surrounding areas, and this urban development may be strongly related to the increase of the flood risks in Jakarta.

1.2. Problem

Jakarta in Indonesia is now enjoying economic development in what may be called a “golden period of growth.” However, there are many social problems and one of which is caused by insufficient infrastructures. Jakarta has experienced many floods in the past, such as those in 1996, 2002, 2007 and 2013, and those floods resulted in not only human casualties but also economic damages (Kure et al., 2014). Jakarta faces various infrastructural, social, and water related problems, such as land subsidence in coastal areas and rapid land-use/cover changes in the upstream region, which have resulted in an increase in the size of the area at risk of flooding. Also, Jakarta has many infrastructure problems, including traffic jams and floods, caused by rapid economic growth and urbanization. Bricker et al. (2014) noted the reduced capacity of the drainage system due to trash clogging flood-gates, which was one of the factors behind the 2013 flood. In addition, Kure et al. (2014) emphasized that a lack of capacity in rivers is a factor that can worsen flooding. As explained above, urbanization has contributed to increased flood damage (Farid et al., 2011; Moe et al., 2016a). In addition to above problems, land subsidence due to groundwater extractions, sedimentary layers and building loads, and their relation to the floods are reported.

The causes of flooding in Jakarta now increasing from year by year as shown in **Figure 1.1** and the flooding situations in 2013 (photos taken by Mr. Tokunaga [ICHARM]) are shown in **Figure 1.2**. According to **Figure 1.1**

the rapid urbanization in Jakarta was started in the beginning 1970. At the same time many people came to Jakarta for seeking jobs to work, and several social problems were started to increase. For example, there are problems such as illegal settlement in the river and coastal regions, trash/garbage disposal to the rivers, and illegal ground water pumping. The ground water pumping contributed to increase the land subsidence in the coastal areas. Accordingly, the urban development with several social problems triggered to increase the flooding in Jakarta.

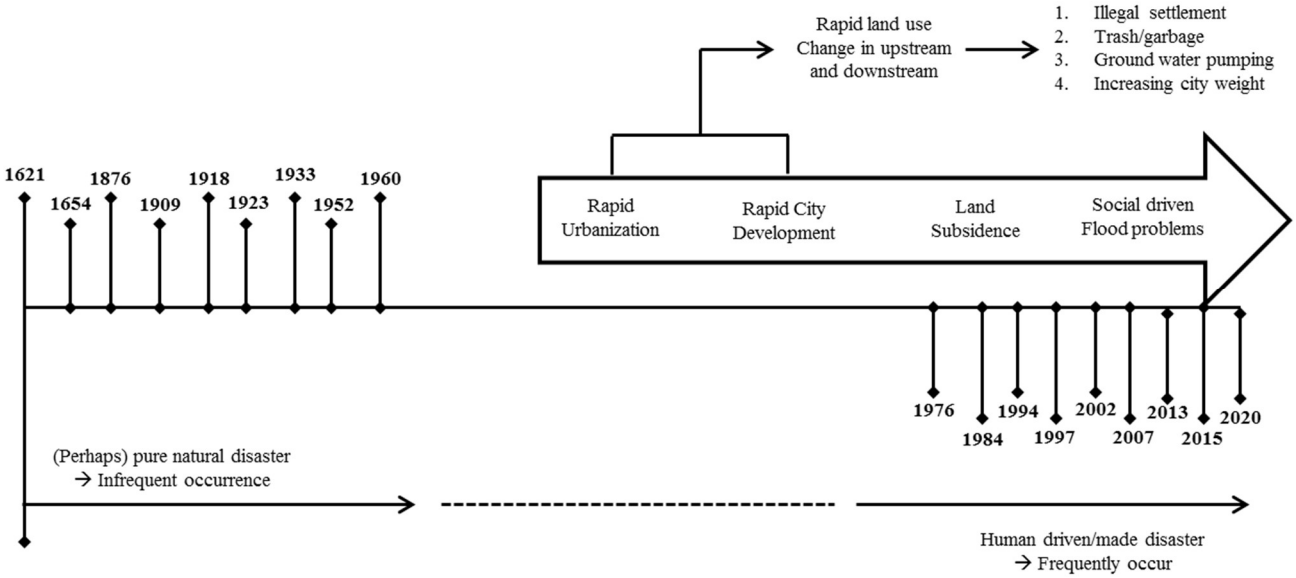

Fig 1.1 Historical flood events (Muhari et al, 2013)

Fig 1.2 Flood inundation situations in the 2013 flood event

1.3. Literature Review

In this section, several previous studies conducted for Jakarta's flood problems are reviewed to identify the critical problems and what further study should be focused to mitigate in the future flood disasters.

1.3.1. Several factors contributing floods in Jakarta

Heavy rainfall in and around Jakarta due to the tropical monsoon may have been a main factor contributing to the 2013 flood (Kure et al., 2014). However, not only heavy rainfall but also several problems causing floods in Jakarta were reported as explained in below. There are many factors contributing to the floods in Jakarta. According to Bricker et al. (2014), the reduced capacity of the drainage system by trash clogging flood gates was raised as one factor for the flooding. Kure et al. (2014) emphasized that the shortage of capacity flow in the lower Ciliwung River is one of the factors for the flooding in the lower sections of Jakarta. Also, other problems were analyzed based on the numerical simulations as explained in the following sentences.

1.3.2. Flood model applications

Several rainfall runoff and flood inundation models were applied to Jakarta to evaluate problems quantitatively and identify the flood risks. Nuswantoro et al. (2014) proposed probabilistic hazard maps for Jakarta using a rainfall runoff and 1D-2D hydraulic model with stochastic rain-storm generator. Also, urban development and land subsidence were modeled and simulated (Farid et al., 2011; Moe et al., 2016a, b, 2017). Flood inundation models were used in the climate change impact studies in Jakarta by Januriyadi et al. (2016) and Budiyono et al. (2016). As such many several flood analysis based on the numerical simulations were conducted in Jakarta. Detailes are explain in the flollowing sentences.

1.3.3. Land use change

Farid et al. (2011) pointed out that the urbanization of the Ciliwung River basin is contributing to increase of the flood flow in the river, and the land use change impacts on the runoff in Ciliwung River basin were evaluated by a numerical simulation. A rapid urbanization of Jakarta due to economic growth accompanied by its rapid population expansion is contributing to the increase of the flood risk in Jakarta. According to Farid et al. (2011), the urbanization of the catchment has caused floods to expand further and faster with the increase of the effective rainfall and surface runoff. Also, Moe et al. (2016a) pointed out that flood inundation area and volume increased with increases in the urbanized area.

1.3.4. Land subsidence

Land subsidence is widely known to be a serious problem causing urban flooding in the lowland areas of Jakarta. Land subsidence in the certain areas (Kure et al, 2014) of the city has spatial relation with flooding during rainy seasons. Land subsidence theoretically leads to expanding inundated areas and deepening water depth in flooded areas. In the northern part of Jakarta, especially coastal areas affected by land subsidence, sea level rise and high tide will contribute directly to increasing water depth and causing flooding to become higher. Also, land use/cover

change and shortage of capacity of rivers and small canals in the urban area also affect subsidence areas during heavy rainfall, resulting in the expansion of flood areas.

According to Atlas (2011), the land subsidence ranging from 0.1 m to 4.0 m occurred in the lowland areas of Jakarta from 1974 to 2010. This land subsidence may be a factor leading to urban flooding in these specific lowland areas. Many parts of the lowland areas are located below mean sea level so these areas are easily inundated by intensive rainfall, and dewatering is difficult due to the need of pumps. Moe et al. (2016b) evaluated that the flood peak and flood inundation volume will increase with the expansion of the urbanized area in and around Jakarta. Also, land subsidence is one of the factors contributing to flooding in Jakarta's lower area (Abidin, 2011). Increase of the ground water extraction due to urbanization was reported as a main factor of the land subsidence in Jakarta (Abidin, 2011). Park et al. (2016) emphasized that all areas including roads and buildings in the northern part of Jakarta are below mean sea level and those areas are vulnerable to flood inundation.

1.3.5. Climate change

Extreme and destructive flooding events may become more frequent in future owing to a combination of urbanization in the upstream region and climate change effects. Thus, a flood mitigation plan considering land use change regulation and climate change adaptation is needed. Hence a detailed future climate change impact assessment will be required considering the future urban development. Budiyono et al (2016) estimated the future flood damage costs in Jakarta, based on a numerical simulation of climate change and urban development scenarios. Combining all the future scenarios, they simulated the median increase in risk to be 180% by 2030. Januriyadi et al (2018) had shown that the combination of climate change and urban development could amplify the mean flood risk in future by 322%–402% by 2050 in Jakarta, with a confidence interval of 95%. Notably, the difference in the increased risks between Budiyono et al (2016) and Januriaydi et al (2018) was due to the different methods for estimating the asset values used in their research (2018).

1.3.6. Counter Measures

The intended plan by the Ministry of Public Works, Indonesia through Directorate General of Water Resources, River Basin Organization of Ciliwung- Cisadane to drain the water out of the city was by constructing a floodway in the shape of a horseshoe surrounding Jakarta. Therefore, the West Canal (Banjir kanal Barat) was constructed and still functions today. However, the construction of the East Canal (Banjir Kanal Timur) delayed and just recently finished because its project faced a financial problem several years ago. As such, some counter measures to reduce flood damages in Jakarta have been proposed and implemented. However, the mechanism of flooding in Jakarta has not been clarified yet, and quantitative evaluations of the proposed counter measures have not been conducted because of the complex flooding mechanism in Jakarta.

Moe et al. (2015) applied a rainfall runoff and flood inundation model to Jakarta and proposed to enlarge the flood flowing capacity of the Ciliwung River as a countermeasure to mitigate the flood damages in Jakarta. Januriyadi et al. (2020) proposed several counter measures in Jakarta and evaluated these based on Benefit-Cost analysis (B/Cs). However, critical and useful counter measures are still not found due to the high cost of the counter measures.

1.3.7. Summary of the literature reviews

According to the literature review, the factors contributing to floods in Jakrta are so complicated as shown in **Figure 1.3**. In these factors, urban development and climate change could be main factors in the near future. Several previous studies had conducted climate change impact analyses in Jakarta, considering future climate and land use changes and land subsidence. However, effects of urban development on the atmospheric environments of cities had not been taken into account in many previous climate change researches conducted in Jakarta or in urban cities across the world. Local urbanization is expected to affect the atmospheric environments of mega cities owing to the changing urban thermal environments, such as the heat island phenomena. In general, local urbanization was considered only for land use changes in runoff and flood inundation simulations. Many developing countries claimed that the climate change was originated from an economic activity of the developed countries, and they still claimed they need to use many fossil energies. They should understand some climate crisis such as urban heat island phenomena are because of their own urban development. Then, immediate research question is how much will the heat island affect for the future flooding in the city. Not only climate change impact but also this heat island should be quantitatively evaluated in the study.

Also, previous studies only considered a land use change scenario (the worst case) toward the future. However, several land use change scenarios should be considered in the climate and land use change study in Jakart in order to show how much CO_2 mitigation plans may work to reduce the flooding.

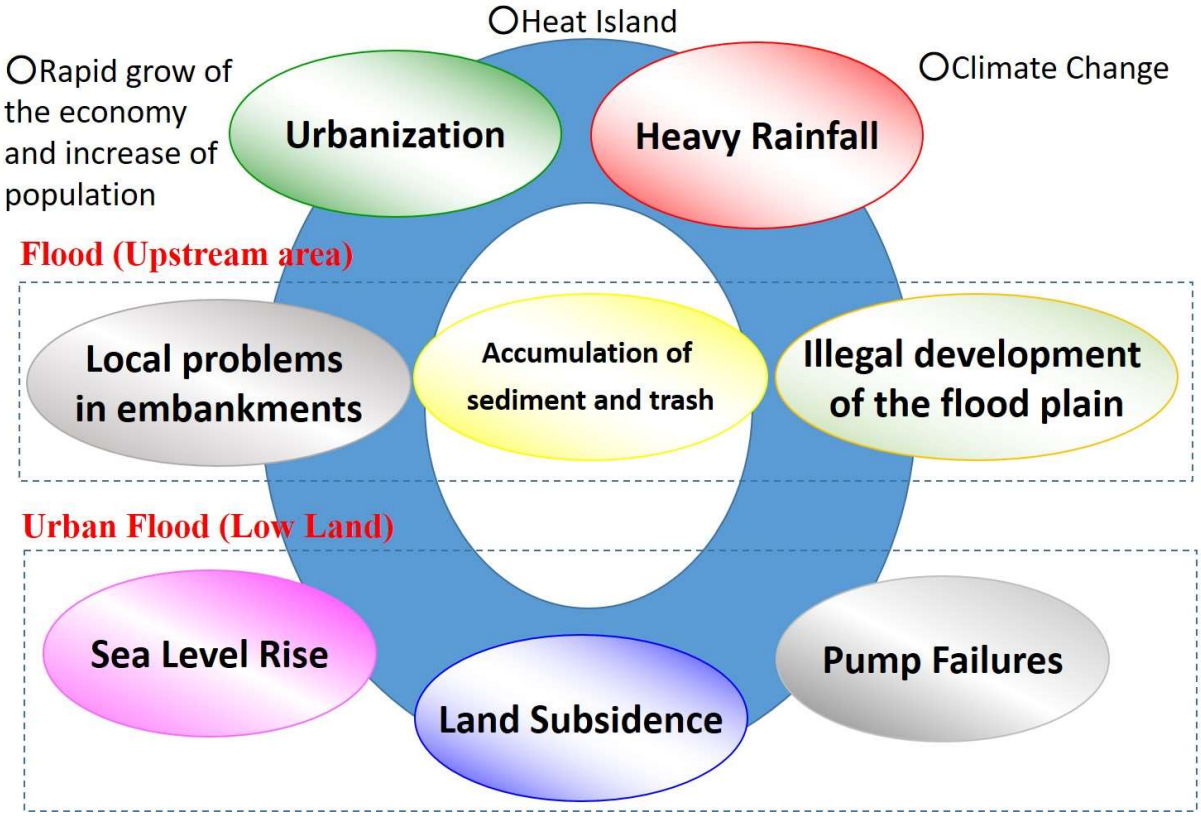

Fig. 1.3 Several factors contributing to the floods in Jakarta (Moe, 2017)

1.4. Objectives

The main objective of this study is to quantify the effects of both land use and climate change on future rainfall and flood inundation in Jakarta based on future urban growth and climate change scenarios including the heat island effects. Also, several counter measures not only structural measure but also non-structural measure such as the flood forecasting are proposed and evaluated in this study.

The originalities of the study are to consider the urban thermal environment (heat island) effects for the future scenarios and to consider the several future development scenarios. Also, the sea level rise was considered and evaluated in this study but this topic and result will be explained in the appendix because the results were not directly connected in the main topic of this thesis.

1.5. Flow chart of the research

A flow chart of the study is shown in **Figure 1.4**.

In **Figure 1.4**, the first step of the research framework is the literature review as explained in this chapter. Also, several hydrological data of rainfall, basin and river information (e.g DEM, River depth) were collected in the chapter 2. A rainfall runoff and flood inundation models were applied to the target area and model calibration and validation were conducted in the chapter 3.

Several scenarios of future urban development were prepared in the chapter 4 and 5. The scenarios of future urban development are consisted of land-use/cover change, land subsidence and climate change associated with a heat island effect. Flood inundation simulations under these scenarios were conducted using the calibrated model. Finally, several structural and non-structural measure will be proposed and evaluated. According to those, the recommendation of reducing the flood damages in Jakarta will be discussed.

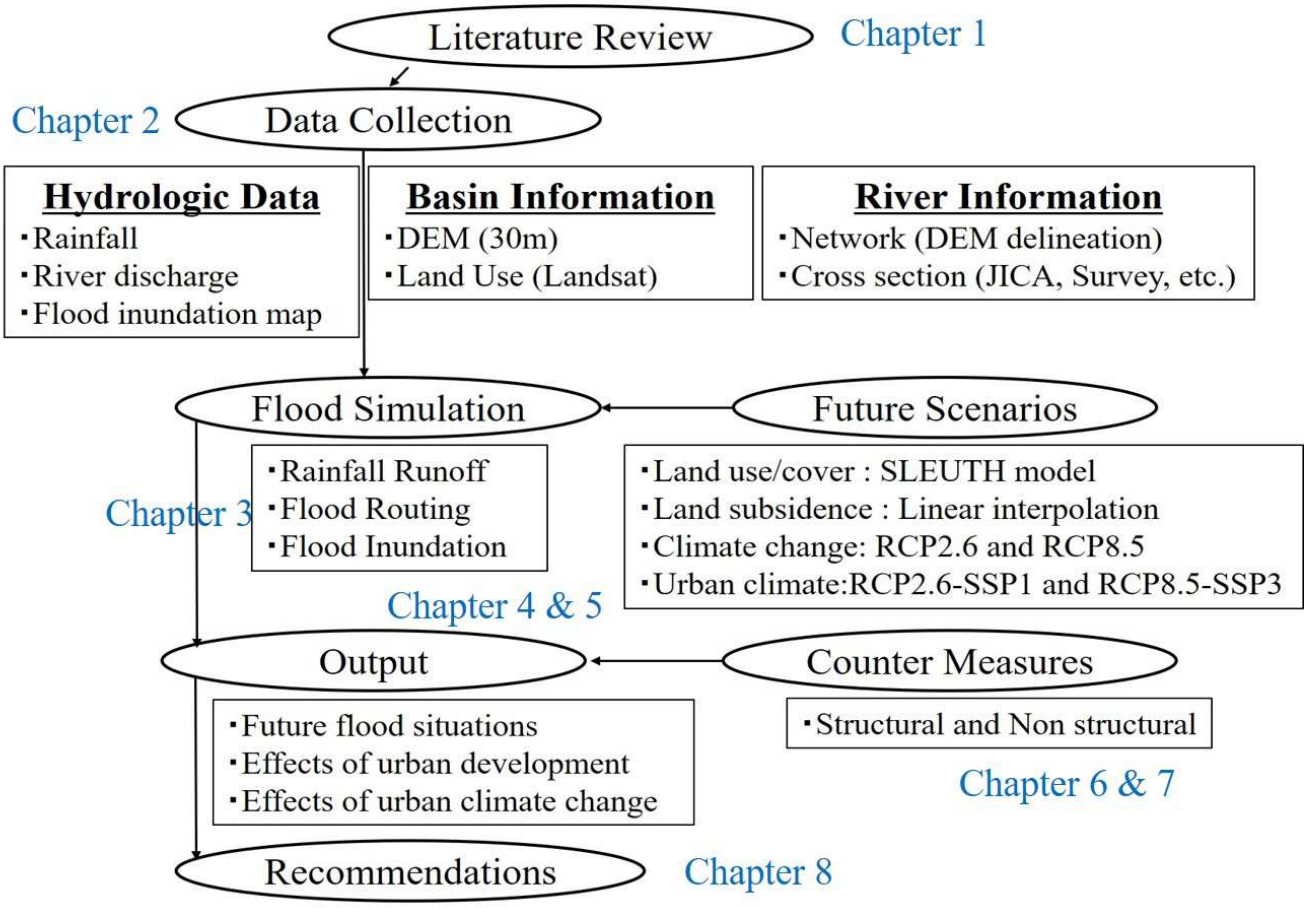

Fig 1.4 Flow chart of this study

1.6. References

Abidin, H.Z., Fukuda, Y., Pohan, Y.E., Deguchi. T. (2011). Land subsidence of Jakarta (Indonesia) and its relation with urban development. Natural Hazards. 59. 1753-1771.

Jakarta Coastal Defense Strategy (JCDS) (2011). ATLAS: Safety beach Jakarta. Ministry of Public Works, Indonesia; 123. http://ja.scribd.com/doc/72755643/ATLAS-Jakarta- Coastal-Defense-Strategy

Bricker, J. D., Tsubaki, R., Muhari, A., and Kure, S. (2014). Causes of the January 2013 Canal embankment Failure and Urban Flood in Jakarta, Indonesia. Journal of Japan Society of Civil Engineers, Ser. B1 (Hydraulic Engineering). 70(4). 91-96.

Budiyono, Y., Ward, J. P., Aerts. (2015). J.H.J.: Flood risk assessment for delta mega-cities: a case study of Jakarta. 2015. https://doi: 10.1007/s11069-014-1327-9).

Budiyono, Y., Aerts, J.C.J.H., Tollenaar, D., Ward, P.J. (2016). River flood risk in Jakarta under scenarios of future change. Natural Hazards and Earth System Sciences. 16. 757-774. https://doi:10.5194/nhess-16-7572016.

Farid, M., Mano, A., and Udo, K. (2011). Modeling Flood Runoff Response to Land Cover Change with Rainfall Spatial Distribution in Urbanized Catchment. Annual Journal of Hydraulic Engineering. 55. 19-24.

Kure, S., Tebakari, T. (2012). Hydrological impact of regional climate change in the Chao Phraya River Basin, Thailand. Hydrological Research Letters. 6. 53-58. https://doi:10.3178/hrl.6.53.

Kure, S., Farid, M., Fukutani, Y., Muhari, A., Bricker, J.D., Udo, K., and Mano, A. (2014). Several Social Factors Contributing to Floods and Characteristics of the January 2013 Flood in Jakarta, Indonesia. Journal of Japan Society of Civil Engineers. 70(5). 211-217.

Moe, I.R., Kure, S., Farid, M., Udo, K., Kazama, S and Koshimura, S. (2015). Numerical Simulation of Flooding in Jakarta and Evaluation of a Countermeasure to Mitigate Flood Damage. Journal of Japan Society of Civil Engineers.71 (5). 29-36.

Moe, I.R., Kure, S., Januriyadi, N.F., Farid, M., Udo, K., Kazama, S., Koshimura, S. (2016). Effect of land subsidence on flood inundation in Jakarta, Indonesia. Journal of Japan Society of Civil Engineers. (Ser. G (Environment). 72. 283-289.

Nuswantoro, R., Diermanse, F., and Molkenthin, F. (2014). "Probabilistic flood hazard maps for Jakarta derived from a stochastic rain-storm generator." Journal of Flood Risk Management. 1-19.

Januriyadi, N.F., Kazama, S., Moe, I.R., Kure, S. (2016). Urban Flood Damage Costs Estimation in Developing Country. Congress IAHR APD. Colombo, Srilanka.

Januriyadi, N.F., Kazama, S., Moe, I.R. and Kure, S. (2018). Evaluation of Future Flood Risk in Asian Megacities: A Case Study of Jakarta. Hydrological Research Letters , 12. 14-22. https://doi.org/10.3178/hrl.12.14

Januriyadi, N.F., Kazama, S., Moe, I.R. and Kure, S. (2020). Effectiveness of Structural and Nonstructural Measures on the Magnitude and Uncertainty of Future Flood Risks. Journal of Water Resource and Protection. 12. 401-415. https://www.scirp.org/journal/jwarp

Park. H., Kwon S., and Hadi S. (2016). Land Subsidence Survey and Policy Development in Pantai Mutiara, Jakarta Bay, Indonesia. Journal of Coastal Research. 75. 1447- 1451.

Chapter 2

Study Area

2.1. Overview

Jakarta is the capital and largest city of Indonesia with a population of about 9.6 million. The central Jakarta is the seat of national government as well as seat of the provincial government of Greater Jakarta. This city is moreover the country's center of finance and business.

Thirteen major rivers flow northwards through Jakarta into the Java Sea. The main river in Jakarta is the Ciliwung River with the upstream area in Pangrango Mountain and the downstream area in Jakarta. The Ciliwung River is the longest river which passes through Jakarta and some areas in West Java Province, as shown in **Figure 2.1**. The Ciliwung River has a catchment area of 382.6 km^2 with the river length of 117 km. The influence of the Ciliwung River on the Jakarta region is the largest among other rivers flowing into Jakarta. Many people think that the occurrence of floods in Jakarta is mainly related to the Ciliwung River, especially in the upper part of the river.

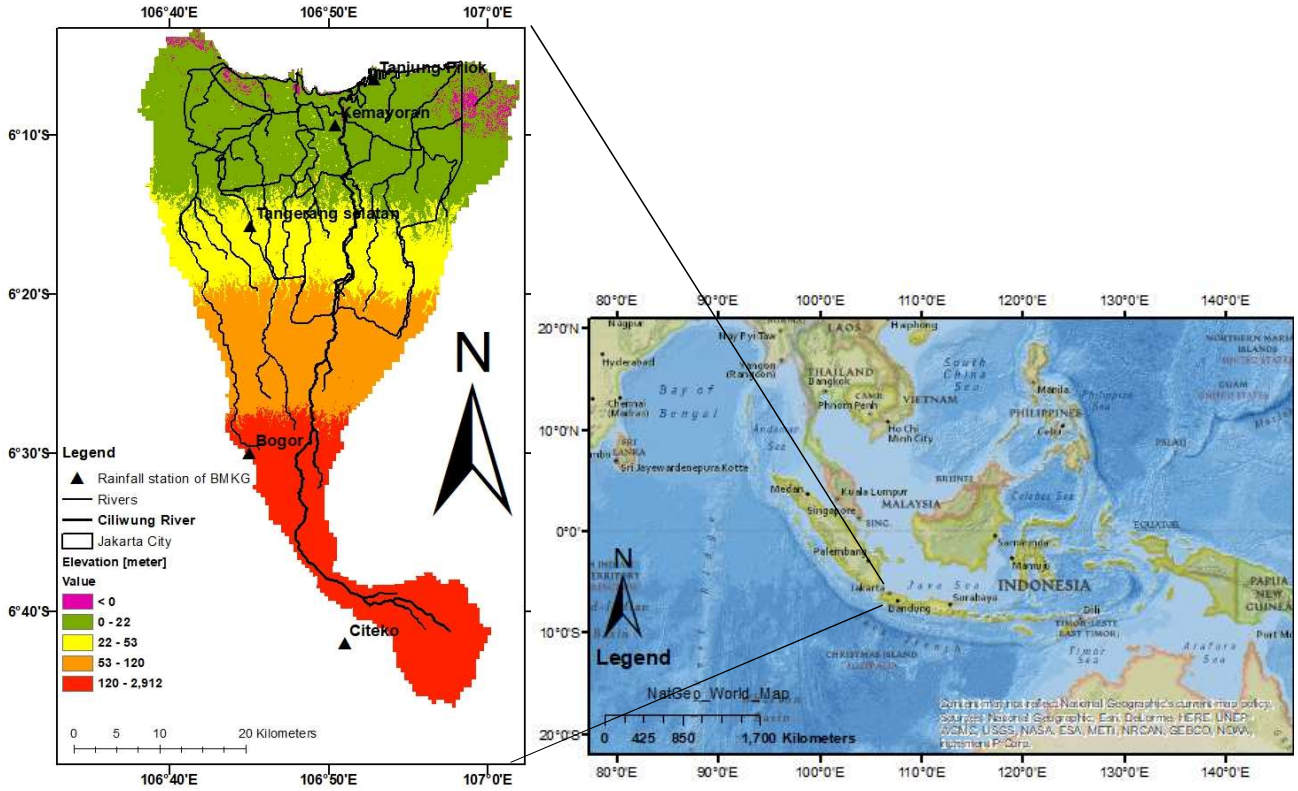

(ArcMap_online)

Fig.2.1 Study area

Figure 2.2 shows the land use/cover change in Ciliwung river basin in 2002. The land use map in 2002 is provided by Ministry of Public Works Republic of Indonesia (PU). The land use categories in 2002 was based on the LANDSAT satellite image analysis (Djakapermana et al, 2008). The categories of land use in 2002 was based on 5 land use classes, i.e. forest, cropland, paddy field, water and urban areas as shown in **Figure 2.2**. The percentage of each land categories for whole target study area can be seen in **Table 1.1**. As shown in **Table 1.1**, 64% of the study

area is covered by the urbanized area, 2.8% of the study area is covered by forest area, 24.2% of the study area is covered by crop land area, 3.3% of the study area is covered by paddy field area, and 5.7% of the study area is covered by water area.

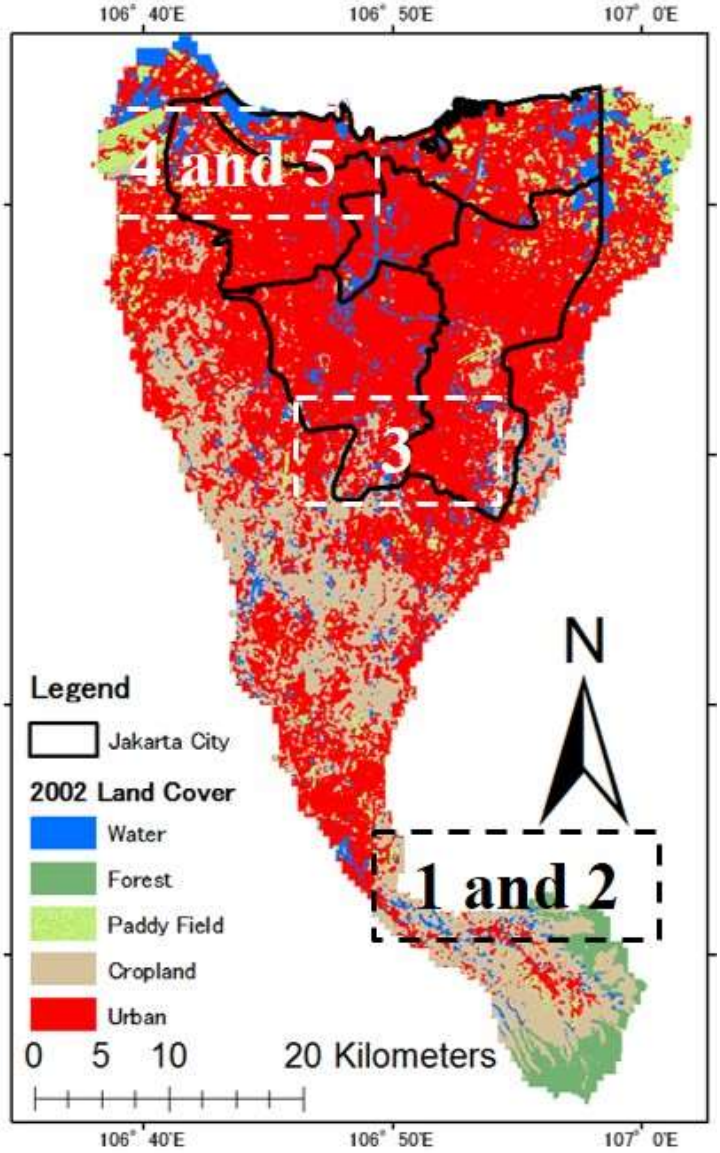

(Source : Moe et al, 2016)

Fig 2.2 Land Use/Cover Change

Table 2.1 Land use/cover categories for 2002 (Moe et al, 2017)

Land-use types [%] for 2002					
Year	Urban	Crop Land	Paddy Field	Forest	Water
2002	64	24.2	3.3	2.8	5.7

Figure 2.3 shows the photos in the study area taken by the author during the on site survey. Locations are specified in **Figure 2.2**. Main vegetations in the upstream areas are Fern, Pinus merkusii, Treelets and Rattan and main agricultures in Jakarta are rice, tea and coffee plantation. Also, several fish ponds can be found at north east side of Jakarta. It was found that some part of the upstream region areas are still covered by various plantations as shown in **Figure 2.3**. However, it also can be found that some urbanized areas are located in the upstream region and those situation relatively match with the land use map in 2002 (**Figure 2.2**). It means that there are still urban developing activities in the upstream region and those activities of urban developing have a high possiblity to be continued in the upstream region in the near future because there are still spaces to be converted from vegetation to urbanized area.

Fig 2.3 Photos of upstream (1-2), middle (3) and downstream (4-5) of ciliwung river basin.

2.2. Recent floods in Jakarta

Almost every year, Jakarta experiences flooding in January and February owing to high rainfall with insufficient capacity flows in the drainage system. The details of the flood events and damage are listed in **Table 2.2**. In **Table 2.2**, the damage cost and main damages were obtained from several sources, such as web online news and several reports, and the values of the rainfall, water level, and flooded area were obtained from the observed data. The details of the flood events were explained in below. It is noted that only flood reports in 2013, 2015, 2017 and 2020 were collected, so that these events are mainly explained.

Table 2.1 Summary of historical flood events

Year	Averaged rainfall (mm)	Maximum water level (cm) at Manggarai	Flood area (km^2)	Death Person	Main damage	Damage Cost (IDR)
1996	421	970	-	10	529 houses were highly damaged	6.4 Trillion
2002	464	1050	160	32	Electrical System Shutdown	9.9 Trillion
2007	340	1060	397	80	Electrical System Shutdown	8.8 Trillion
2013	168	1020	132	41	Embankment failure	1.5 Trillion
2014	581	830	201	26	134,662 persons were affected	5 Trillion
2015	310	890	196	5	Electrical System Shutdown	1.5 Trillion
2016	275	580	152	2	-	3 Trillion
2017	322	700	139	6	1,178 houses were inundated	147 Billion
2018	346	775	79	1	42 houses were highly damaged	150 Billion
2019	154	890	84	2	-	100 Billion
2020	196	965	150	67	Electrical System Shutdown	1 Trillion

(Source : result analysis (2021), Moe et al (2015), News online)

2.2.1. 2013 flood event

The January 2013 floods are a complex problem because the rainfall intensity was smaller than that during the 2007 floods, yet Jakarta's wealthy commercial and governmental core, which escaped the 2007 floods, was inundated (IRIDeS report, 2013). One improtant poin of the event is breaching of a section of embankment along the west drainage canal flooded downtown areas below the canal (**Figure 2.4**). The canal embankment overtopping itself may have been the result of inconsistent embankment height (a locally lower embankment in the breach area) or/and seepage along the embankment/structure interface at a concrete structure (a highway bridge pier or a tower) built on the embankment at the breach site. Related this embankment breach, the problem of trash (**Figure 2.5**) is a critical problem because clogging of the Karet gate (downstream of the canal breach site, and observed by Deltares during the flood) by trash may have been a principle cause of high water level at the canal breach site and at Manggarai gate, resulting in canal embankment failure and the ensuing flooding of Jakarta's commercial/governmental core.

The IRIDeS report (2013) investigated the causes of casualties due to the flood. Unexpected casualties, such as those which occurred when the underground parking area of building flooded, can be attributed to lack for flood response. Unlike after Jakarta's previous floods, deaths due to leptospirosis and dengue have not been reported this time, even though most of Jakarta's population has no access to sewage or septic systems, meaning that floodwaters inevitably contain much human waste. However, acute respiratory infections (ARI), diarrhea, gastritis, typhoid, and skin disease were common after the January 2013 flood due to continuous rain, cold living conditions, and lack of hygiene and sanitation in flooded and refuge areas. In addition to disease, the floods affected residents by interrupting the supply of clean water and electricity, and by temporarily putting affected health care facilities out of operation.

The photos in **Figure 2.4** show the overtopping of the flood flow provided by BNPB. Also, **Figure 2.5** shows the trash accumulation situations at the Karet gate in the Chiliwun River. This photo was taken and provided by Deltares.

Fig. 2.4 Overtopping situations at the section of embankment along the west drainage canal (Photos provided by BNPB)

Fig. 2.5 Trash accumulation situations at the Karet gate after the flood event (Photos provided by Deltares)

Table 2.2 shows the average actual flood damage per house hold for the 2013 flooe event (Wijayanti et al., 2017). From this table, the flood damage situations could be slightly understood. A significant house damage by a severe flood inundation flows is not so often and house contend damages at the inside and outside due to the flood inundation are main damage (63%). As IRIDeS report specified, some peple claimed life in the floodplain in Jakarta is not so bad, because they are only flooded 1 month of the year, so have the remaining 11 months to live normally, especially after adapting to the flooding by building 2-story homes. From these damage situations and people's comment, it might be said that Jakarta people underestimate the impact of the floods in Jakarta.

Table 2.2 Average actual flood damage per house hold for the 2013 flood event (Wijayanti et al., 2017)

Damage	Value (US$)	Percentage (%)
1 Direct		
1a Structural damage	43	14
1b Content damage (inside and outside)	193	63
2 Indirect		
2a Clean-up cost	25	8
2b Loss of income	30	10
2c Evacuation and temporary house	12	4
2d Cost of illnesses	5	2
Total	308	100

2.2.2. 2020 flood event

Heavy rain since Tuesday, December 31, 2019 flushed all regions in Jakarta and its surroundings until 07.35 am, the rain continued to flush. As a result, a number of areas in Jakarta and surrounding areas were flooded after being rained overnight. The water level at the Katulampa dam is 170 centimeters, rain conditions and alert status number 2 (Human initiative, situation report, 2020). A number of areas in Jabodetabek are flooded with varying heights from 30 cm to 200 cm. Data from the BNPB states there are 6 areas with water levels of more than 2 meters, including Cipinang Melayu East Jakarta, Jatikramat Bekasi, Bekasi Exile, Margahayu Bekasi, Duren Jaya Bekasi, and Bintaro South Jakarta. In this event, 67 people were dead due to landslides, hypothermia, drowning, and electrocution. Many parts of the city had been left without power, as the power was switched off for safety reasons by the state-owned electricity firm, PLN. This event was the area's worst flooding since 2007 when the rainfall intensity was 340 millimetres per day and 80 people were dead in 10 days. **Figure 2.6** shows the flooding situations in Jakarta in January 2020.

Figure 2.6 flooding situations in 2020 flood event (Source: USAtoday news, on February 25, 2020)

2.2.3. Summary of the recent flood events

From recent flood events in Jakarta, we could understand the flood damage situations and flood physical behaviors in Jakarta. The catchment area of the Cilliwun River is 382.6 km^2, and this size is not so large compared to other countries main rivers. So significant flood damage to the infrastructures and houses are not main damages in Jakarta flooding. Embankment failure is reported in only 2013 flood event. However, other social problems such as electrical shutdown, traffic jams, and human health problems are considered to be additional problems and characteristics in Jakarta flooding. These problems are significantly affecting the Jakarta's economy, so that we must consider the counter measures against Jakarta's flooding.

2.3. Data availability

The Digital elevation model (DEM) from Shuttle Radar Topography Mission (SRTM) with resolution 30 meters was employed in this study. For the soil data, the dataset from the Food and Agriculture Organization of the United Nations (FAO) was employed for the determination of model parameters used in this study. The data of cross sections of rivers and the drainage system were obtained from the project authority of JICA on the Ciliwung River in 2011. Rainfall data in the target area was provided by the BMKG (Badan Meteorologi, Klimatologi dan Geofisika: Indonesian Agency for Meteorology, Climatology and Geophysics), and water level data of the Ciliwung River and flood inundation map of Jakarta were provided by the BPBD (Badan Penanganan Bencana Daerah: Jakarta Disaster Management Agency).

For the river cross sections, the measured data by JICA project were employed in this study. However, there are no observed data available from upstream rivers and small tributaries. In that case we assumed the river cross sections as having a rectangular shape, and river width data were measured from Google Map views and mean river

bed elevations were extracted from DEM. Also, the river depths were assumed by using simple empirical equations proposed by Carpenter et al. (1999).

The dataset was used to apply the flood simulation model explained in the following chapter.

2.4. References

Carpenter, T.M., Sperfslage, J.A., Georgakakos, K.P., Sweeney, T., and Fread, D.L. (1999). National threshold runoff estimation utilizing GIS in support of operational flash flood warning systems. Journal of Hydrology. 224. 21-44.

Djakapermana R. D. (2008, March 31). Kebijakan Penataan Ruang Jabodetabekjur. Paper dipresentasikan pada Seminar Sehari Memperingati Hari Air Sedunia, Kelompok Keahlian Teknologi Pengelolaan Lingkungan. FTSL ITB, Bandung.

Human Initiative (Situation Report). (2020). Floods in Jabodetabek.

IRIDeS. (2013, Ferbruary 13). IRIDes(2nd Report) Fact-finding missions to Jakarta, Indonesia .

Wijayanti, P., Zhu, X., Budiyono, Y., and Van Lerland, E.C. (2017). Estimation of river flood damages in Jakarta, Indonesia. Natural Hazards. 86. 1059-1079.

Chapter 3

Flood Simulation Model

3.1. Overview of the flood inundation model

In this study, a physical model of rainfall-runoff and flood inundation was used to simulate the flood inundation in Jakarta that would result from various changes due to the urban development (Moe et al., 2017). The model consisted of modules representing the rainfall-runoff in each sub-basin, a hydrodynamic module representing the river and canal networks, and a flood inundation module for predicting the status of the floodplains. The details are explained in below.

3.1.1. Rainfall runoff module

For the rainfall runoff simulation, the model proposed by Kure et al. (2004; 2008) was employed. The model is based on the kinematic wave theory for a hillslope, and it computes surface and subsurface flows based on the geological and hydrological characteristics at each sub basin. Model parameters are determined by DEM and soil datasets.

For the rainfall runoff simulation, a physically based distributed rainfall-runoff model (Kure et al, 2004) was employed because this model can simulate the hortonian overland flow in urban areas and the subsurface flow and saturation overland flow in mountainous areas depending upon the relationship between the soil and geological characteristics and the rainfall intensity in a hill slope.

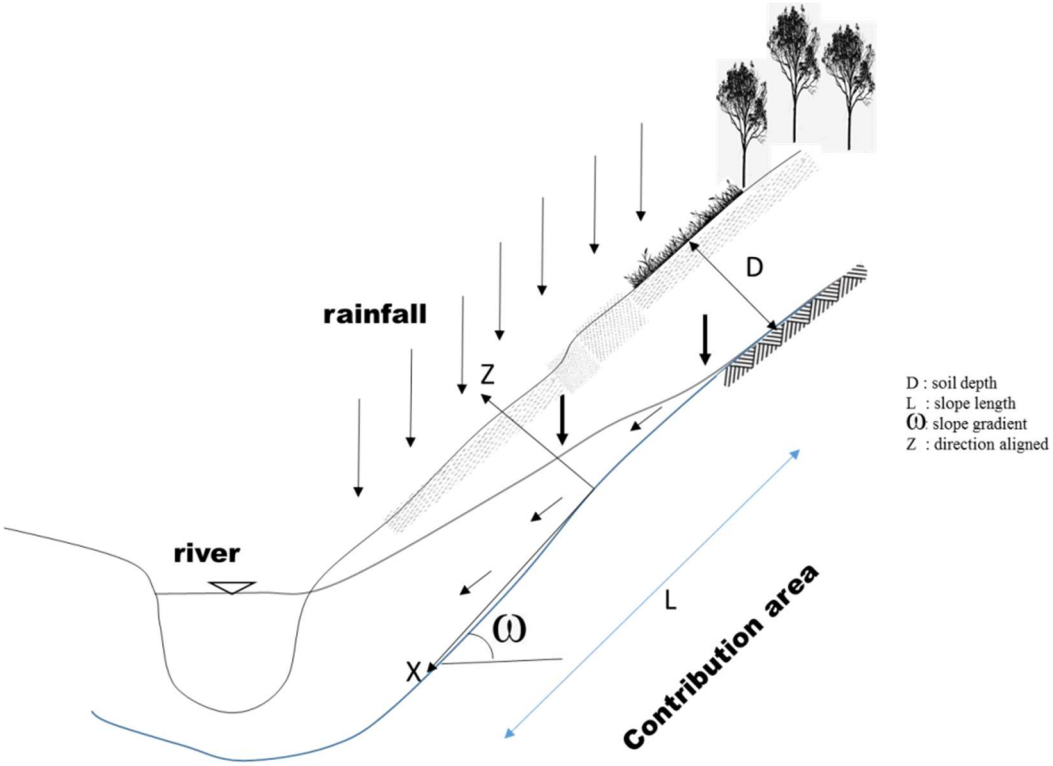

Fig.3.1. Schematic representation of the rainfall runoff processes in a slope

$$\frac{dq_s}{dt} = a_s q_s^{\beta_s}\left(r(t) - q_0 - q_s\right)$$ Surface flow (3-1)

$$\frac{dq_*}{dt} = a_0 q_*^{\beta}\left(q_0 - q_*\right)$$ Subsurface flow (3-2)

$$\frac{dq_0}{dt} = \left(r(t) - q_0\right)\frac{q_0 - K_s}{h + h_k} - \frac{q_0}{\left(\theta_s - \theta_i\right)}\frac{\left(q_0 - K_s\right)^2}{K_s\left(h + h_k\right)}$$ Vertical infiltration flow (3-3)

$$\frac{dh}{dt} = r(t) - q_0 - q_s$$ Surface water depth (3-4)

Where $a_0 = (m+1)\alpha^{\frac{1}{m+1}} L^{\frac{-1}{m+1}}$, $\beta = \frac{m}{m+1}$, $\alpha = \frac{Ks \sin\omega}{D^m w^{m+1}}$

Where

- r(t) is the effective rainfall (mm/h),
- q_0 is the vertical infiltration rate (mm/h),
- q_s is the surface runoff (mm/h),
- q_* is the subsurface runoff (mm/h),
- h is the water depth of overland flow (mm),
- K_s is the saturated hydraulic conductivity (mm/h),
- h_k is the capillary negative pressure of the wet line (cm),
- θ_s is the saturated water content of the soil,
- θ_i is the residual water content of the soil,
- m is the runoff parameters,
- L is the slope length (mm)
- D is the thickness of surface soil layer (mm)
- w is the effective porosity
- ω is the slope gradient

For the computation of a_s and β_s, m=2/3 (manning's law for the overland flow) is used.

The values of the soil parameters were calibrated in the 2013 flood event simulation based on four classes of land cover: forest, cropland, paddy field, and urban area. From a sub basin delineation tool in Arc Map (ver.10.1) with DEM 30 m data, 40 sub basins with an area ranging from 0.04 km^2 to 88.6 km^2 were delineated. Slope gradients at individual sub basins in the target area are mostly mild ranging 2 – 16 degrees. The soil parameters were obtained from FAO data by means of Kure et al. (2011) and then soil parameters were calibrated based on trial

and errors under the discharge simulations. Soil depth for A_0 layer was determined with a range of 97 mm to 215 mm, and the total porosity ranging from 0.45 to 0.5 was obtained.

The 4th order Runge Kutta method was used to numerically simulate the eq. (3-1), (3-2), (3-3) and (3-4). Computation time is less than 1 second to simulate a flood event of 40 subbasins with the Δt=1 second with 6 core CPUs (Intel Xeon E-2286G 4.00GHz) and 64.0 GB memory.

3.1.2. Flood routing module,

The hydrodynamic module used to simulate the river and canal networks was composed of a continuous equation, and an equation for the momentum at steady flow (Saint-Venant equation). For the flood routing and inundation, MIKE FLOOD (DHI), integrated system of MIKE 11 and MIKE 21, were employed in this study. A flood routing in rivers and a drainage system were conducted based on the MIKE 11. MIKE 11 simulates a 1D flow with dynamic wave description by solving the vertically integrated equations of conservation of continuity and momentum (the Saint-Venant equations). The Saint-Venant equations for conservation of continuity and momentum are written as follows:

$$\frac{\partial A}{\partial t} + \frac{\partial Q}{\partial x} = q_l \tag{3-5}$$

$$\frac{\partial Q}{\partial t} + \frac{\partial \left(\alpha \frac{Q^2}{A}\right)}{\partial x} + qA\frac{\partial h}{\partial x} + \frac{gn^2|Q|Q}{R^{4/3}A} = 0 \tag{3-6}$$

where, Q is the discharge (m^3/s), A is the area of cross-section (m^2), q_l is the lateral inflow (m^2/s) or outflow distributed along the x-axis of the watercourse, n is the manning's roughness coefficient, α is the momentum distribution coefficient, g is the acceleration of gravity, R is the hydraulic radius and h is the water level (m).

Figure 3.2 shows that the modeled river channel network in Jakarta. The calibration also included Manning's roughness coefficients of these river networks, which were set to between 0.02 and 0.4 for the beds of each river section after model calibration. It is noted that we could find several high values of the manning's roughness coefficients around 0.1-0.4 in the river beds. This may be from the insufficient river cross section information.

The numerical scheme for these equations is 6-point Abbott-scheme that make fast and stable computations of the flood routing in MIKE 11. Upper boundary conditions were set as constant discharge values in the upstream and lower boundary conditions were set as the tide level in Jakarta bay. For the numerical simulation, Δt was set as 1 second and Δx was set as 100 m. The simulation takes about 30 minutes for a 5 days flood event simulation with 6 core CPUs (Intel Xeon E-2286G 4.00GHz) and 64.0 GB memory.

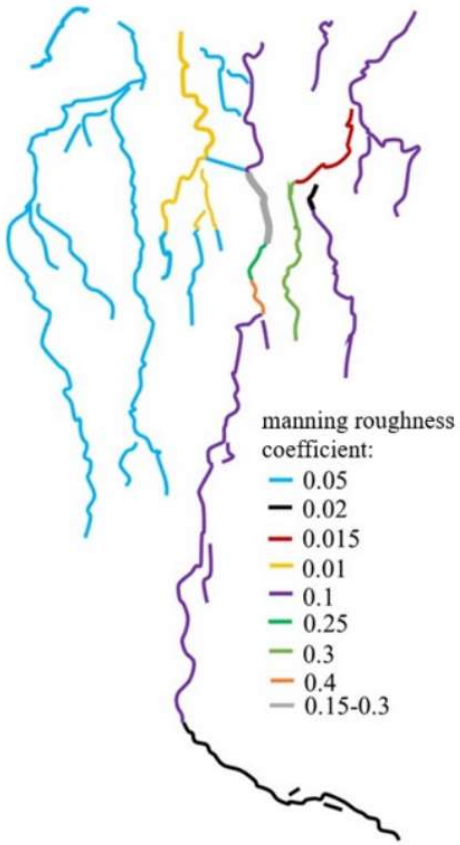

Fig. 3.2. Modeled river network in Jakarta

3.1.3. Flood inundation module

For the flood inundation, the unsteady two- dimensional flow equations consisting of the continuity equation and momentum equation are numerically solved in MIKE 21. The flood routing simulation by MIKE 11 and the flood inundation by MIKE 21 are dynamically integrated through the MIKE FLOOD system. The river (MIKE 11) is linked laterally to floodplain (MIKE 21) to represent spilling from the river to the flood plain and drainage back into the river.

$$\frac{\partial h}{\partial t}+\frac{\partial p}{\partial x}+\frac{\partial q}{\partial y}=0 \tag{3-7}$$

$$\frac{\partial p}{\partial t}+\frac{\partial}{\partial x}\left(\frac{p^2}{h}\right)+\frac{\partial}{\partial y}\left(\frac{pq}{h}\right)+gh\frac{\partial \zeta}{\partial x}+\frac{gp\sqrt{p^2+q^2}}{C^2-h^2}-\frac{1}{\rho_w}\left[\frac{\partial}{\partial x}(h\tau_{xx})+\frac{\partial}{\partial y}(h\tau_{xy})\right]=0 \tag{3-8}$$

$$\frac{\partial q}{\partial t}+\frac{\partial}{\partial y}\left(\frac{q^2}{h}\right)+\frac{\partial}{\partial x}\left(\frac{pq}{h}\right)+gh\frac{\partial \zeta}{\partial y}+\frac{gq\sqrt{p^2+q^2}}{C^2-h^2}-\frac{1}{\rho_w}\left[\frac{\partial}{\partial y}(h\tau_{yy})+\frac{\partial}{\partial x}(h\tau_{xy})\right]=0 \tag{3-9}$$

Where;

- $C(x,y)$ is the Chézy resistance ($m^{1/2}$ s^{-1}),
- ρ_w is the density of water (kg m^{-3}),
- τ_{xx}, τ_{xy}, and τ_{yy} are the components of effective shear stress (kg m^{-1} s^{-2}),
- g is the acceleration of gravity (m s^{-2}).
- $\zeta(x,y,t)$ is the water elevation (m),
- $p(x,y,t)$, $q(x,y,t)$ are the flux densities (m^3 s^{-1} m^{-1}) in the x- and y-directions,
- $h(x,y,t)$ is the water depth (m).

Manning's roughness coefficients for land surface were set to 0.1 $m^{-1/3}$ s for all floodplains. A so-called Alternating Direction Implicit (ADI) technique to integrate the equations for mass and momentum conservation in the space-time domain. The equation matrices that result for each direction and each individual grid line are resolved by a Double Sweep (DS) algorithm. For the details, see the MIKE 21 Scientific Documentation. These numerical schemes make fast and stable computations of the flood inundation simulation in MIKE 21. At the domain boundary, the flux is assumed to be zero. For the numerical simulation, Δt was set as 0.5 s and Δx and Δy were set as 30 m as the same as the DEM data. The simulation takes about 4 days for a 5 days flood event simulation with 6 core CPUs (Intel Xeon E-2286G 4.00GHz) and 64.0 GB memory.

3.2. Simulation results

The flood inundation model was applied to the target areas for the 2013 flood event of January 14 –18, 2013. The 2013 flood was selected as the target event, because an observed inundation map and the radar rainfall of Jakarta exists for this event. In the study area, it was difficult to obtain rainfall data with high temporal and spatial resolutions from the ground stations. For the 2013 flood event, only 7 of 17 rain gauges provided hourly rainfall data, which was inadequate to achieve a good spatial distribution of hourly rainfall data as a model input. The other gauges record rainfall data at daily intervals, and hourly data are unavailable. In September 2007, a C-band Doppler radar was installed (Yamanaka et al., 2008) in Serpong, a southwestern suburb of Jakarta. Therefore, radar rainfall information was used as the input for the rainfall-runoff model in this study.

The comparison of the simulated and observed discharge hydrographs at the Depok and Katulampa stations are shown in **Figure 3.3**. The simulated discharge is calculated by using the radar rainfall data with the ground observation data. Radar data bias was corrected based on ground observations (Moe et al., 2016a). The radar rainfall data were provided by the BPPT. It can be seen from **Figure 3.3** that the simulation results reasonably well matched with the observed discharge. Their correlation coefficients are 0.81 and 0.80 and the root mean square errors are 6.4 m^3/s and 15.4 m^3/s at Katulampa and Depok, respectively. Also, the high Nash Index of 0.75 and 0.95 at Depok and Katulampa stations are confirmed.

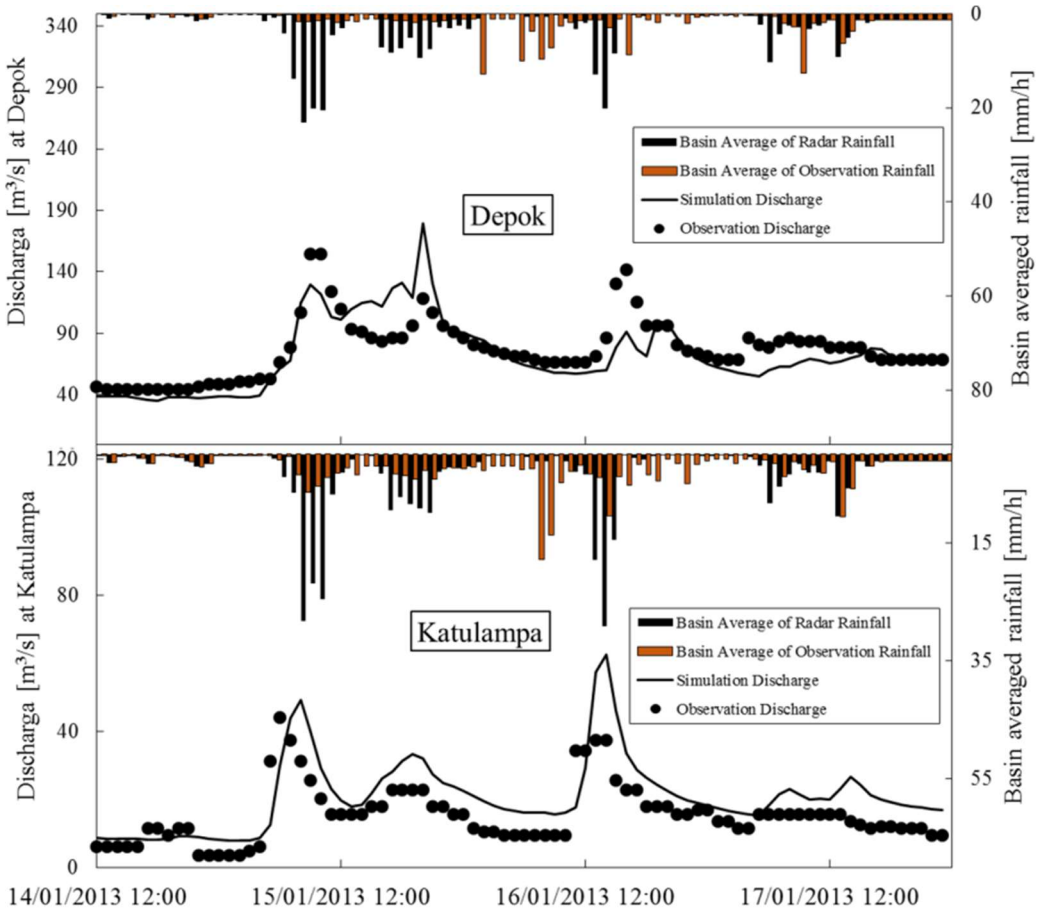

Fig. 3.3. Time series of the observed and simulated discharge at Katulampa and Depok stations for 2013

Additionally, the visual-graph comparisons between the simulated flood inundation distribution and the observed inundation map indicated an acceptable agreement, as shown in **Figure 3.4**. The observed flooded area data were provided by the Badan Penanggulangan Bencana Daerah (BPBD; Jakarta Province Regional Disaster Management Agency).

Here, we quantify the agreement based on the following Fit index:

$$\text{Fit } (\%) = \frac{IA_{obs} \cap IA_{sim}}{IA_{obs} \cup IA_{sim}} \tag{3-10}$$

Where IA_{sim} is the inundated pixels predicted by the model (we assumed a depth greater than 0.1 m as the simulated flood extent in this study) and IA_{obs} is the identified flooded pixels by the observation map. To get the area of IA_{obs}, the map shown in **Figure 3.4** was digitized and converted to a raster data set having the same grid size as the model simulation. From equation (3-10), the Fit value was obtained as 0.21, which is relatively low. For this reason, it should be emphasized the observed flooded area was based on the eyewitness reports at each district by government officers during the flood event and interviews with local residents after the event although there are some uncertainties. For example, only slight area was actually inundated, but the whole district was judged as the inundated zone in Fig. 5. Also, there were discrepancies between the reported and simulated inundation areas,

especially in the northcentral and northeast areas. This may have been caused by the numerous local fish ponds located in these areas. The local fish ponds are initially filled with water but this initial water was not captured by the land-use map used in this study, leading to the underestimation of the flood inundation simulation of this study. It is also noted that the inundation in the northern coastal area is affected by ocean flooding. The simulated inundation area in the target area matched relatively well with the observation results, namely, at the north-west of Jakarta and the upstream area of the Manggarai gate point.

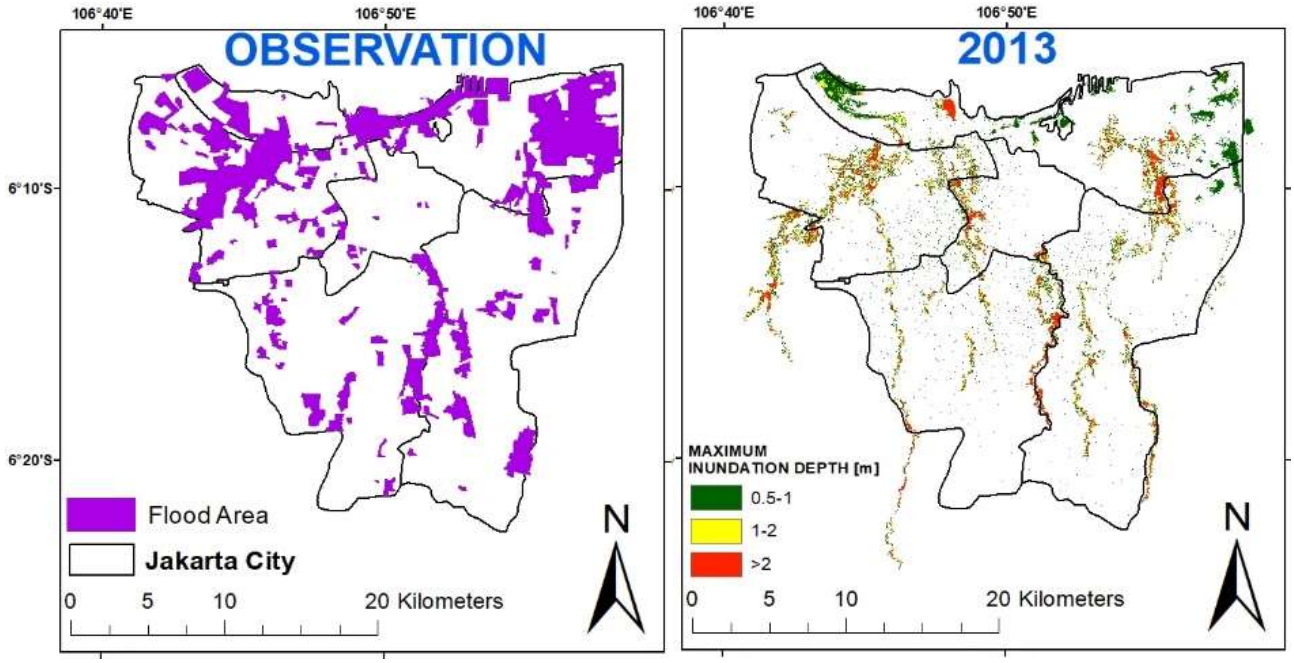

Fig. 3.4. Comparisons between the simulated (left) and observed (right) inundation areas

3.3. Original source of the flood inundations

The flood inundation volumes originated from each source were computed, and those inundation areas were represented in **Figure 3.5**. The flood volumes were computed by the maximum inundation depth and inundated area in Jakarta derived from the simulation results. River flood volumes without land subsidence was computed by simulations without the land subsidence DEM data. In 2002 land use condition, the area with the shortage of capacity flow in the lower part of the Ciliwung River contributed 10.3% and the shortage of capacity flow in other rivers contributed 53.2%, of the total flood inundation volume. Also, the land subsidence, coastal effects and local fish ponds in the northern part of Jakarta occupied 36.5% of the total volume.

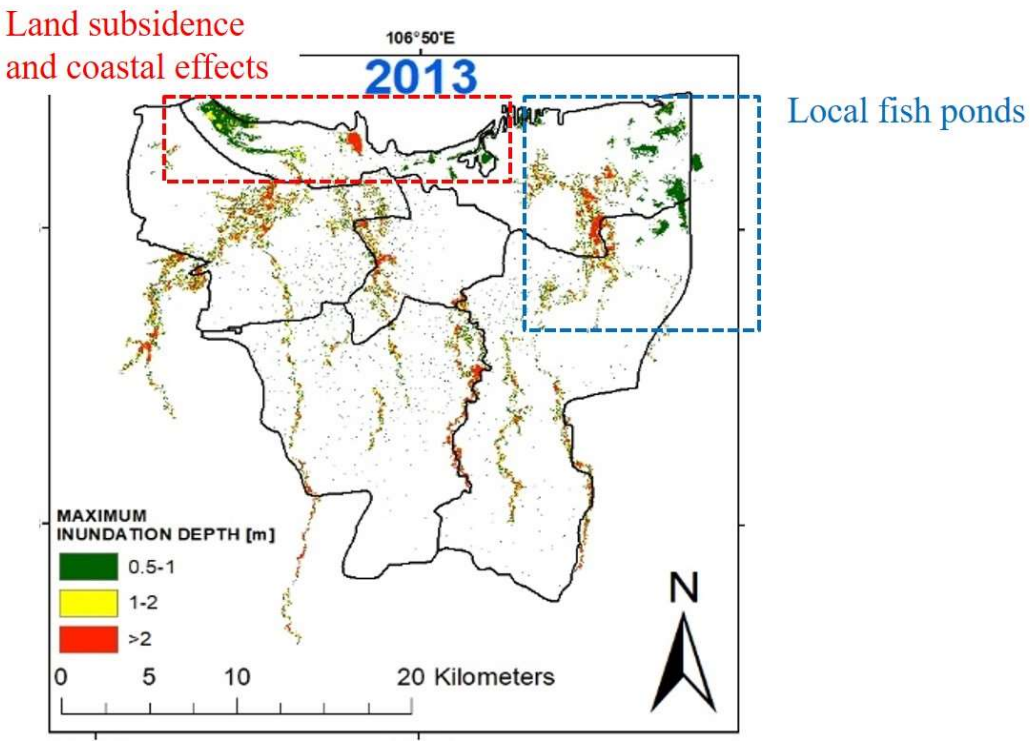

Fig. 3.5. Original sources of the flood inundation (Shortage of capacity flow in the Ciliwung river: 10.3%, shortage capacity flow in other rivers: 53.2% and land subsidence, coastal effects and local fish ponds: 36.5%)

3.4. Model improvement

The above explained model was used to simulate future flood inundation situations in Jakarta considering the urban development and climate change in this region. In addition, the model was improved to consider the other factors such as the sea level rise of the climate change. The original model (Moe et al., 2017) did not consider the water from the ocean as making the boundary condition as a no flow condition but the improved model consider the water from the ocean depending on the sea tide level and coastal bathymetry. This is because the sea level rise impact needs to be evaluated at the same time with the urban development. This effect will be discussed in the Appendix.

3.5. References

Kure, S. and Yamada, T. (2004). Nonlinearity of runoff and estimation of effective rainfall in a slope. Proceedings of the 2nd Asia Pacific Association of Hydrology and Water Resources Conference. 2. 76-85.

Kure, S., Watanabe, A., Akabane, Y., and Yamada, T. (2008). Field Observations of Discharge and Runoff Characteristics in Urban Catchments Area. Proceedings of the 11th International Conference on Urban Drainage, United Kingdom. 1-10.

Moe, I.R., Kure, S., Januriyadi, N.F., Farid, M., Udo, K., Kazama, S., Koshimura, S. (2016). Effect of land subsidence on flood inundation in Jakarta, Indonesia. Journal of Japan Society of Civil Engineers, Ser. G (Environment). 72. 283-289.

Moe, I.R., Kure, S., Januriyadi, N.F., Farid, M., Udo, K., Kazama, S., and Koshimura, S. (2017). Future Projection of Flood Inundation Considering Land Use Change and Land Subsidence in Jakarta, Indonesia. Hydrological Research Letters. 11(2). 99-105.

Yamanaka, M.D., Mori, S., Wu, P.M., Hamada, J.I., Sakurai, N., Hashiguchi, H., Yamamoto, M.K., Shibagaki, Y., Kawashima, M., Fujiyoshi, Y., Shimomai, T., Manik, T., Erlansyah., Setiawan, W., Tejasukmana, B., Syamsudin, F., Djajadihardia, Y.S., Anggadiredja, J.T. (2008). HARIMAU radar-profiler network over Indonesian maritime continent: A GEOSS early achievement for hydrological cycle and disaster prevention. Journal of Disaster Research. 3. 78-88.

Chapter 4

Effects of Land Use/Cover Change and Land Subsidence

This chapter is based on the following paper:

Priyambodho A.B., S. Kure, I.R. Moe, and S. Kazama (2018) “Numerical Experiments of Future Land Use Change for Flood Inundation in Jakarta, Indonesia” Journal of Japan Society of Civil Engineers, Ser. G (Environment), Vol.74, No.5, I_265-I_271.

Land subsidence and land-use changes in Jakarta are ongoing, and significant changes are expected to continue in the future. In this chapter, effects of the land use/cover change and land subsidence due to the urbanization on the flood inundation are examined based on the flood model simulations and future urban development scenarios.

4.1 Methodology

4.1.1. Land Subsidence

In this study, a land subsidence projection for the future derived by Moe et al. (2016a) was used. In order to evaluate the situation of land subsidence in Jakarta for the historical and future periods, accumulated land subsidence from 1974 - 2010 reported by another study (Abidin et al, 2011) was extracted at each grid point to make a spatially interpolated land subsidence accumulation map over Jakarta by using the inverse distance weighted method. Then, those accumulated values were adjusted to obtain the year average subsidence rate [m/year] by dividing with the total year of accumulation from 1974 – 2010 under the assumption that the land subsidence speed is constant in time. The digital elevation model shown in **Figure 1.1** by JAXA with the resolution (JAXA, 2016) of 30 meters was selected as the base data. The data was observed by ALOS equipped with the Panchromatic Remote-sensing instrument for Stereo mapping (PRISM), to acquire elevation from 2006 to 2011 that was the operational period of ALOS (JAXA, 2016). Therefore, we assume that the data provided from ALOS represents the Jakarta's land surface elevation situation in 2009 as the base year.

From the base data of 2009, Moe et al (2016a) reconstructed and projected the land elevation in Jakarta for the historical and future periods by using a linear extrapolation based on the subsidence rate at each grid as shown in **Figure 4.1**. **Figure 4.2** shows a projected land subsidence situation in Jakarta in 2050 compared to 2009. It was found that more than 4 m land subsidence from 2009 can be found in the northwestern part of Jakarta in 2050. However, it should be emphasized that the land subsidence situation for the future period derived from the linear extrapolation was one of the worst scenarios based on the assumption that there would be increase of ground water withdrawal and high-rise buildings in Jakarta keeping land subsidence speed constant. Murakami et al. (2003) and Yasuhara et al. (2015) developed an observational prediction method of land subsidence based on the observed data at the target area. According those studies, time series of the land subsidence at several areas were successfully reproduced by an exponential equation, and they pointed out that land subsidence rate was affected by ground water level. As such, the land subsidence situation projected in this study should be considered as the worst scenario.

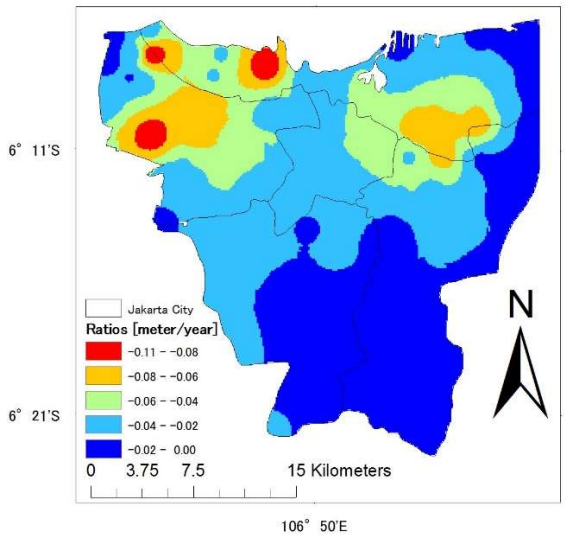

Fig. 4.1 The annual land subsidence rate in Jakarta.

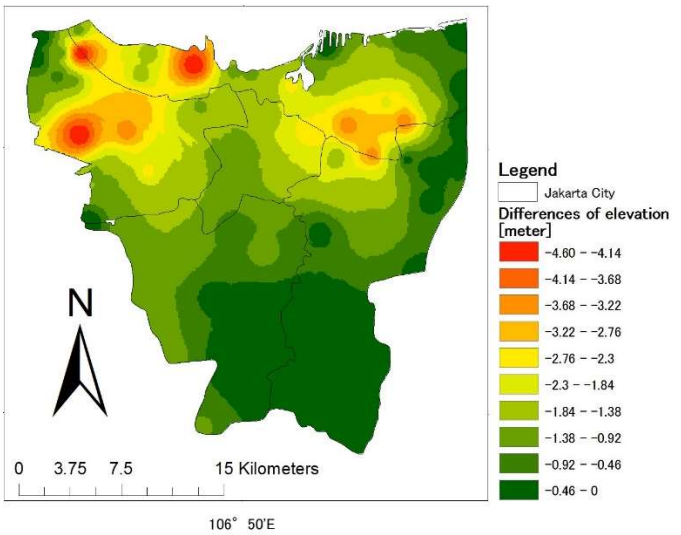

Fig. 4.2 Projected land subsidence situation in Jakarta in 2050 compared to 2009 (Moe et al, 2016b).

4.1.2. Land use/cover change

The effects of changes in land use on flooding in Jakarta by predicting future land use using the SLEUTH model (Dietzel et al., 2006), which estimates urban growth based on historical slopes, land use, exclusion, urban growth, transportation, and hill-shade data. Varquez et al. (2017) applied SLEUTH to Jakarta under the RCP8.5-SSP3 (worst-case) and RCP2.6-SSP1 (compact-growth) scenarios, and we used the resulting projected land-use/cover maps in this study. Although a previous study by Moe et al. (2017) investigated the impact of land-use changes in only the worst-case scenario, several additional scenarios must be evaluated to develop realistic strategies for future land-use management.

The necessary inputs for the SLEUTH model are slope, land cover, excluded region, urban cover, transportation, and hill shade in the study area. Excluded region, means areas where urban growth is restricted (e.g. water bodies, parks). From the inputs, Varquez et al (2017) calibrated the necessary growth coefficients (dispersion=1, breed=14, spread=89, slope=65, and road=28) for urban growth using 1000 iterations of the Monte Carlo Simulation. Under the RCP8.5-SSP3, direct application of the calculated growth coefficients provided the urban extents of 2050. To limit urban expansion (i.e. consistency with RCP2.6-SSP1), the coefficients (e.g. spread=22) were reduced. For more details, please see the reference (Varques, et al; 2017).

In this study, I consider four scenarios for future land use in Jakarta: the worst-case, compact-growth, and controlled-growth-I and -II scenarios. The worst-case scenario assumed that historical levels of urbanization are maintained (BaU: Business as Usual). In the compact-growth scenario, we reduced the spread coefficients of the SLEUTH model to represent less urban growth than in the worst-case scenario. The output from the SLEUTH model were not used for the controlled-growth scenarios. Instead, I reduced the total urbanization ratio obtained from the compact-growth model of the target area. I have 40 sub-basins for the rainfall-runoff simulations in the study area. Four land cover ratios of these sub-basins were calculated by the SLEUTH model under the worst-case

and compact-growth scenarios, and then, these land cover ratios were used in the rainfall-runoff simulations. For the controlled-growth scenarios, some of the urban areas were uniformly converted to the forest areas over the upstream regions. These new urbanization and mountainous ratios in the sub-basins were used for the rainfall-runoff simulations of the controlled-growth.

The compact-growth and controlled-growth-I scenarios differed by a constant ratio (0.03) for every year (2020, 2030, 2040, and 2050) of urbanization between 2050 (0.90) and 2040 (0.87). Thus, the aim of the controlled-growth scenario was to decrease the growth rate and delay the progress of urbanization by 10 years compared to the compact-growth scenario in 2050. I set the constant difference ratio between levels of urbanization according to the compact-growth and controlled-growth-II scenarios in 2050 (0.90) and 2030 (0.81) to 0.09, based on the ratio of the compact-growth scenario to the controlled-growth-II scenario. This allowed us to increase our control of urban development in the upstream region. Relative to the compact-growth scenario, the controlled-growth-II scenario delayed development by 20 years and the controlled-growth-I and -II scenarios replaced urban areas in the upper region with forested areas.

Figure 4.3 shows the predicted changes in land use in and around the target area in 2020 and 2050 based on the compact-growth scenario and worst scenarios. **Figure 4.4** shows a time series of the total urbanization ratios in the target area for each scenario. These figures imply that the entire target area would be almost fully urbanized by 2050, even in the compact-growth and controlled-growth scenarios. It should be noted that the urbanization speed in **Figure 4.4** is gradually decreasing even in the worst-case scenario that assumed historical levels of urbanization are maintained. This is because there is no more space for the urbanization in the study area except for the excluded areas or steep mountainous areas that are not suitable for the urban development. I used the land elevation data provided by Moe et al (2016a) to evaluate land subsidence. I assumed that historical land-subsidence speeds in the target area varied linearly over time. The historical land-use data were provided by PU. Models with entirely forested or entirely urban target areas were also simulated in two further numerical experiments. I then applied the rainfall-runoff and flood inundation models using these land-use conditions and elevations. The results are discussed in the next section.

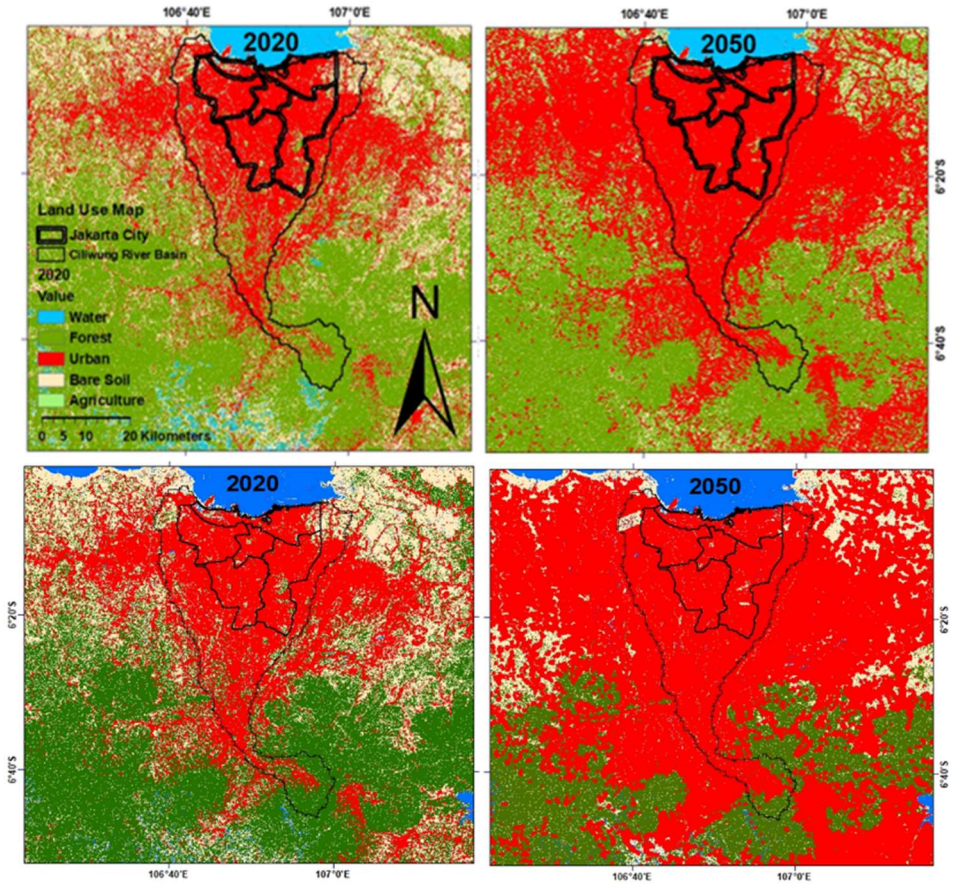

Fig.4.3 Projected future land-use map of the compact-growth scenarios for 2020 (top left), 2050 (top right) and worst scenarios for 2020 (bottom left) and 2050 (bottom right)

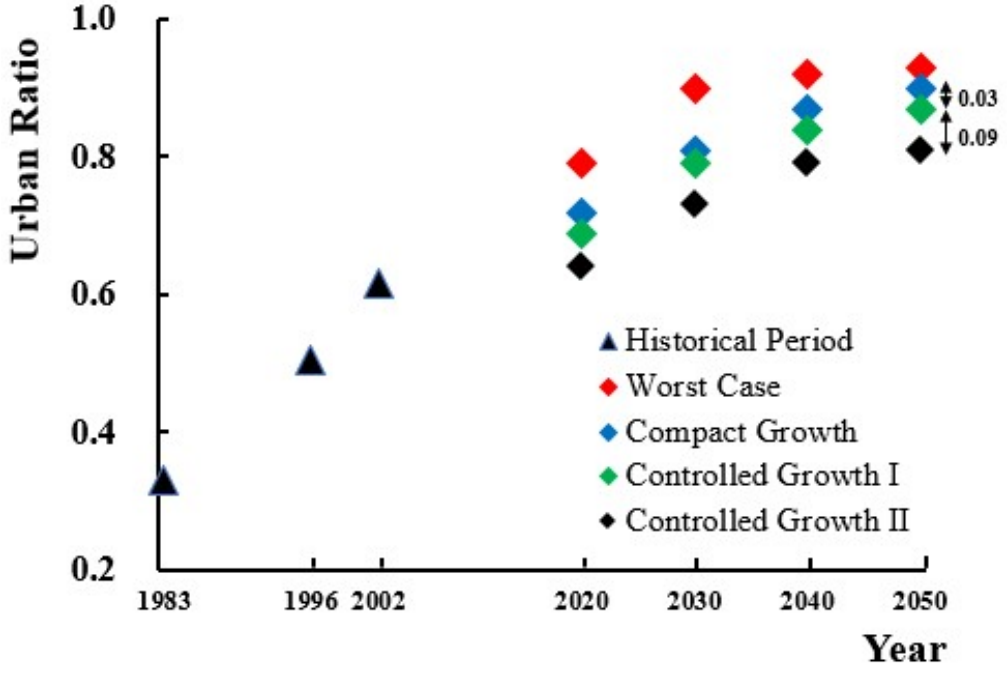

Fig. 4.4 Time series of the total urban ratio of each scenario in the historical and future periods

4.2. Results

For the rainfall-runoff simulation, projected-land-use information was used to compute the land-use categories in each sub-basin by area and percentage (%). I used the values used for the calibration simulation (Moe et al, 2015, 2016a) of the 2013 flood event for other inputs such as rainfall and the model parameters for each land-use category. It is noted that the same rainfall input data of the 2013 flood event was used as the input for the future and historical simulations. It means that we did not consider the impacts from the climate change on the flood inundation in this paper.

Figure 4.5 shows simulated hydrographs at Katulampa Station (**Figure 1.1**) in 2020 and 2050, under each land-use scenario. The flood peak and volume increase with future increases in the size of the urbanized area. Examples of the simulations are shown in **Figure 4.6**. This indicates the flood inundation in 2020 and 2050 according to the historical calibration simulation (2013) together with observations and the compact-growth scenario with the land subsidence. Each of the urban and forest situations is also presented in the figure. These figures clearly show that in the compact-growth scenario, extensive flooding occurs in 2050, whereas flooding is limited in the scenarios in which forest is retained.

Figure 4.7 shows a time series of the areas and volumes of historical and future flood inundation under each land-use condition with the land subsidence. The inundation area and volume increase with increasing urbanization under each scenario. The largest inundation area and greatest volume occur in the worst-case scenario, but the other scenarios also result in extensive inundation. I calculated the total worst-case-scenario inundation volumes in 2013 and 2050 as 4,050,171 and 2,960,121 m^3, respectively. The flood inundation volume in 2050 in the controlled-growth-II scenario would be 3,752,756 m^3. The changes in land use between 2013 and 2050 would increase the flood inundation volume in the worst-case and controlled-growth-II scenarios by 35% and 25%, respectively. It should be emphasized that flood inundation would increase significantly due to changes in land use with land subsidence even if urban development in the upper region were delayed, such as in the controlled-growth-II scenario. This is because, except for some areas in the upper forest, much of the study area was already occupied by urban areas in 2013. The impact on flood inundation of converting the remaining forested areas into urban areas would be significant. Based on this, I conclude that the government should control and regulate changes in land use in the regions upstream and land subsidence in the regions downstream of Jakarta as soon as possible.

Figure 4.8 shows the relationship between the urbanization ratio of the whole area and flood inundation volumes, with and without land subsidence. I analyzed the impact of land subsidence by simulating flooding both with and without land subsidence. High urbanization ratios are clearly associated with high flood inundation volumes, with the figure showing that the urbanization ratio varies linearly with the flood inundation volume. I found that land subsidence also would have the impact to the flood inundation. The land subsidence itself has small impacts as reported by Moe et al. (2017) but the combination of the land-use change and land subsidence would have a much greater impact to the flood inundation than only land subsidence or land-use change.

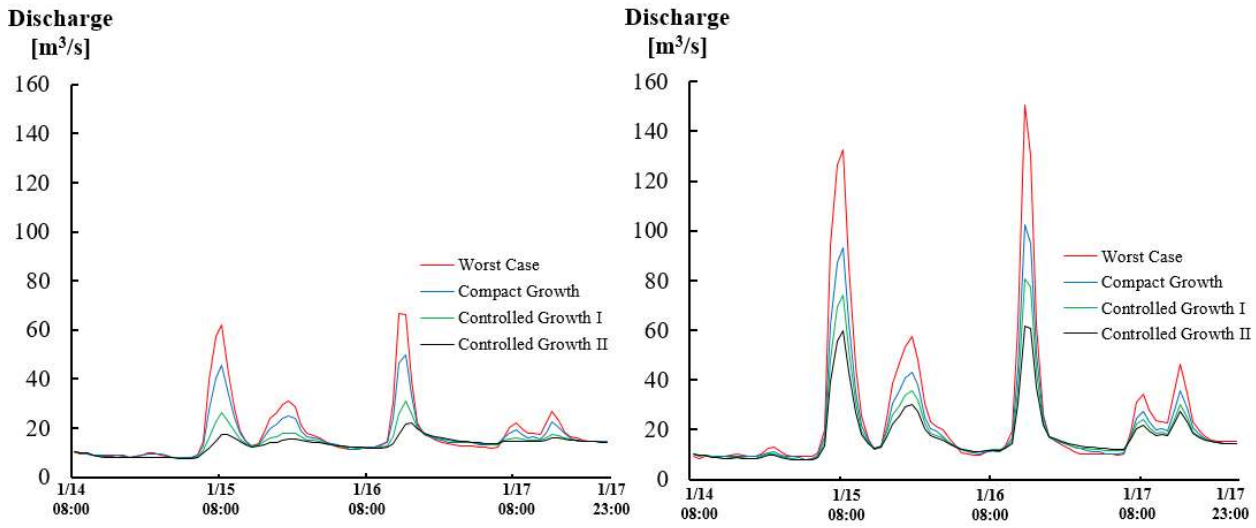

Fig. 4.5 Simulated river discharge [m^3/s] of each scenario at Katulampa Station in 2020 and 2050

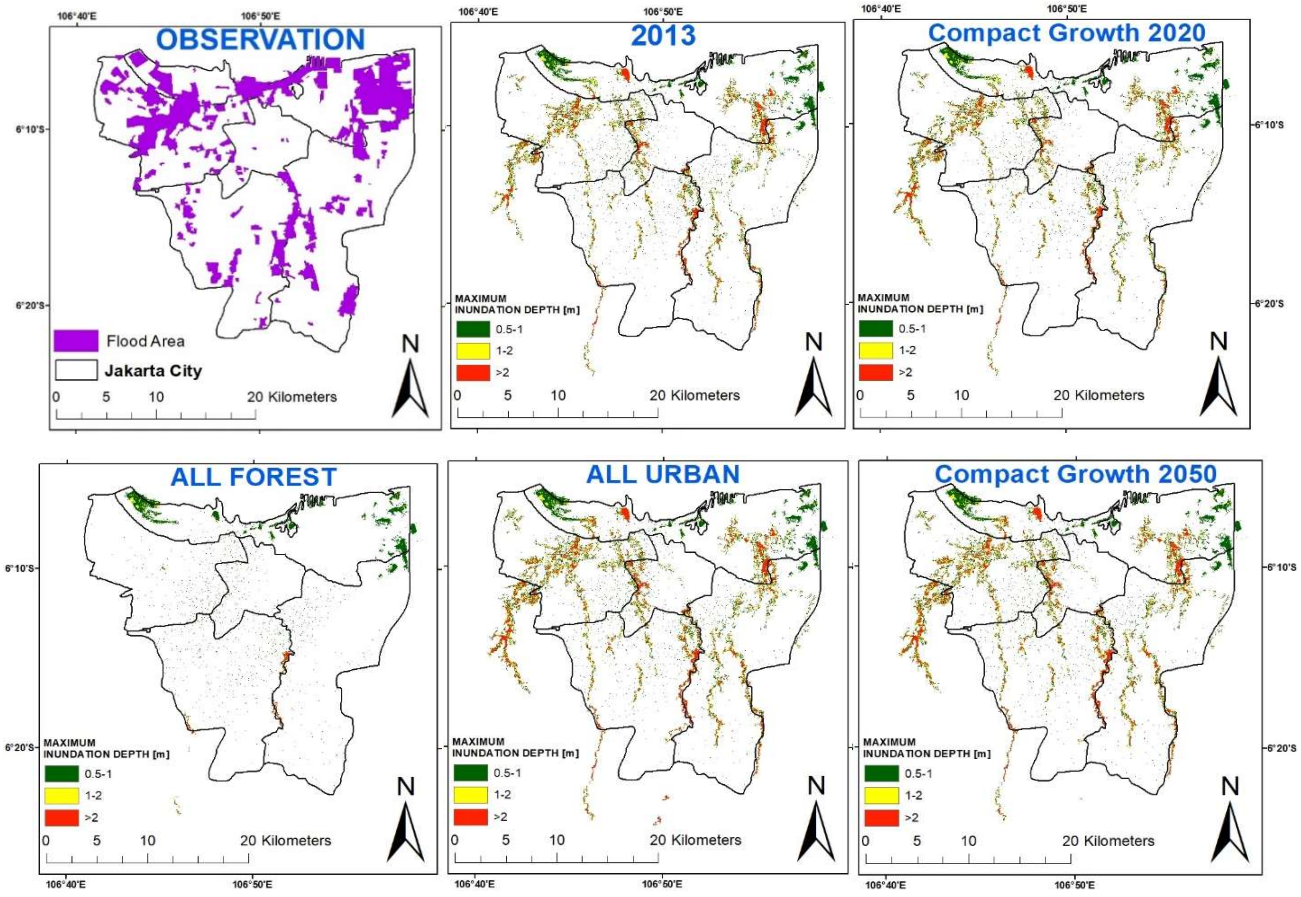

Fig. 4.6 Simulated flood inundation areas of the example scenarios

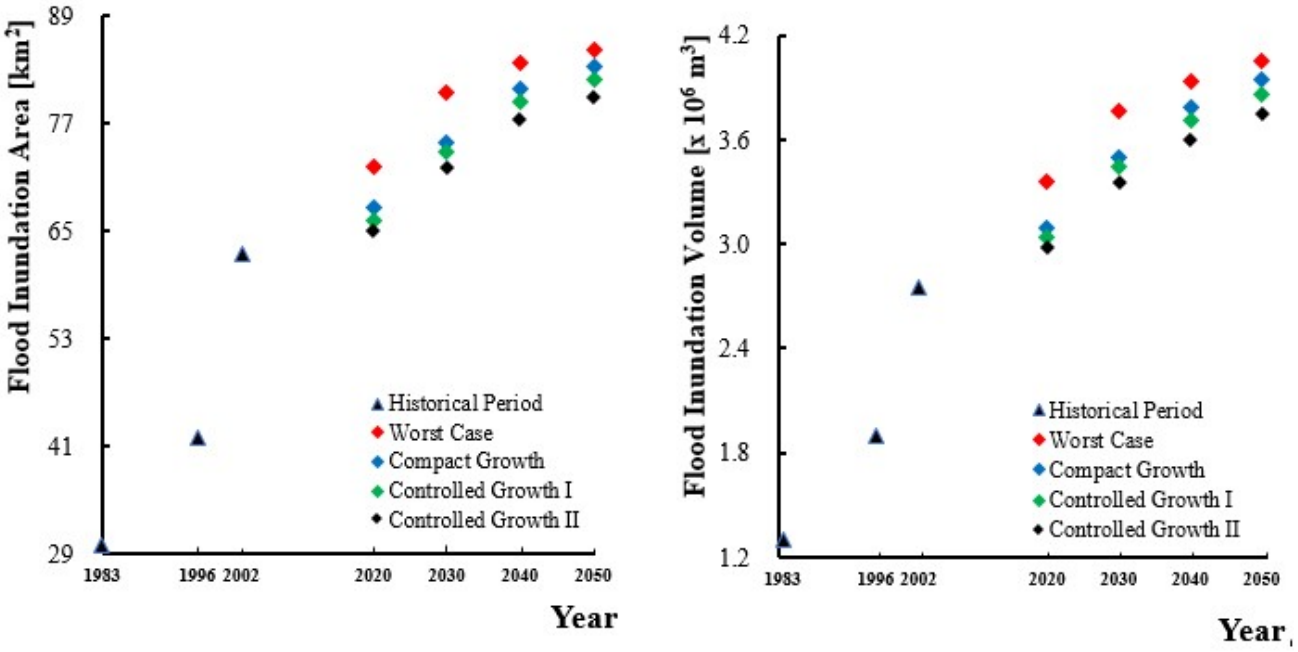

Fig. 4.7 Time series of the simulated flood inundation areas and volumes of each scenario in the historical and future periods

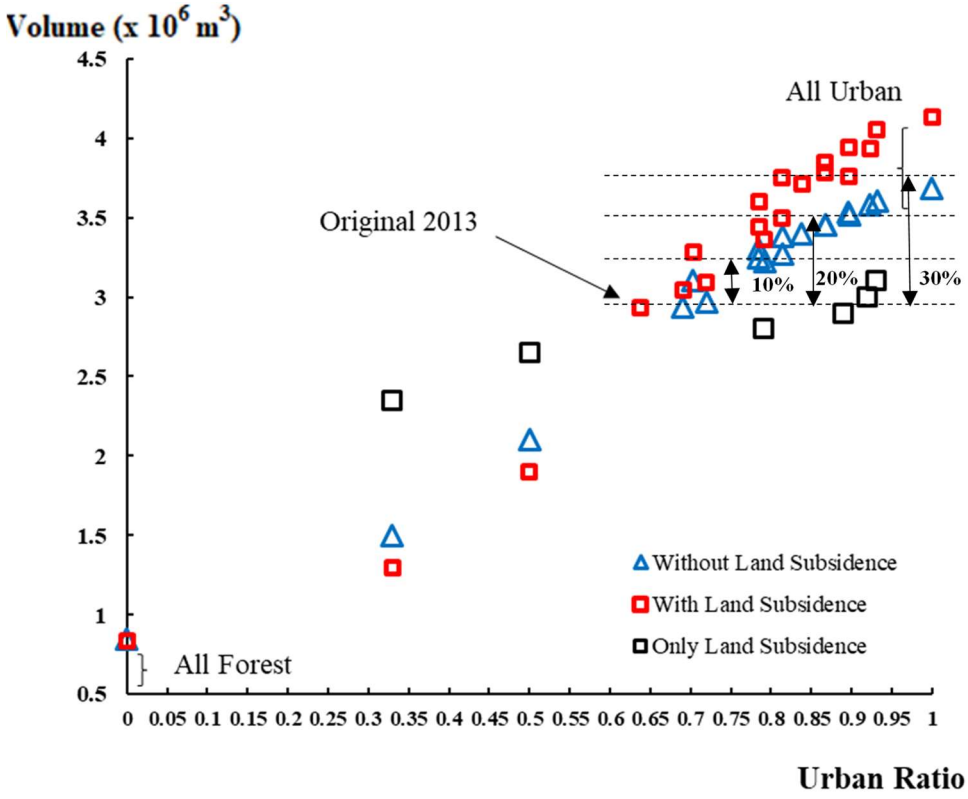

Fig. 4.8 Relationship between total urbanization ratios and flood inundation volumes with, without land subsidence and only land subsidence

4.3. Discussion

Since becoming more frequent in recent years, flooding in Jakarta has been investigated by several studies. Moe et al (2017) reported that the extent of flood inundation in Jakarta was much more sensitive to land-use changes than to other factors. However, they considered only urban areas in a future scenario with the worst-possible socio-economic conditions, namely the RCP8.5-SSP3 scenario. They suggested that further investigations to evaluate other future land-use scenarios, and stated this would be the subject of their next study. Accordingly, in this study, I analyzed the compact-growth scenario as in the RCP2.6-SSP1 scenario together with other controlled-growth scenarios (controlled-growth I and II). The simulated flood inundation volume under the several scenarios in this study are summarized in **Table 4.1**.

Table 4.1 Percentages of the flood inundation volume increase compared to the original 2013 flood.
(LU: only land-use change, LS: only land subsidence, and LU+LS: land-use change with land subsidence)

Year	LS	Worst Case		Compact Growth		Controlled Growth I		Controlled Growth II	
		LU	LU+LS	LU	LU+LS	LU	LU+LS	LU	LU+LS
2020	1	7	12	-1	1	-2	1	-4	-1
2030	2	18	25	9	17	9	15	6	12
2040	5	20	31	15	26	13	24	10	20
2050	7	20	35	18	31	15	29	13	25

It should be emphasized that, even the controlled-growth-II scenario, which delayed urban development in the upper region of Jakarta, resulted in significantly increased flood inundation because of the additional impacts from land subsidence. Hence, land use in the upper region and land subsidence in the lower region of Jakarta should be urgently controlled or regulated. **Figure 4.8** implies that the urbanization ratio in the target areas should be maintained at below 0.7 (70% of the target area is urbanized) and 0.8 in the future to restrict the increase in flood inundation volumes to within 10% and 20% of present levels (2013), respectively. The urbanization ratio is currently 0.63, implying that there is little or no more space available for urbanization in upstream regions, and an urgent need to regulate changes in land-use/cover.

4.4. CONCLUSIONS

In this chapter, I examined four possible scenarios for future changes in land use and used a flood inundation model to evaluate their impact. The results indicate that by 2050 changes in land use with land subsidence would cause flood inundation volumes to increase by 35% and 25%, respectively, relative to those of 2013, in the worst-case and controlled-growth-II scenarios. Of the scenarios modeled, the worst-case scenario had the greatest impact on flood inundation. However, flooding increased significantly even in the controlled-growth-II scenario. In addition, the effects of changes in land use on the extent of flood inundation in Jakarta were increased by land subsidence even

under the delayed urban development's scenarios.

Based on these results, I strongly recommend that the Jakarta government specify regulations for changes in land use in the forested upper regions and land subsidence in the lower regions as soon as possible to reduce future flood damage in the city.

However, in this chapter, climate change impact was not considered for the future projections. Next chapter will focus on the climate change and heat island effects associated with the urban development.

4.5. References

Abidin, H.Z., Fukuda, Y., Pohan, Y.E., Deguchi, T.(2011). Land subsidence of Jakarta (Indonesia) and its relation with urban development. Natural Hazards. 59. 1753-1771.

Dietzel, C., Clarke, K.C., (2006). The effect of disaggregating land use categories in cellular automata during model calibration and forecasting. Computers, Environment and Urban Systems. 30. 78–101. https://doi: 10.1016/j.compenvurbsys.2005.04.001.

JAXA, (2016, May 11). ALOS WORLD 3d – 30 m. http://www.eorc.jaxa.jp/ALOS/en/aw3d30/index.html

Moe, I.R., Kure, S., Farid, M., Udo, K., Kazama, S., and Koshimura, S. (2015). Evaluation of Flood Inundation in Jakarta Using Flood Inundation Model Calibrated by Radar Rainfall. Journal of Japan Society of Civil Engineers, Ser. B1 (Hydraulic Engineering). 72. 4. 1243-1248.

Moe, I.R., Kure, S., Januriyadi, N.F., Farid, M., Udo, K., Kazama, S., Koshimura, S. (2016). Effect of land subsidence on flood inundation in Jakarta, Indonesia. Journal of Japan Society of Civil Engineers, Ser. G (Environment). 72. 283-289.

Moe, I.R., Kure, S., Farid, M., Udo, K., Kazama, S., Koshimura, S. Evaluation of flood inundation in Jakarta using flood inundation model calibrated by radar rainfall. Journal of Japan Society of Civil Engineers, B1 (Hydraulic Engineering). 72(4). I_1243–I_1248.

Moe, I.R., Kure, S., Januriyadi, N.F., Farid, M., Udo, K., Kazama, S., Koshimura, S.(2017). Future projection of flood inundation considering land use change and land subsidence in Jakarta, Indonesia. Hydrological Res Lett. 11(2). 99–10.

Murakami, S., Yasuhara, K., and Mochizuki, N. (2003). An observational prediction of land subsidence applied for GIS. Journal of Japanese Association of Groundwater Hydrology .45(3). 391-407.

Varquez, C.G.A., Darmanto, N., Kawano, N., Takakuwa, S., Kanda, M., Xin, Z.. (2017). “Representative urban growing scenarios for future climate models”. Journal of Japan Society of Civil Engineers, Ser. B1 (Hydraulic Engineering). 73.

Yasuhara, K., Murakami, S., Mimura, N. (2015). Inundation Caused by Sea-Level Rise Combined with Land Subsidence. Geotechnical Engineering Journal of the SEAGS & AGSSEA. 46(4).

Chapter 5

Effects of Urban Climate Change

This chapter is based on the following paper:

Priyambodho A.B., S. Kure, N.F. Januriyadi, M. Farid, A.C.Varquez, M. Kanda and S. Kazama (2022) “Effects of Urban Development on Regional Climate Change and Flood Inundation in Jakarta, Indonesia” Journal of Disaster Research, Accepted.

Several previous studies had conducted climate change impact analyses in Jakarta, considering future climate and land use changes, land subsidence, and sea level rise. However, effects of urban development on the atmospheric environments of cities had not been taken into account in many previous climate change research conducted in Jakarta or in urban cities across the world. Local urbanization is expected to affect the atmospheric environments of mega cities owing to the changing urban thermal environments, such as the heat island phenomena. In general, local urbanization was considered only for land use changes in runoff and flood inundation simulations. Darmanto et al. (2019) coupled global climate change with distributed urbanization scenarios, based on projections of future urban morphology and anthropogenic heat emissions, in a mesoscale weather model. They projected future air temperature and rainfall in Jakarta, considering both climate change and local urbanization. The effects of future changes on flood inundation, as a result of climate change and local urbanization in cities, would need detailed investigations. In this study, I aimed to quantify the effects of both land use and climate change on future rainfall and flood inundation in Jakarta based on future urban growth and climate change scenarios.

5.1. Methodology

Fig. 5.1 shows the schematic representation of the research method used in this chapter. Details are explained in below.

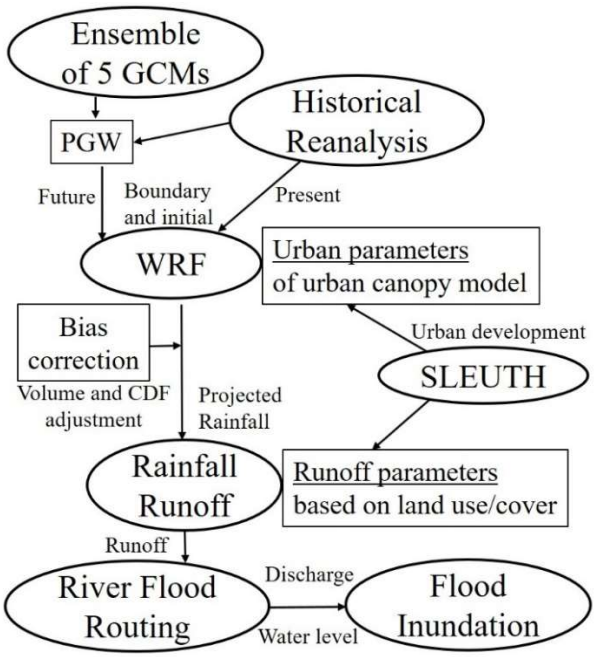

Fig.5.1. Schematic representation of the method of the chapter 5

5.1.1 Future projected rainfall

Darmanto et al (2019) had simulated the present and future urban climate in Jakarta based on high-resolution 1-km

regional climate modeling. The high-rainfall seasons in the present (2006–2015) and future (2046–2055) climate were simulated using the Weather Research and Forecasting (WRF) model coupled with a modified version of the single-layer urban canopy model to represent important urban morphological parameters. In this single-layer urban canopy model, the estimations of the bulk transfer coefficients for each building facet have been revised based on the Simple Urban Energy Model for Mesoscale Simulation (SUMM). Also, the actual urban fractions were considered rather than the constant values used in the default WRF model. Further descriptions of the modified WRF can be found from the references (Darmanto et al., 2019).

For future conditions, four scenarios were used, so that the month of January, in the last 10 years of the historical period and next 40 years (10 years x 4 scenarios), could be simulated in the WRF runs. For the present simulation, the historical reanalysis data of NCEP-FNL was used for the boundary and initial conditions of the WRF simulation.

The future global climate scenario was downscaled using a pseudo global warming (PGW) method with ensembles of five CMIP5 global climate models (GCMs) namely HadGEM2-ES, IPSL-CM5A-LR, MIROC-ESM-CHEM, NorESM1-M, and GFDL-ESM2M as inputs for RCP2.6 and RCP8.5. The PGW is a non-direct downscaling delta approach used to realize a finer resolution and effective performance of future climate projections using a mesoscale regional climate model (Kimura and Kitoh, 2007). It has been used and validated in several studies. Using this approach, we considered the 10-year average of future climate values of each GCM in January during the period 2046–2055. The values necessary for the PGW method include three-dimensional wind components (3- and 6-hourly), temperature components (3-hourly, 6-hourly, daily, and monthly), pressure components (6-hourly), and humidity components (3-hourly, 6-hourly, and monthly). Ensemble averaging was done for each meteorological component value from 2046-2055. The ensemble averages were subtracted from the ensemble averages of 2006-2015. The difference of the ensembles was added to the meteorological boundaries of the historical NCEP-FNL to be used as the meteorological boundary for 2046-2055. Specific details of the PGW method can be found in Kimura and Kitoh (2007).

RCP2.6 and RCP8.5 were selected considering the best and worst emission scenarios, respectively. Urban parameters were projected based on socio demographic parameters from SSP1 and SSP3. SSP1 represents low challenges for mitigation (resource efficiency) and adaptation (rapid development). In the contrary, SSP3 represents high challenges for mitigation (regionalized energy / land policies) and adaptation (slow development). The two urban expansion scenarios based on the SLEUTH model, namely compact and business-as-usual (BaU) adaptation strategies, where the compact scenario was derived from SSP1 and the BaU scenario was derived from SSP3 (**Fig. 5.2**).

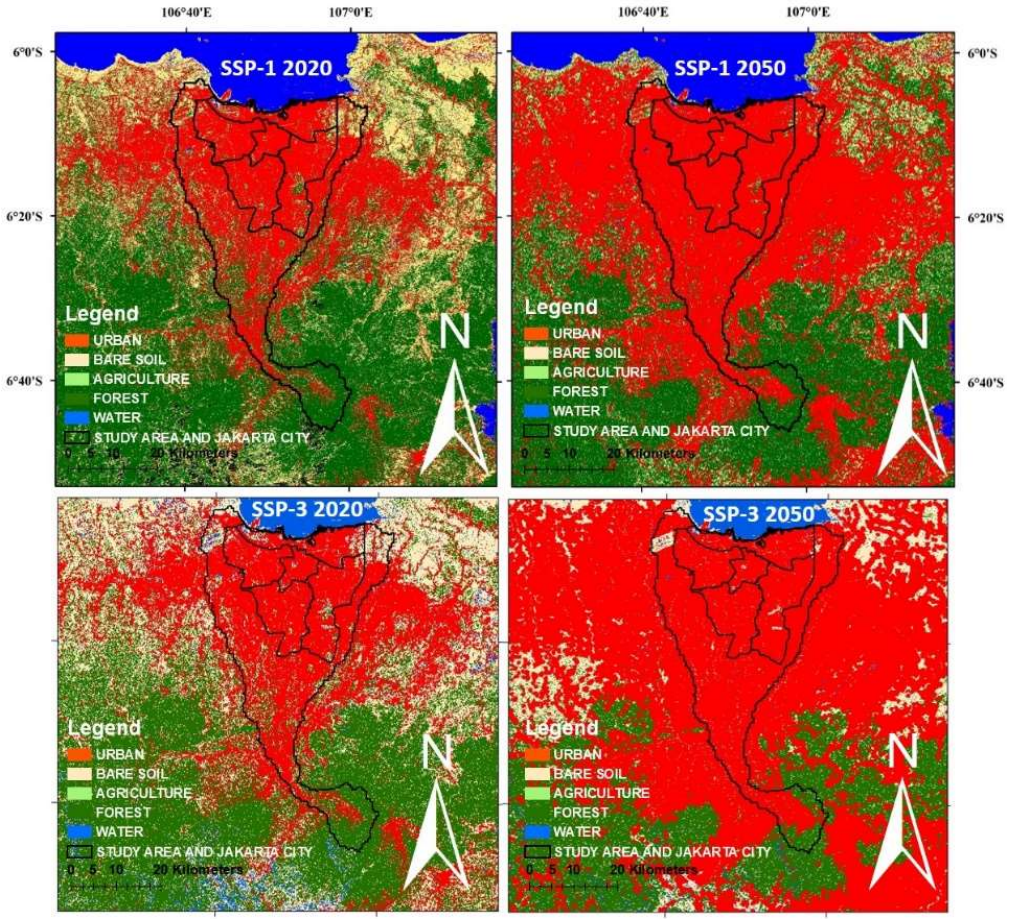

Fig. 5.2 Land use/cover in 2020 and 2050(SSP1 and SSP3)

The urban ratios of SSP1 and SSP3 in 2050 were 0.89 and 0.93, respectively. The urbanized speed in the study area was high, therefore, there were no significant differences in the study area between SSP1 and SSP3 could be confirmed (Priyambodho et al, 2018). The global and urbanization scenarios were then coupled in the WRF simulation runs. In addition, RCP2.6 and RCP8.5, without urban development, were simulated. Finally, rainfall data were projected to future periods based on the four scenarios (RCP2.6, RCP8.5, RCP2.6-SSP1, and RCP8.5-SSP3) and the historical period (Januriyadi et al, 2018). **Table 5.1** summarizes the experimental cases used in this study.

Table. 5.1. Experiment cases

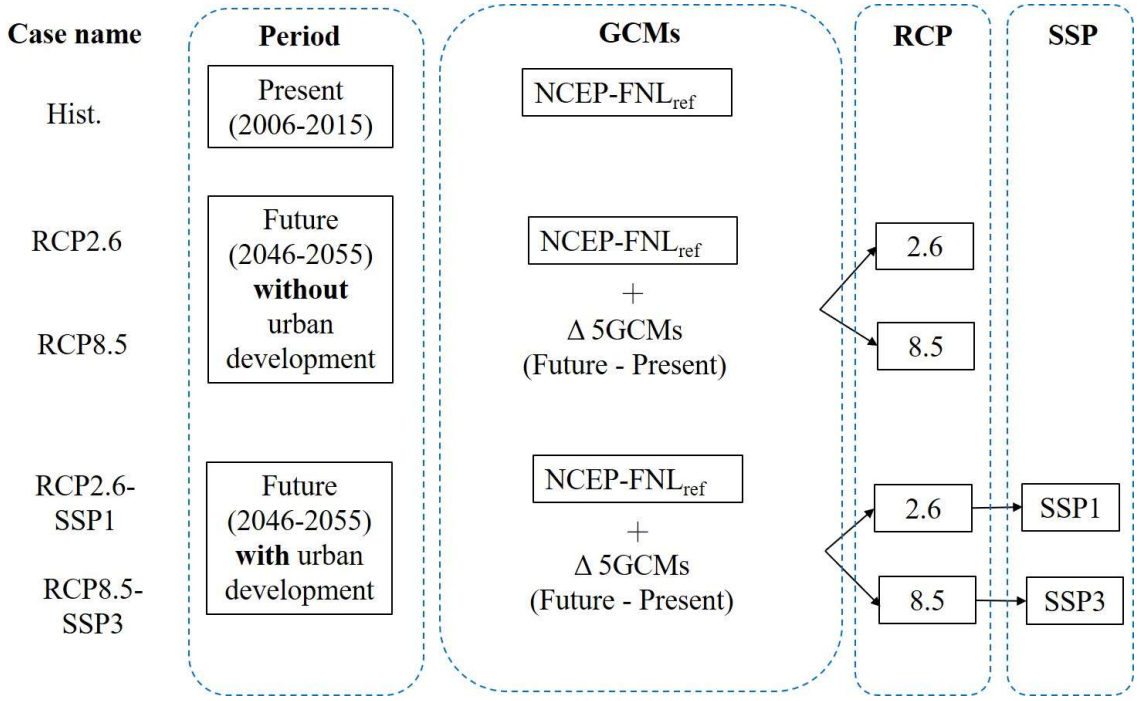

A bias correction was conducted for the projected rainfall to obtain a realistic magnitude of the rainfall in the basin and flood discharge in the rivers because the rainfall data of the downscaled NCEP-FNL by the WRF simulation have a bias in volume and frequency compared to the observed data. It is noted that the NCEP-FNL is the historical reanalysis data simulated considering the historical atmospheric observations but rainfall values have the biases at the local basin scale. Firstly, the monthly rainfall volume in the historical and future periods were adjusted based on the values based on the observation rainfall data in 30 years used in the previous study (Januriyadi et al., 2018). The volume adjustment was conducted as there was an over estimation of the simulated monthly rainfall volume compared with the observed rainfall, which might be because of the accuracy of the NCEP-FNL reanalysis data at the basin scale in Jakarta and short span of the simulation period taken for the analysis (10 years). It is noted that the previous study's bias information were used in this study because the bias information was obtained from much longer simulation periods (30 years). Secondly, the empirical cumulative distribution function (CDF) for the downscaled historical GCMs and hourly observed rainfall data of 10 years (2006-2015) were calculated, and the projected rainfall bias was corrected using the inverse of the CDF of GCMs with observation distribution parameters to adjust the frequency of the high-intensity rainfall. These adjustments were extended to future projected rainfall data. This bias correction was based on the CDF analysis for the rainfall intensity distribution to adjust the frequency and magnitude of the extreme rainfall events in the historical period. However, it was noted that further analysis and bias correction based on the longer simulation periods of WRF simulations were required because 10-year simulation periods are too short to compute the long term climate situations.

After this bias correction, the projected rainfall data were used as inputs for the rainfall-runoff and flood inundation model to project future flood inundation situations.

5.1.2 Future land use and cover change

This chapter also used land use/cover maps for 2050, based on the RCP8.5-SSP3 and RCP2.6-SSP1 scenarios for rainfall-runoff and flood inundation simulations, the same as used in the chapter 4. **Figure 5.2** shows the land use/cover maps for the present and 2050 (RCP2.6-SSP1 and RCP8.5-SSP3). It is noted that the land subsidence in Jakarta, which affected inland and coastal flooding, was not considered in this study.

5.2 Comparisons

5.2.1 Rainfall comparisons

Fig. 5.3 and 5.4 show the comparison of the relative frequency and changes in the exceedance probability of hourly and daily rainfall in the target area and over the studied time periods. The projected rainfall was spatially and temporally averaged over the target area in January over 10 years in both historical and future periods. Generally, high rainfall was projected toward the high RCP and SSP future scenarios. The RCP8.5-SSP3 scenario was found to show the highest rainfall intensity among all. RCP2.6-SSP1 and RCP8.5-SSP3 show higher rainfall values with high probabilities more than those of only RCPs. **Fig. 5.5** shows the monthly rainfall in both historical and future periods under each scenario. In this figure, the error bars for each scenario show 95% confidence intervals. The monthly rainfall was clearly found to increase toward the high RCP and SSP scenarios.

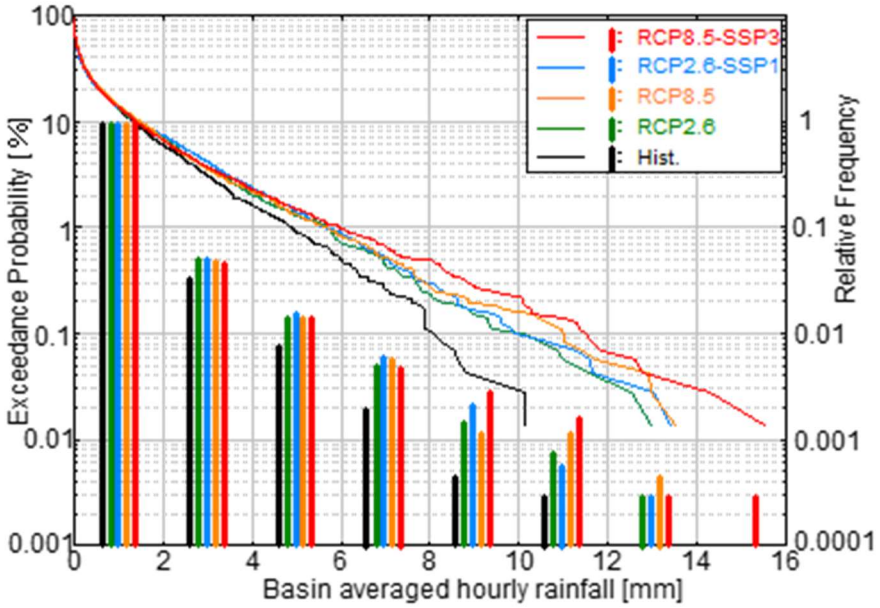

Fig. 5.3. Comparison of the relative frequencies of hourly rainfall in each scenario

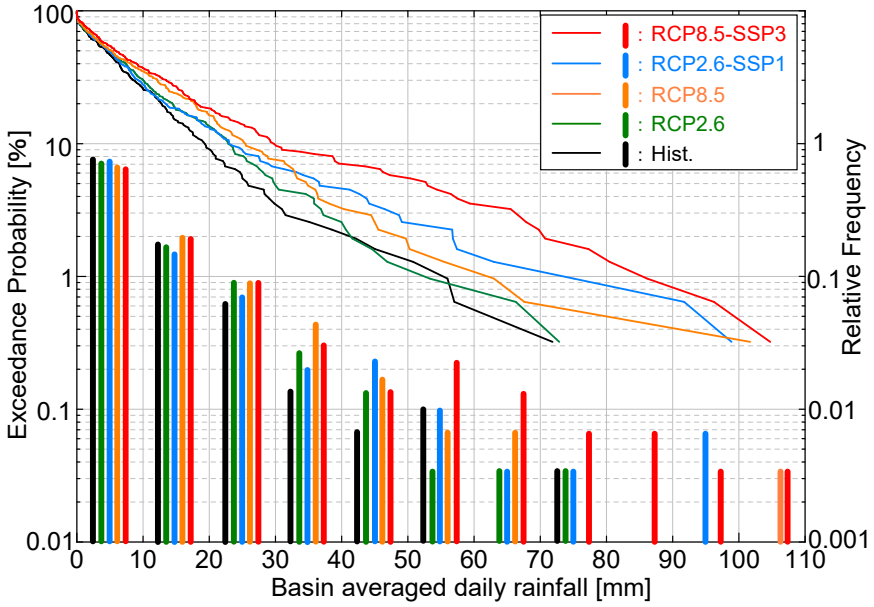

Fig. 5.4 Comparison of the relative frequencies of daily rainfall in each scenario

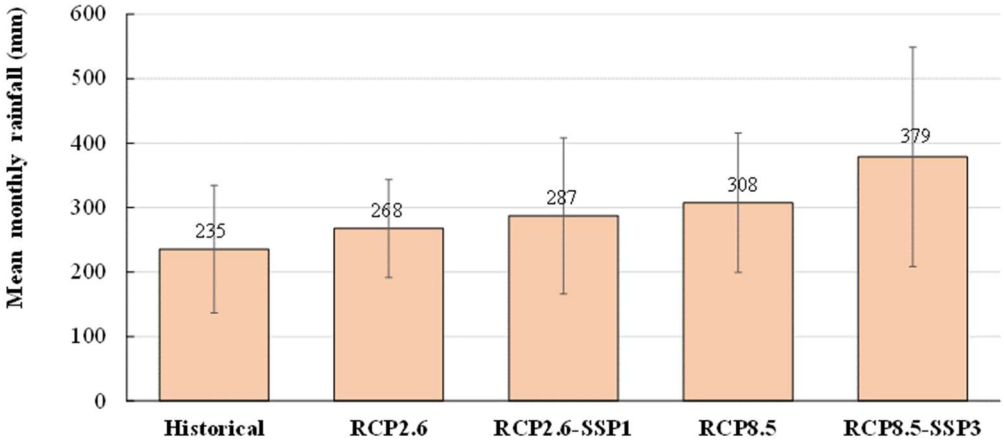

Fig. 5.5 Comparison of the average monthly rainfall in each scenario

The average monthly rainfall of RCP2.6-SSP1 was approximately 7% more than that of RCP2.6, whereas the average value of RCP8.5-SSP3 was approximately 23% more than that of RCP8.5. As such, the increase of the rainfall in RCP8.5-SSP3 is significant compared with those in RCP2.6-SSP1.

5.2.2 Flood peak discharge comparisons

Fig. 5.6 shows the comparisons of the hourly simulated peak river discharge at the three stations of Ciliwung River during both the historical and future periods under each scenario. As seen from the figure, peak discharge generally increased toward the high RCP and SSP scenarios in the future due to the high rainfall and land use change. Significantly, the RCP2.6-SSP1 showed higher peak discharge values than RCP8.5, owing to the combination of land use change and increased rainfall.

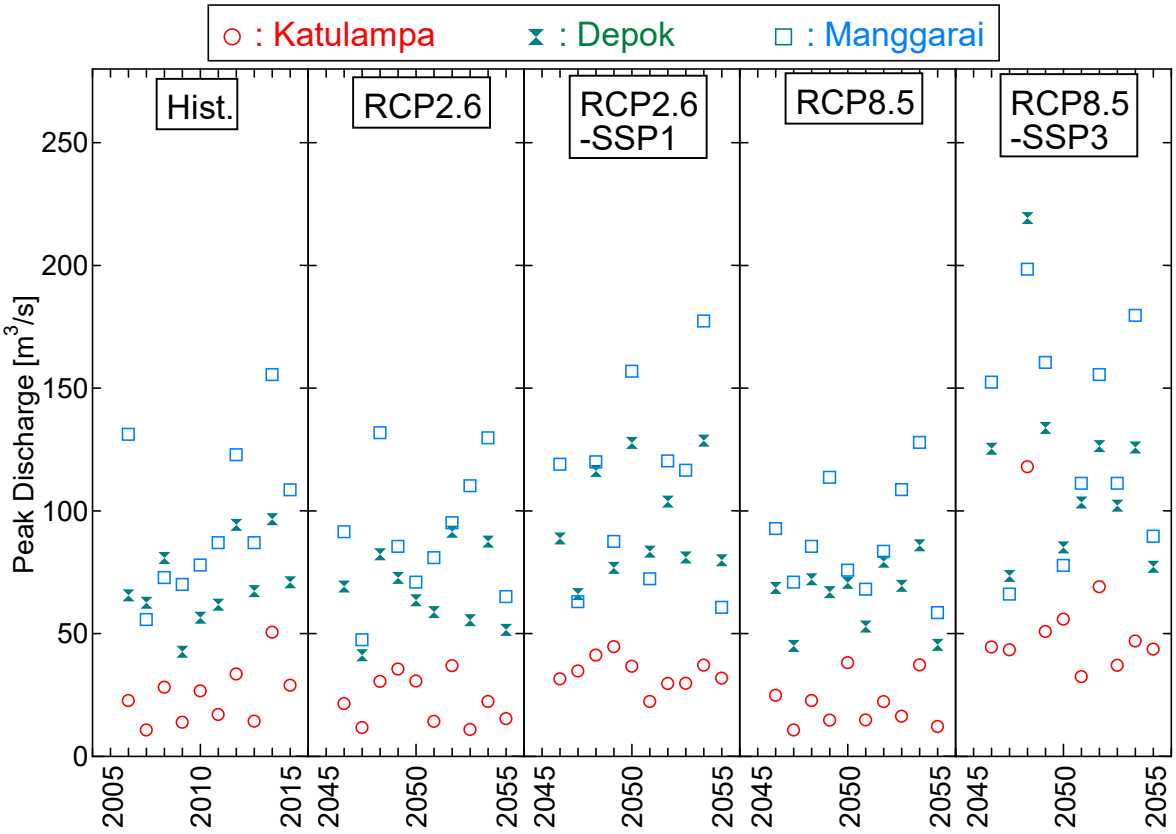

Fig. 5.6 Comparison of the relative frequencies of daily rainfall in each scenario

5.2.3 Flood inundation comparisons

Fig.5.7 shows a comparison of the average maximum flood inundation depths and the computed values of the flooded volumes. The simulated maximum flood inundation depths were averaged for each grid in the 10-year events. Additionally, the difference between with and without SSPs are shown in the figure. A high maximum flood inundation depth was computed in the RCP8.5-SSP3. However, in a simulated event from RCP2.6-SSP1, a large inundation in the west side of Jakarta was computed as shown in **Fig.5.7**. Hence, spatial distribution of rainfall is also important to analyze but only this case shows the high rainfall in West Jakarta. Moreover the ensemble numbers of the simulations may have to be increased to analyze the spatial distribution patterns of rainfall. The largest flood inundation was simulated under the RCP8.5-SSP3 scenario, the second largest flood inundation was simulated under the RCP2.6-SSP1 scenario, and not in RCP8.5 because urban development had not been considered in the RCP8.5-only scenario.

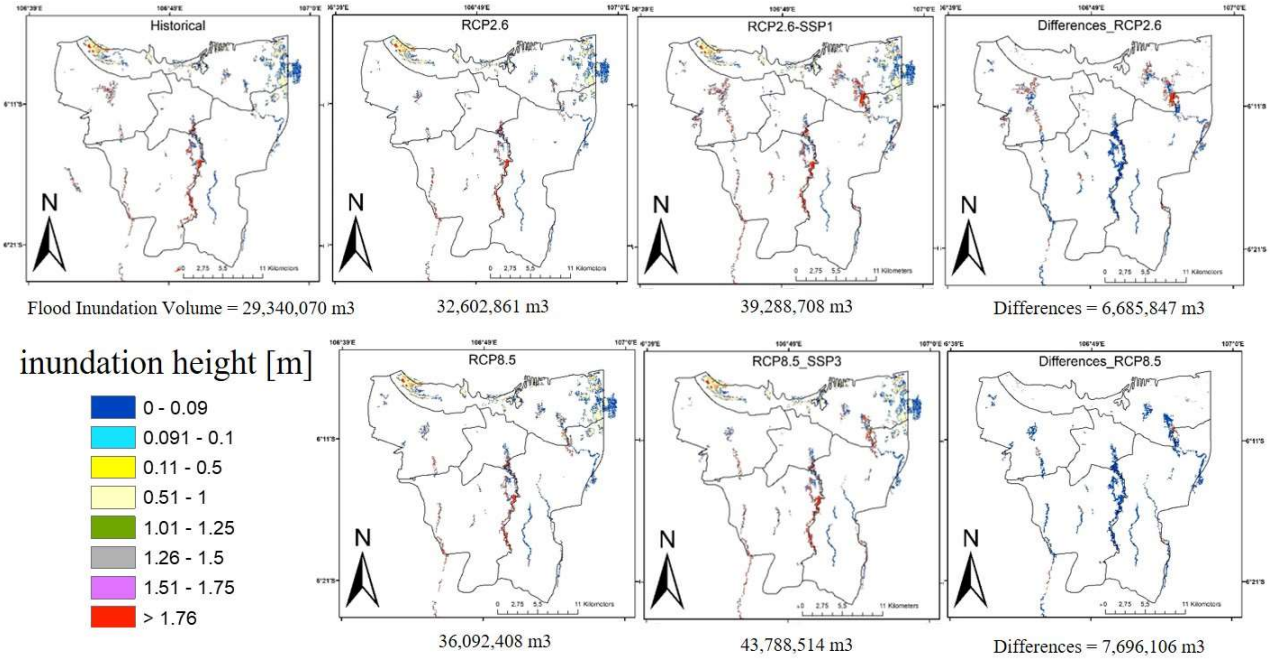

Fig. 5.7. Comparison of the simulated averaged maximum flood inundation depths in each scenario and the differences of w/wo SSPs

Fig. 5.8 summarizes the monthly rainfall, runoff, and flood inundation volumes in both historical and future periods under each scenario. The largest flood inundation was simulated under the RCP8.5-SSP3 scenario, and the second largest flood inundation was simulated under the RCP2.6-SSP1 scenario, not RCP8.5, owing to the urban development that had not been considered in RCP8.5-only scenario. These simulation results clearly indicated that the urban development scenario should be considered in the climate change assessment of cities, not only for atmospheric conditions, but also for flood inundation situations. I concluded that the combined effects of urban development on the atmosphere and flooding should be considered in climate change analysis of cities.

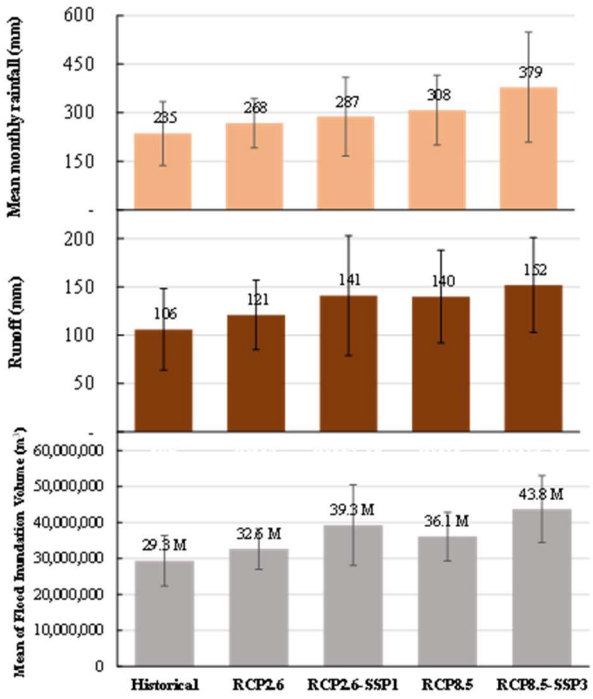

Fig. 5.8. Comparison of average monthly rainfall with the simulated runoff and flood inundations in each scenario

5.3. Discussion

In this study, the effects of urban development on the atmosphere and flood inundation have been discussed. Jakarta and its surroundings are highly urbanized areas, and convectional rainfall typically occurs in the urban areas of humid tropical regions. Additionally, the heat island phenomenon has been progressing significantly in Jakarta; moreover, urban thermal influence on the background environment of convectional rainfall also prevails in the region (Sugawara et al, 2018). This kind of heat island effect had not been considered in many previously conducted climate change studies because of the difficulties in modeling the urban heat environments in course grid simulations. In this study, urban development was considered for both rainfall and flood projections.

From the comparisons between with and without SSPs (**Fig. 5.3 and 5.4**), it is evident that the extreme rainfall events of the hourly and daily time scale were enhanced due to urbanization. These urbanization and heat island impacts on rainfall were reported from several previous studies (Yu et al, 2020; Singh et al, 2020). Urban land use changes also lead to high river flood discharge in the urbanized area. The peak river flood discharge and inundation volume in RCP2.6-SSP1 were larger than those in RCP8.5 (**Fig. 5.6**, **5.7**, and **5.8**). The chapter 4 analyzed the land use change impact on flood inundation without considering climate change and reported that the flood inundation volume increased about 18% (SSP1) and 20% (SSP3) in 2050. We can simply compute these increase as 5.2 Mm^3 (SSP1) and 5.8 Mm^3 (SSP3) increase in the flood inundation volume because the current inundation volume is 29.3 Mm^3 as computed in this chapter. Also, in the current chapter, much higher increases were computed while comparing RCP2.6-SSP1, RCP2.6 (6.7 Mm^3), and Historical (10 Mm^3); these increases were also observed while

comparing RCP8.5-SSP3, RCP8.5 (7.7 Mm^3), and Historical (14.5 Mm^3) as specified in **Figure 5.8**. It can be inferred from the results herein and in the chapter 4 that the urbanization impacts on atmospheric rainfall contributed to the flood inundation volume of 1.5 Mm^3 in RCP2.6 and 1.9 Mm^3 in RCP8.5; we assumed that if land use change could increase the flood inundation volume by 18% and 20% as reported in the chapter 4, then a similar increase was applicable in this study. These increases amount to approximately 5–7% of the current flood inundation volume; hence we speculate that the urban development effects on the increases in rainfall will contribute to an increase of the flood inundation volume by approximately 5–7% in a target area. Based on these results, urban development was found to affect the rainfall increase because of changes in the urban thermal environment and flood inundation associated with land use and rainfall changes in the future.

However, in this study, simulations for only a 10-year period was performed within a scenario owing to the requirements of extremely heavy computations for high-resolution urban atmospheric simulations. Thus, the relatively large flood inundation result in the west side of Jakarta was only simulated in the RCP2.6-SSP1. However, only 10 events are insufficient to discuss the spatial distribution patterns of rainfall. Moreover, because of the less number of ensemble members of the future projections, we could not analyze the statistical significance of future changes caused by urban development. For future studies, the simulation period has to be increased to evaluate the uncertainty of impacts of future climate and urban development in Jakarta. Furthermore, the statistical significance, more physical patterns such as the spatial distribution of the rainfall have to be assessed; in addition, a more realistic bias correction that may be applicable under future land use and urban environment situations should be evaluated.

5.4. Conclusions

In this study, future flood inundation situations were projected considering both climate change and effects of urban development. The future projected rainfall data of RCP2.6 and RCP8.5, without urban development, and RCP2.6-SSP1 and RCP8.5-SSP3, based on the WRF simulation, were used as inputs for the rainfall-runoff and flood inundation simulations in Jakarta. Future land use change was also considered in the rainfall-runoff simulations based on the SLEUTH model outputs in Jakarta and surrounding areas in 2050. Based on the results of this analysis, urban development was clearly seen to increase not only the rainfall intensity and volume in future but also the runoff from the basin, river flow discharges, and flood inundations in Jakarta, due to the combination of land use change and increased rainfall. It should be emphasized that the urban development effects on the increases in rainfall will contribute to an increase of the flood inundation volume by approximately 5–7% in a target area. I concluded that the effects of urban development on both the atmosphere and runoff processes should be considered in climate change studies in cities.

5.5. References

Priyambodho, B.A., Kure, S., Moe, I.R., and Kazama, S. (2018). Numerical Experiments of Future Land Use Change for Flood Inundation in Jakarta, Indonesia.. *Journal of Japan Society of Civil Engineers, Ser. G (Environment)*. 74(5). I_265-I_271.

Sugawara, H., Oda, R., and Seino, N., (2018). Urban Thermal Influence on the Background Environment of Convective Precipitation. *Journal of the Meteorological Society of Japan*. 96A. 67-76.

Singh, J., Karmakar, S., PaiMazumder, D., Ghosh, S., and Niyogi, D. (2020). Urbanization alters rainfall extremes over the contiguous United States. *Environment. Research. Letters*. 15, 074033.

Kimura and Kitoh. (2007). Projection of Global Warming onto Regional Precipitation over Mongolia Using a Regional Climate Model. *Journal of Hydrology*. 333(1). 144-154. DOI:10.1016/j.jhydrol.2006.07.023.

Yu, M., Liu, Y., Miao, S. (2020). Impact of urbanization on rainfall of different strengths in the Beijing area. *Theoretical and Applied Climatology*. (139. 1097-1110).

Januriyadi, N.F., Kazama, S., Moe, I.R., and Kure, S. (2018). Evaluation of future flood risk in Asian megacities: a case study of Jakarta. *Hydrological Research Letters*. 12(3). 14-22.

Darmanto, N.S., Varquez, A.C.G., Kawano, N., and Kanda, M. (2019). Future urban climate projection in a tropical megacity based on global climate change and local urbanization scenarios. *Urban Climate*, 29. 100482.

Chapter 6

Evaluation of Counter Measures

6.1. Introduction

To address flood hazards, various adaptation measures (i.e., either structural or nonstructural measures) have been utilized. Moe et al. (2015) examined the reduction in the inundation frequency and volume by improving the flow river capacity in Jakarta. They found that a 150% increase in the river capacity could reduce flood inundation by 15%. The construction of embankments or levees represents one option for increasing river capacity (Radhakrishnan, 2018; Dyer, 2004), and these options are sometimes combined with nature-based protection (Wesenbeeck,et al; 2017; Vuik et al, 2016; Stark et al, 2016). In addition, nonstructural measures, such as early warning systems, could alleviate the damage costs caused by floods (Parker et al, 2005; Pilarczyk, 2005).

As explained in the previous chapters, future floods are expected to increase due to the urban development with the climate change. To reduce the magnitude of future floods, this study applies several adaptation measures, either structural or nonstructural. In this chapter, structural measures are first evaluated and compared with the results obtained from previous study (Januriyadi et al., 2020). And then, nonstructural measures will be discussed in the chapter 7.

6.2. Methodology

6.2.1. Counter measures

In this chapter the effects of counter measures on reducing the flood extent and volume in Jakarta are quantitatively evaluated by the flood inundation model. The counter measures discussed in this chapter are to increase the flood flow capacity in the whole river. The scenarios for the counter measures are Case 1: increasing river bank height (1 m) and Case 2: dredging bed level (1 m) with Case 1. The flood inundation simulations were conducted with and without the counter measures and the flood inundation area, flood damage cost and cost benefit analysis (B/C) results are obtained and discussed.

6.2.2. Damage cost estimation

This study used flood damage costs evaluation method based on Januriyadi et al. (2018, 2020). Damage cost estimation was divided into two steps. First, the damage costs were estimated based on return period rainfall events. Second, the expected annual damage costs (EADC) were calculated. The damage cost estimation was based on the land use classification. Januriyadi et al. (2018, 2020) used the damage-depth function of the Ministry of Land, Infrastructure, Transportation, and Tourism in Japan (MLIY, 2015) applied by Kazama et al. (2009) to estimate the flood damage costs throughout all of Japan. Furthermore, the EADC were calculated by integrating the flood damage costs over the overall return periods (Zhou et al, 2012). This model assumes that the flood damage costs correspond to the depth of inundation. Kreibich and Dimitrova (2010) found that the water level of floods has a significant connection to flood damage costs, especially for riverine floods.

Damage costs in agricultural fields were calculated using the inundated area and the depth of inundation as the main components while considering the price of the rice or crop and the production rate.

$$DC_{Agr} = \sum_{depth=1}^{5} prd \text{ x } Price \text{ x } A_{depth} \text{ x } DR_{Agr} \quad (6\text{-}1)$$

where DC_{Agr} is the damage costs for agriculture (USD), *prd* is the average of the crop or rice production (ton/km^2), *Price* is the average price of the crop or rice (USD/ton), A_{depth} is the inundated area for different depth classifications (km^2), and DR_{Agr} is the damage rate value for the agriculture sector based on the water depth.

In the housing sector, the calculation of damage costs includes the building and the house content damage as follows:

$$DC_H = \sum_{depth=1}^{5} A_{depth} \ (BP \text{ x } DR_B + HC \text{ x } DR_{HC}) \quad (6\text{-}2)$$

where DC_H is the flood damage costs for housing (USD) and *BP* is the building price (USD/m^2), which is different depending on the location. DR_B and DR_{HC} are the damage rate values for the building and house contents based on the water depth, respectively.

Similar to the housing sector, the manufacturing and services sectors were also calculated for building and nonbuilding asset damage, as follows:

$$DC_M = \sum_{depth=1}^{5} A_{depth} \ (BP \, x \, DR_B + Asset_M \, x \, DR_{Asset}) \quad (6\text{-}3)$$

$$DC_S = \sum_{depth=1}^{5} A_{depth} \ (BP \, x \, DR_B + Asset_S \, x \, DR_{Asset}) \quad (6\text{-}4)$$

where DC_M and DC_S are the flood damage costs for the manufacturing and service sectors (USD), respectively. DR_{Asset} is the damage rate value for the no building asset based on the water depth.

The final step is calculating the expected annual damage costs (EADC). The EADC is a strong indicator for a given area showing how vulnerable it is to flood risk and how much can be gained by implementing, e.g. climate change adaptation measures (Olsen et al., 2015). Olsen et al. (2015) compared the methods for estimating the EADC, i.e. statistical, numerical and analytical methods. They found three methods yield very similar results, and the identified shift in costs occurring at the design return period was more important than the method to calculate the EADC. Furthermore, this study used the numerical method for estimating the EADC (Olsen et al., 2015). For the details of the estimation of the damage cost, see the references (Januriyadi et al., 2018; 2020)

6.2.3. Future scenarios

It is noted that the future climate and land use change conditions are different from the chapter 4 and 5 in this study, and the future scenarios used in Januriyadi et al. (2018; 2020) were used in this chapter. The reason of this is to compare the counter measures evaluated by Januriyadi et al., (2018; 2020) and this study under the same conditions. The land use change of RCP8.5-SSP3 (the worst case) and land subsidence on 2050 were used and the 3 RCPs scenarios and 6 GCMs were used for the climate change computations in Januriyadi et al. (2018; 2020).

6.3. Results

The expected annual damage cost (EADC) were divided by near future (2011-2050) and far future (2050-2100). The EADC of original condition and two scenarios of countermeasures were shown in **Figure 6.1**, **6.2** and **6.3**. Also, summary of these results is shown in **Figure 6.4**. It can be seen from these figures that the counter measures work well and contributed to reduce the flood damages in Jakarta. And it was found that the case 2 has more strong impact to reduce the damage. It is obvious that the two combination of the counter measures are more useful. However, these structural measures may be expensive to actually implement in Jakarta due to the high construction fees and so on. So, the cost and benefit analysis (B/C) were conducted in the next sentences.

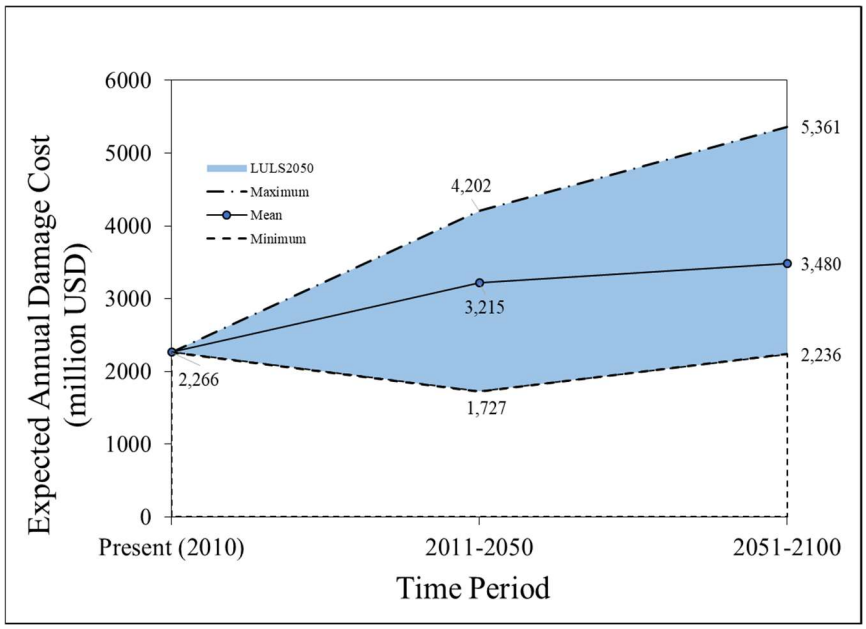

Fig. 6.1. Simulated EADC in the near and far future without a counter measure

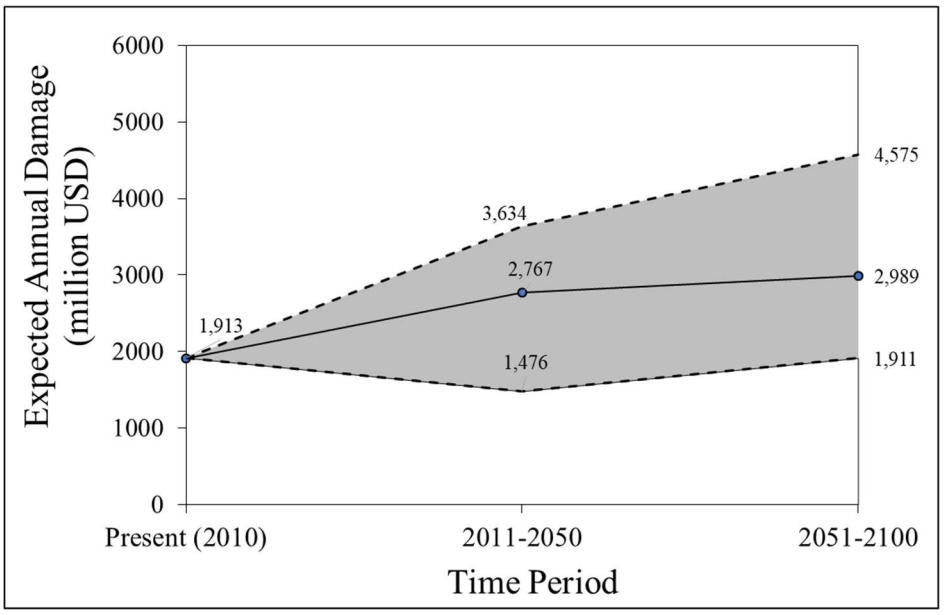

Fig. 6.2. Simulated EADC in the near and far future with Case 1

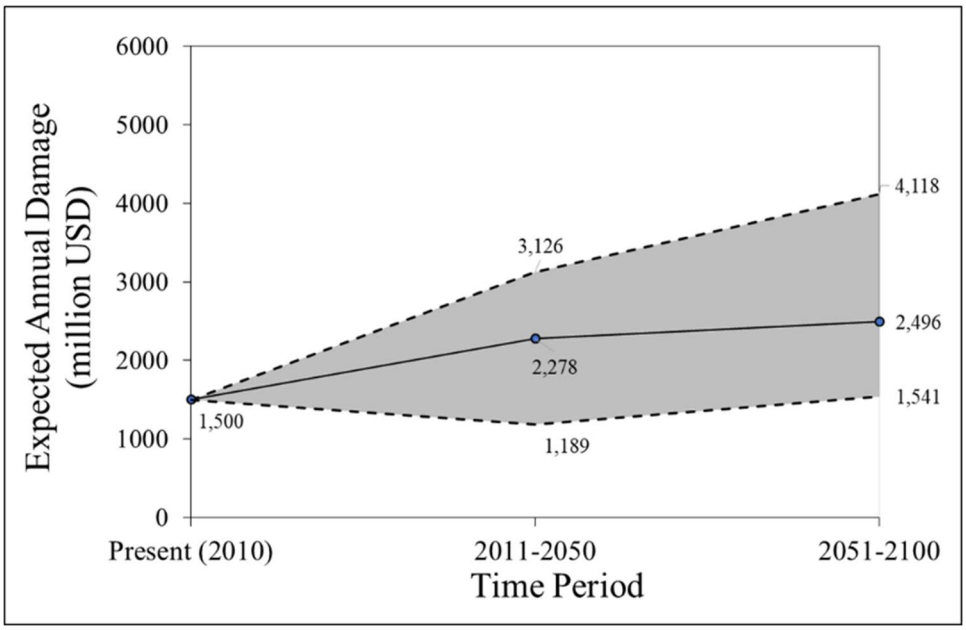

Fig. 6.3. Simulated EADC in the near and far future with Case 2

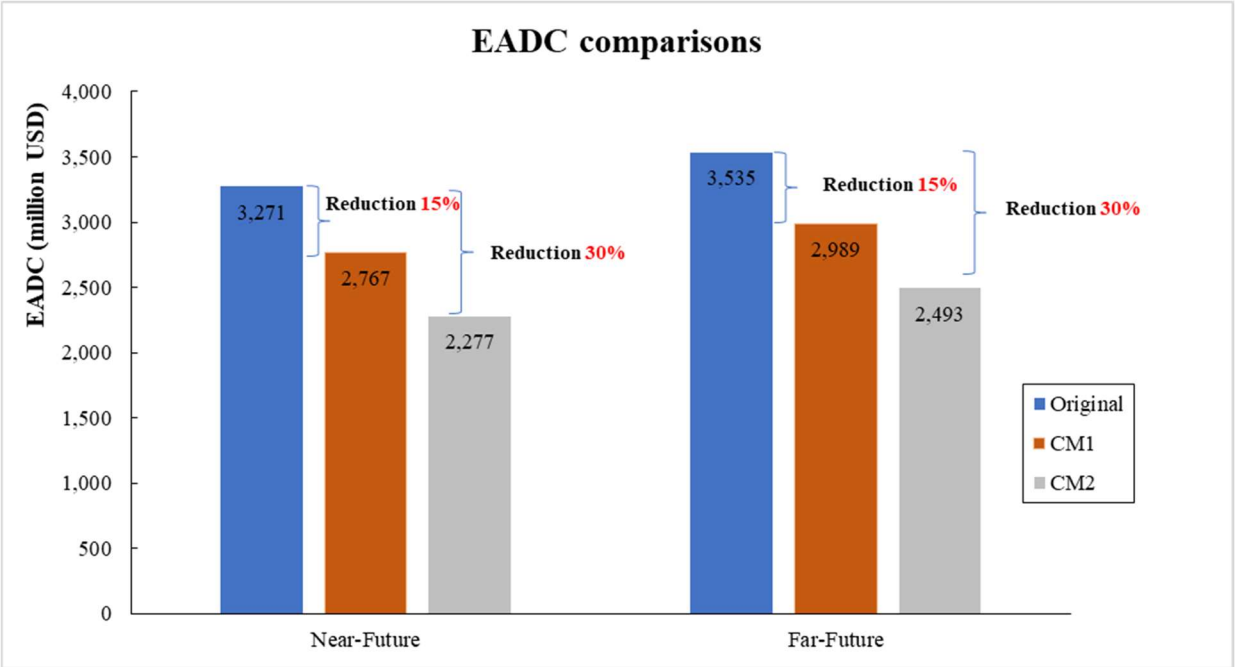

Fig. 6.4. EADC comparisons between original, Case 1 and Case 2

6.4. Cost and benefit analysis (B/C analysis)

The costs of countermeasures were estimated by considering the construction, land acquisition (if any) and other costs related to build up materials for the countermeasures. The cost of construction is difference between one place and another place. In general, Indonesia government and PU were released the standard cost of construction at each region. However, the cost construction in the Indonesia Rupiah, not in US Dollar, so I needed to convert from Indonesia Rupiah (IDR) into the US dollar (USD) to make same unit with the benefit. The benefits are obtained from differences between the EADC with and without the countermeasures.

The benefit of countermeasure Case 1 for near-future is 504 million USD and far-future is 546 million USD. The cost for the Case 1: increasing the bank height 1 meter to whole rivers was computed by using the cost of the NCICD's project within period 2015 – 2020 as a reference. They conducted a similar construction for the river length about 2,200 m and the cost was 418,381,000,000 IDR. This cost was converted to this study, and the total cost of the Case 1 is 11,544,094,858 USD. Also, the results of B/C were computed for near future as 0.044 and far-future as 0.047.

The benefit of countermeasure Case 2 for near-future is 994 million USD and far-future is 1,042 million USD. The cost for dredging bed level 1m of whole rivers was computed by total volume of dredging in the whole rivers and multiply by a dredging cost of each 1 m^3. The cost for 1 m^3 dredging is 250,000 IDR from the reference of PU. Then the total cost of Case 2 was 11,771,731,349 USD. Also, the result of B/C for near future is 0.080 and for far-future is 0.088.

The benefist-cost ratio for far future were computed and compared by the previous results as shown in **Table 6.1**. In here, RPPs represents the recharge and retention ponds, RWs represents the recharge wells, SWP represents the seawall protection and GI represents the green infrastructure. RPPs and RWs show good B/C values. For the details, see the reference (Januriyadi et al., 2020). The benefit-cost ratio for the Case 1 is 0.047 and the case 2 is 0.088 as shown in **Table 6.2**. It can be concluded that the structual counter measures are too much expensive and the B/Cs are too low to implement such same as the SWP and GI. Next chapter, nonstructual conter measure is evaluated in this study.

Table 6.1 Benefit-Cost Ratio (sources: Fajar et al, 2020)

Adaptation measures	Benefit-Cost Ratio (BCR)
RPPs	2.193
RWs	9.076
SWP	0.045
GI	0.004

Table 6.2 Benefit-Cost Ratio of this study

Adaptation measures	Benefit/Cost Ratio (BCR)
CM1	0.047
CM2	0.088

6.5 References

Dyer, M. (2004). Performance of Flood Embankments in England and Wales. Proceedings of the Institution of Civil Engineers. Water Management. 157. 177-186.

Radhakrishnan, M., et al. (2018). Coping Capacities for Improving Adaptation Pathways for Flood Protection in Can Tho, Vietnam. Climatic Change. 149. 29-41.

Januriyadi, N.F., Kazama, S., Moe, I.R., and Kure, S. (2018). Evaluation of future flood risk in Asian megacities: a case study of Jakarta. Hydrological Research Letters. 12(3). 14-22.

Januriyadi, N.F., Kazama, S., Moe, I.R., and Kure, S. (2020). Effectiveness of Structural and Nonstructural Measures on the Magnitude and Uncertainty of Future Flood Risks. Journal of Water Resource and Protection. 12. 401-415.

Kazama, S., Sato, A., Kawagoe, S. (2009). Evaluating the cost of flood damage based on changes in extreme rainfall in Japan. Sustainability Science. 4. 61–69. https://doi: 10.1007/s11625-008- 0064-y.

Kreibich, H. and Dimitrova, B. (2010). Assessment of Damages Caused by Different Flood Types. FRIAR. 3-11. Milan.

Moe, I.R., Kure, S., Farid, M., Udo, K., Kazama, S and Koshimura, S. (2015). Numerical Simulation of Flooding in Jakarta and Evaluation of a Countermeasure to Mitigate Flood Damage. Journal of Japan Society of Civil Engineers, Ser. G (Environment). 71(5). I_29-I_36 .

MLIT. (2005). The Flood Control Economy Investigation Manual (Proposed). Ministry of Land, Infrastructure, Transport and Tourism.

Olsen, A.S., Zhou, Q., Linde, J.J., Arnbjerg-Nielsen, K. (2015). Comparing methods of calculating expected annual damage in urban pluvial flood risk assessments. Water 7. 255–270. https://doi: 10.3390/w7010255

Parker, D., Tunstall, S. and Wilson, T. (2005). Socio-Economic Benefits of Flood Forecasting and Warning. International Conference on Innovation Advances and Implementation of Flood Forecasting Technology. Tromsø. 11.

Pilarczyk, K.W. and Nuoi, N.S. (2005). Experience and Practices on Flood Control in Vietnam. Water International. 30. 114-122.

Stark, J., Plancke, Y., Ides, S., Meire, P. and Temmerman, S. (2016). Coastal Flood Protection by a Combined Nature-Based and Engineering Approach: Modeling the Effects of Marsh Geometry and Surrounding Dikes. Estuarine, Coastal and Shelf Science. 175. 34-45

Van Wesenbeeck, B.K., de Boer, W., Narayan, S.W., van der Star, R.L. and de Vries, M.B. (2017). Coastal and Riverine Ecosystems as Adaptive Flood Defenses under a Changing Climate. Mitigation and Adaptation Strategies for Global Change. 22. 1087-1094.

Vuik, V., Jonkman, S.N., Borsje, B.W. and Suzuki, T. (2016). Nature-Based Flood Protection: The Efficiency of Vegetated Foreshores for Reducing Wave Loads on Coastal Dikes. Coastal Engineering. 116. 42-56.

Zhou, Q., Mikkelsen, P.S., Halsnæs, K. and Arnbjerg-Nielsen, K. (2012). Framework for Economic Pluvial Flood Risk Assessment Considering Climate Change Effects and Adaptation Benefits. Journal of Hydrology. 414-415. 539-549.

Chapter 7

Flood Prediction as a Nonstructural Counter Measure

This chapter is based on the following paper:

Priyambodho A.B., Kure, S., Yagi, S. and Januriyadi, N.F. (2021) “Flood Inundation Simulation Based on GSMaP Satellite Rainfall Data in Jakarta, Indonesia” Progress in Eath and Planetary Science.

7.1. Introduction of GSMAP satellite rainfall data

In these flood-prone situations, several countermeasures have been implemented in Jakarta to mitigate flood damages, such as dredging and diversion tunnels. However, flood risk in Jakarta is still high, and more than 60 people were killed in Jakarta during the most recent flood event that occurred in January 2020 (Berlinger and Yee 2020). Also, as explained in the previous chapter, structural counter measures are too much expensive to implement in Jakarta. Thus, a flood-forecasting system as a nonstructural measure is required in Jakarta to ensure early evacuation and prevent traffic jams during flood disasters.

Nevertheless, the development of a flood-forecasting system in Jakarta is a challenging task because the rapid flooding of rivers and canals will not provide sufficient lead time for a prediction based on the water levels in the upstream regions (Miyamoto et al. 2012). In addition, the shortage of rainfall data, such as radar rainfall and ground gauge data, results in uncertainty and low accuracy in predicting flood hydrographs and inundations based on hydrologic models owing to insufficient rainfall input accuracy, model calibrations, and data assimilation opportunities (Kure et al. 2013).

In this study, I analyzed whether satellite rainfall data can be used as an input for real-time flood forecasting in Jakarta because of the discontinuation of rainfall radars in 2013 owing to high maintenance costs. Various satellite rainfall products can be accessed and downloaded freely, and the data are provided in near real-time worldwide. We used global satellite mapping of precipitation (GSMaP) products as the satellite rainfall data in this study because of their high spatial and temporal resolutions suitable for flood simulations in highly urbanized areas. GSMaP products have been evaluated and verified through comparison with observational data from several previous studies. Based on a verification study of hourly GSMaP rainfall conducted by Setiawati and Miura (2016), GSMaP-MVK data can potentially be used to replace rain gauge data, particularly for lowland areas in the Kyusyu region, Japan, if inconsistencies and errors are resolved. However, without bias correction, significant underestimation or overestimation of heavy rainfall events will be observed. Moreover, the former algorithm of the GSMaP microwave radiometer does not consider topographical effects (Setiawati and Miura 2016). Other researchers have also reported an underestimation via the GSMaP (Fu et al. 2011; Admojo et al. 2018; Pakoksung and Takagi 2016). Fu et al. (2011) evaluated the accuracy of the GSMaP using a gauge station in a basin in China and found that GSMaP products generally underestimated the precipitation amount. Additionally, GSMaP rainfall data are less accurate when used for mountainous regions than flat areas owing to the occurrence of topographical rainfall (Fu et al. 2011). Conversely, Tian et al. (2010) reported that satellite products (e.g., GSMaP) overestimate rainfall in the summer based on the estimations over the contiguous United States.

Hence, GSMaP rainfall products provide less accurate results compared with gauge-based rainfall networks or radar rainfall information systems. Nevertheless, GSMaP rainfall products are often used as inputs for hydrological models in simulating flood events. Admojo et al. (2018) and Pakoksung and Takagi (2016) statistically evaluated satellite rainfall products, including the GSMaP, and applied hydrological simulations to a large river basin in Thailand using satellite data. They showed acceptable model results (high correlation coefficient: 0.85) to simulate the observed discharge in a river basin, but underestimations (NSE = 0.37) of simulated runoff were reported in a previous study (Admojo et al. 2018). To improve the flood simulation results based on satellite data, bias correction

(Sayama et al. 2012) of satellite rain- fall products, and ensemble flood simulation methods (Jiang et al. 2014) have been successfully used for flood simulations in large-scale basins. Sayama et al. (2012) applied a hydrological model with a bias-corrected GSMaP for flood inundation simulation in Pakistan to provide additional information for flood relief operations. The simulated flood inundation area reasonably matched well (the fit index: 0.61, peak discharge ratio: 1.0, and inundated area ratio: 1.0) with the actual area, even though the satellite rainfall products were used as the input for the simulation.

These literature reviews indicate that the accuracy of GSMaP data should be verified for several cities and regions before being used in practice. In several studies, hydrological models were applied with satellite rainfall data to large basins, where the flood travel time is relatively slow (Sayama et al. 2012). However, GSMaP evaluation investigations of highly urbanized cities prone to rapid flooding in rivers and subjected to local convective rainfall owing to urban heat environments or humid tropical climates have not been conducted in detail. Satellite-based rainfall can be used to reconstruct historical flood events. A problem faced by developing countries is the evaluation of historical flood events with insufficient survey and hydrological observation data. Thus, GSMaP data were also evaluated in this study as input rainfall data to simulate the historical flood events in Jakarta, including the most recent large-flood event that occurred in January 2020.

7.2. Method

7.2.1. Satellite rainfall products

The GSMaP project was implemented in 2002 to develop retrieval algorithms for rainfall rates and to produce high-resolution global precipitation maps based on satellite data (Ushio et al. 2009; Aonashi and Liu 2000). GSMaP products are distributed by the Japan Aerospace Exploration Agency (JAXA) Global Rainfall Watch. GSMaP Now, GSMaP NRT, and GSMaP MVK are provided by JAXA. GSMaP Now only allows the extrapolation of rain- fall maps every 30 min; therefore, the accuracy of the data may be relatively low. Moreover, it only provides data for 2017, 2018, and 2019. GSMaP MVK is a reanalysis version of GSMaP NRT and has a resolution of 0.1°/h with a domain coverage from 60° N to 60° S. It was available from March 2000 until December 2010. GSMaP NRT uses the same algorithm as GSMaP MVK, and it has been available since October 2008. GSMaP NRT is released every hour (4 h latency), and a Kalman filter algorithm is applied to the data (Ushio et al. 2009). GSMaP Gauge V7 is a calibrated version based on the ground gauge data and yields high accuracy. Its data have been available since March 2014.

In this study, I evaluated the data using GSMaP NRT and GSMaP Gauge V7. GSMaP NRT can be used as the input for a real-time flood-forecasting system, and the GSMaP Gauge can be used for reconstructing past flood events. The simulated data were compared with ground observation data.

7.2.2. Ground observation rainfall data

Hourly rainfall data were obtained for the target area from Badan Meteorologi, Klimatologi dan Geofisika (Indonesian Agency for Meteorology, Climatology, and Geophysics). We evaluated the uncertainties in the hourly

satellite rainfall data from the Citeko, Darmaga, Pondok Betung, Kemayoran, and Tanjung Priok stations. The locations of the stations are shown in **Figure 1.1**. **Table 7.1** shows the total rainfall values at the stations during flood events. Then, the satellite product rainfall data for January and February of 2015–2020 were obtained from both GSMaP NRT and GSMaP Gauge data.

Table 7.1. Summary of historical flood event

Year	Averaged rainfall (mm)	Maximum water level (cm) at Manggarai	Flood area (km^2)	Death person	Main damage	Damage Cost (IDR)
1996	421	970	-	10	529 houses were highly damaged	6.4 Trillion
2002	464	1050	160	32	Electrical System Shutdown	9.9 Trillion
2007	340	1060	397	80	Electrical System Shutdown	8.8 Trillion
2013	168	1020	132	41	Embankment failure	1.5 Trillion
2014	581	830	201	26	134,662 persons were affected	5 Trillion
2015	310	890	196	5	Electrical System Shutdown	1.5 Trillion
2016	275	580	152	2	-	3 Trillion
2017	322	700	139	6	1,178 houses were inundated	147 Billion
2018	346	775	79	1	42 houses were highly damaged	150 Billion
2019	154	890	84	2	-	100 Billion
2020	196	965	150	67	Electical System Shutdown	1 Trillion

Six yearly largest flood events from 2015 to 2020 were selected as the target in this study because both GSMaP NRT and GSMaP Gauge data are available for these flood events. These events produced the highest water levels at the stations in the Chiliwung river during these years. The event periods lasted for approximately a week in January or February.

I compared the agreement of the GSMaP products and examined the rainfall data of the study area. Statistical validation methods, such as the root mean square error (RMSE), correlation coefficients (CCs), and volume bias, were used as evaluation indexes; these were employed to evaluate the relationship between the GSMaP and observed rainfall data. The RMSE was used to compare the magnitude of the error between the GSMaP and observation data sets. CC represented the correlation between the data sets; its value ranged between zero and one. The volume bias (%) is the difference in the percentages of the total rainfall volume between the GSMaP and ground rainfall observation. It is calculated using the following equation: (100 × ((GSMaP − Observation)/Observation)). For the flood hydrograph comparisons, the Nash–Sutcliffe efficiency index (NSE) was computed. The NSE values ranged from minus infinity to 1, and an efficiency index of 1 indicated a perfect match.

7.3. Results

7.3.1. Rainfall comparison

Good performances on a daily scale with respect to the CCs and volume bias were observed for the 2015, 2019, and 2020 events, as listed in **Table 7.2**. **Figures 7.1** and **7.2** show the hourly and daily comparisons, respectively, between the basin-averaged GSMaP and rainfall observation data for the 2015 flood event. In this case, we

confirmed relatively strong correlations for the daily basin-averaged gauge rainfall, particularly for the GSMaP Gauge and observation data (0.79 for the daily basin- averaged gauge rainfall). **Figures 7.3** and **7.4** show the hourly and daily comparisons, respectively, between the average basin observation and GSMaP data for the 2020 flood event. It is noted that the observed rainfall in 2020 only provides the data at 3 h intervals, so that hourly data was made from these 3 h intervals assuming uniform time distributions at each hour. In this case, the best correlation existed (0.99, for the daily basin-averaged rainfall), but weak correlations could be confirmed on an hourly time scale. **Table 7.2** summarizes the evaluation index data. The values for the other years are listed in **Table 7.2**. The agreement of the GSMaP data was not very high (**Table 7.2**). Only weak correlations were found for the flood events from 2016 to 2018, both hourly and daily. Overestimation of the GSMaP was observed for the 2016, 2017, and 2018 events except for the GSMaP NRT in 2018, whereas slight underestimation was observed for the 2019 and 2020 events. It should be noted that the volume bias in the Pondok Betung station in 2019 showed an extremely large overestimation for both hourly and daily scales. This is because the observed rainfall in the Pondok Betung station in the 2019 event was 21 mm, which is too small compared with the values at other stations. The data quality of the rainfall stations during heavy rainfall events should be checked in Jakarta.

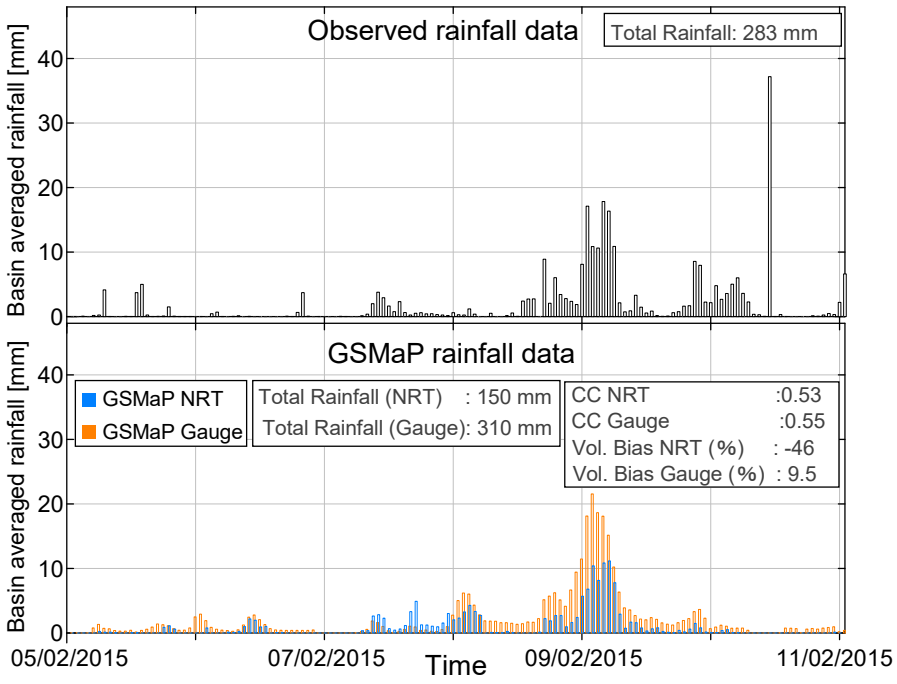

Fig. 7.1. Comparisons of hourly rainfall between GSMaP products (NRT & Gauge V7) and observation for flood event of 2015

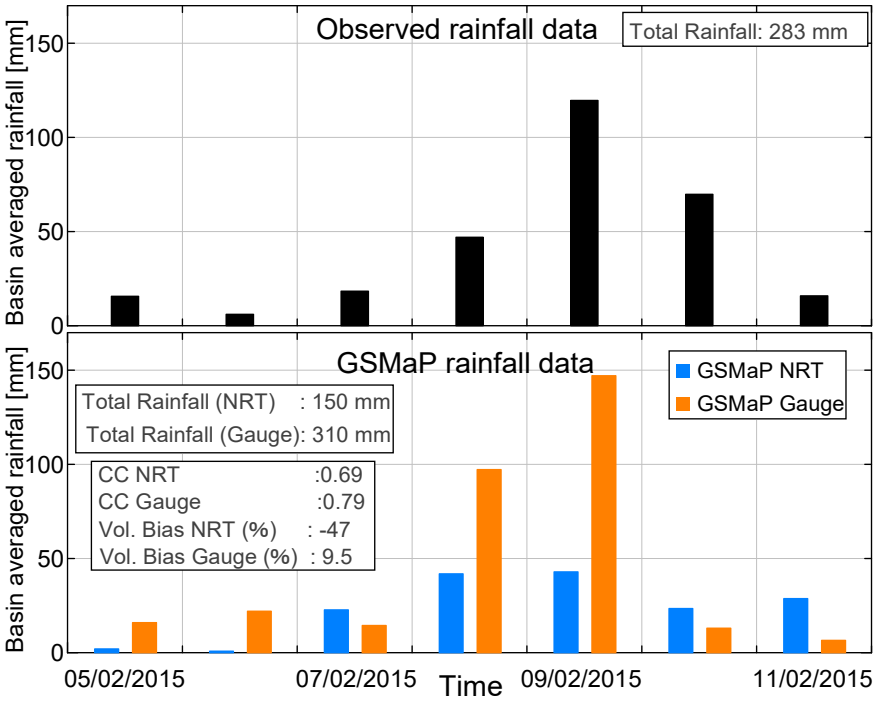

Fig.7.2. Comparisons of daily rainfall between GSMaP products (NRT & Gauge V7) and observation for flood event in 2015

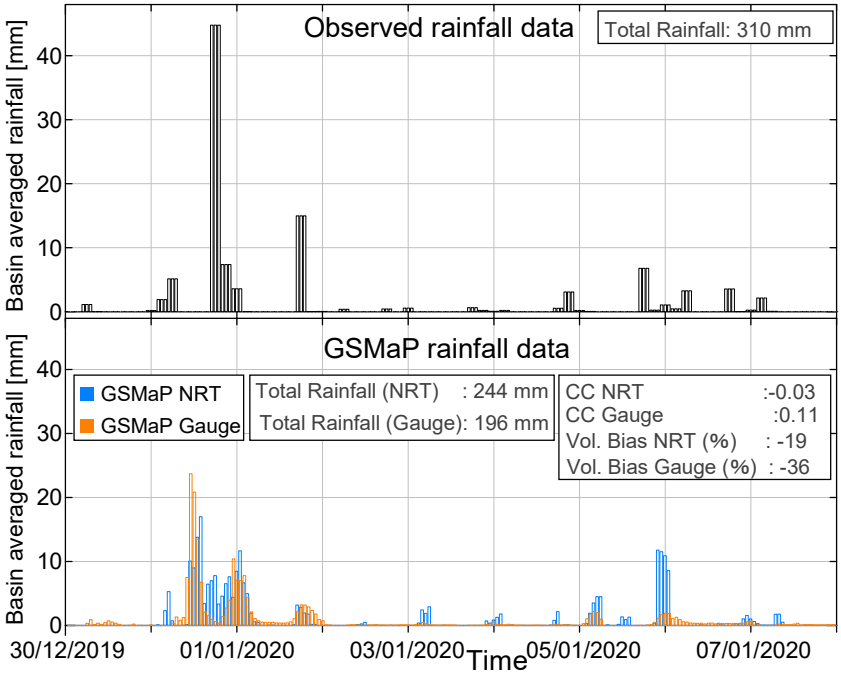

Fig.7.3. Comparisons of hourly rainfall between GSMaP products (NRT & gauge.v7) and observation for flood event of 2020

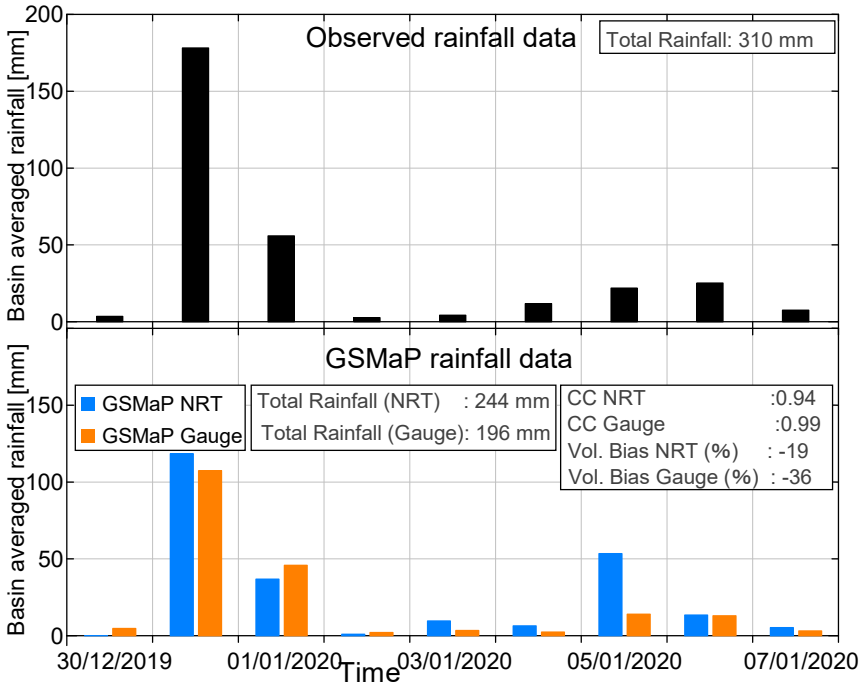

Fig.7.4. Comparisons of daily rainfall between the GSMaP products (NRT & Gauge V7) and observation for flood event of 2020

Table 7.2. Evaluation index of rainfall comparisons

Period	Location/ coverage area	Observed Rainfall (mm)	Altitude (m)	GSMaP NRT						GSMaP Gauge					
				Volume Bias (%)	Total Rainfall (mm)	Hourly Rainfall Correlation coefficients (CCs)	Hourly Rainfall RMSE (mm)	Daily Rainfall Correlation coefficients (CCs)	Daily Rainfall RMSE (mm)	Volume Bias (%)	Total Rainfall (mm)	Hourly Rainfall Correlation coefficients (CCs)	Hourly Rainfall RMSE (mm)	Daily Rainfall Correlation coefficients (CCs)	Daily Rainfall RMSE (mm)
Event 2015	Citeko	160	920	-34	107	0.07	4	0.04	24	81	290	0.10	5	0.28	49
	Darmaga	206	190	-52	98	0.05	5	-0.45	42	17	240	-0.08	5	-0.34	58
	Pondok Betung	156	50	24	193	-0.03	10	-0.28	60	127	353	-0.03	11	-0.18	84
	Kemayoran	505	4	-61	196	0.47	9	0.92	66	-44	282	0.44	8	0.91	55
	Tanjung Priok	425	2	-54	196	0.45	9	0.82	74	-41	250	0.40	9	0.90	63
	Basin Averaged	283		-46	150	0.53	4	0.69	34	12	310	0.55	4	0.79	28
Event 2016	Citeko	176	920	8	189	0.01	3	-0.12	22	52	268	0.01	3	-0.25	31
	Darmaga	126	190	31	165	-0.01	6	-0.30	36	114	270	-0.04	6	-0.34	43
	Pondok Betung	104	50	90	198	-0.02	3	0.15	29	180	292	-0.05	4	-0.01	41
	Kemayoran	178	4	94	346	0.35	5	0.81	28	53	273	0.43	4	0.43	33
	Tanjung Priok	256	2	37	350	0.20	5	0.84	22	-3	248	0.39	4	0.96	14
	Basin Averaged	172		83	316	0.16	3	0.49	30	59	275	0.15	2	0.47	24
Event 2017	Citeko	361	920	-24	273	0.02	4	-0.34	34	-6	338	-0.06	4	-0.19	32
	Darmaga	146	190	-100	282	-0.03	4	-0.17	34	129	333	-0.03	4	-0.25	31
	Pondok Betung	111	50	121	246	0.00	3	0.04	20	203	336	-0.02	3	0.03	27
	Kemayoran	233	4	-9	212	0.09	3	-0.08	20	27	295	0.17	3	0.27	19
	Tanjung Priok	543	2	-53	253	0.04	6	0.19	45	-46	292	0.01	6	-0.32	52
	Basin Averaged	228		14	260	-0.02	3	-0.37	28	41	322	0.005	3	-0.21	33
Event 2018	Citeko	497	920	-84	80	-0.01	6	0.09	60	-46	268	0.00	6	0.29	53
	Darmaga	258	190	-73	69	-0.04	4	-0.37	28	71	440	0.05	4	0.17	41
	Pondok Betung	143	50	-39	87	0.02	3	0.07	12	101	290	0.00	3	0.07	19
	Kemayoran	213	4	-53	100	0.18	1	0.30	7	19	253	0.21	2	0.53	19
	Tanjung Priok	213	2	-28	154	-0.04	3	0.61	11	17	250	-0.04	3	0.29	15
	Basin Averaged	188		-49	96	-0.03	2	-0.02	15	74	325	0.07	2	0.35	23

Table 7.2. Evaluation index of rainfall comparisons (Continued)

Period	Location/ coverage area	Observed Rainfall (mm)	Altitude (m)	GSMaP NRT						GSMaP Gauge					
				Volume Bias	Total Rainfall	Hourly Rainfall		Daily Rainfall		Volume Bias	Total Rainfall	Hourly Rainfall		Daily Rainfall	
						Correlation coefficients (CCs)	RMSE	Correlation coefficients (CCs)	RMSE			Correlation coefficients (CCs)	RMSE	Correlation coefficients (CCs)	RMSE
				(%)	(mm)		(mm)		(mm)	(%)	(mm)		(mm)		(mm)
Event 2019	Citeko	1141	920	-81	217	-0.09	12	-0.10	122	-82	204	-0.10	12	0.46	116
	Darmaga	174	190	28	222	-0.01	5	-0.14	26	25	216	0.00	4	-0.29	26
	Pondok Betung	21	50	508	128	0.18	1	0.29	12	520	130	0.08	1	0.14	12
	Kemayoran	151	4	-43	86	0.06	2	0.50	13	-13	132	0.08	2	0.50	16
	Tanjung Priok	186	2	-56	82	0.15	4	0.41	22	-32	126	0.29	3	0.44	20
	Basin Averaged	215		-41	128	0.22	2	-0.05	15	-29	154	0.46	2	0.65	13
Event 2020	Citeko	563	920	-68	181	0.12	10	0.52	80	-68	181	0.13	10	0.60	78
	Darmaga	230	190	-26	170	0.10	4	0.91	16	-20	183	-0.01	4	0.90	16
	Pondok Betung	343	50	-23	265	0.23	9	0.98	23	-41	203	0.03	9	0.98	43
	Kemayoran	445	4	-46	240	0.48	7	0.91	61	-62	169	0.50	7	0.99	68
	Tanjung Priok	424	2	-29	301	0.35	7	0.79	59	-63	156	0.51	7	0.92	69
	Basin Averaged	310		-19	244	-0.03	6	0.91	27	-36	196	0.11	6	0.99	24

7.3.2 Flood hydrograph

I performed rainfall-runoff and flood inundation simulations at an hourly time step using the GSMaP rainfall data as the input and compared the observed and simulated results. **Figures 7.5**, **7.6**, **7.7**, **7.8**, **7.9** and **7.10** show the hydrographs for the observations at the Katulampa, Depok, and Manggarai stations and the corresponding simulations for the 2015–2020 flood events. The locations of the stations are shown in Fig. 1. The simulated hydrographs showed relatively good agreement with the observations on an hourly time scale with respect to CCs (the average CCs of the Gauge simulation is 0.53), but some underestimations and/or overestimations with respect to the peak discharge bias (from 62 % to 134 % in the Gauge simulations) occurred. For the Nash index, generally low performance was confirmed, except for the 2019 and 2020 events.

For the 2015 flood event **(Figure 7.5**), flood peak discharges were captured through GSMaP Gauge simulations at the Katulanmpa and Depok stations, but apparent peak time and volume differences were observed. These differences in the flood event resulted in the worst Nash index values of all events, although the hourly rainfall correlations in **Figure 7.1** performed well, as discussed in the previous sentences. At the Manggarai station, the GSMaP Gauge simulation was overestimated in the peak dis- charge compared with the observation. For 2016 and 2017 flood events (**Figures 7.6** and **7.7**), several high flood-flow fluctuations were observed and simulated, but the simulated flood hydrograph occasionally overestimated and underestimated the observations. The simulation results of the GSMaP Gauge simulations for the 2018 event showed good correlations (**Figure 7.8**) in CCs (0.64–0.73), good peak discharge biases (− 39–35%), and relatively acceptable Nash index values (0.38 and 0.39). The flood peak timing and values of the 2018 flood event were accurately simulated, but the GSMaP NRT simulations did not show any floods in the event. This is because significant underestimations of the rainfall of the GSMaP NRT during the event were found at all stations (**Table 7.3** and **Figure 7.10**), even though GSMaP NRT captured the rainfall well in the 2018 rainy season, except during this flood event. One possibility of this underestimation might be due to shallow orographic rainfall, because large rainfall observation values at high elevations can clearly be observed in this event, as shown in Table 2. This type of rainfall may still be difficult to capture by the satellite after a new orographic/non-orographic rainfall classification scheme was installed (Kubota et al. 2020). this will be discussed further in the discussion section.

For the 2019 flood event (**Figure 7.9**), good CCs and Nash index values were observed in the gauge simulation. The best Nash index values were confirmed for the 2019 flood event. For the 2020 flood event (**Figure 7.10**), CCs show more than 0.6 in all stations for both the GSMaP NRT and gauge simulations. The relatively acceptable Nash index values (0.15–0.54) were observed, except at the Manggarai station. As such, the 2019 and 2020 events show good flood simulation results because these events show good daily rainfall correlations and volume bias of the GSMaP Gauge data compared with the observations. The simulation results for the hourly time scales are presented in **Table 7.3**. The peak bias (%), CCs, RMSE, and NSE were computed (**Table 7.3**). From **Table 7.3**, it can be observed that the gauge simulations are better than the NRT simulation, especially for the 2018 event. The gauge simulation results in **Table 7.3** show that stations at higher altitudes show good RMSE and NSE values because of the small catchment size and sub-basin numbers and few opportunities to have uncertainty (Moriasi et al. 2007). Several NRT simulations yielded negative NSE values, which signified that these simulations were not useful for flood prediction. Based on the comparison, GSMaP Gauge simulations were found to be significantly better than GSMaP NRT based simulations. Significant underestimation of the GSMaP NRT simulation occurred compared with the observation. GSMaP NRT data were designed as input for the flood-forecasting simulations because these data sets provided near real-time rainfall data. However, in terms of agreement, the GSMaP NRT data were unsuitable for the real-time forecasting of flooding in Jakarta, and significant bias corrections or modifications are required to obtain more accurate simulation results. Finally, it should be emphasized that GSMaP Gauge simulations showed relatively good performance. These results encourage us to use satellite-driven rainfall data to reconstruct historical flood events in poorly gauged basins and developing countries, even when the target areas are highly urbanized.

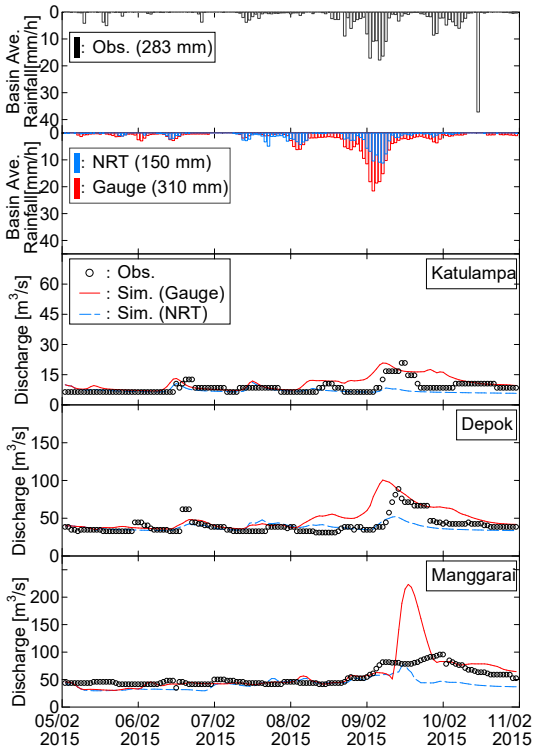

Fig.7.5. Hydrograph comparisons for flood event of 2015

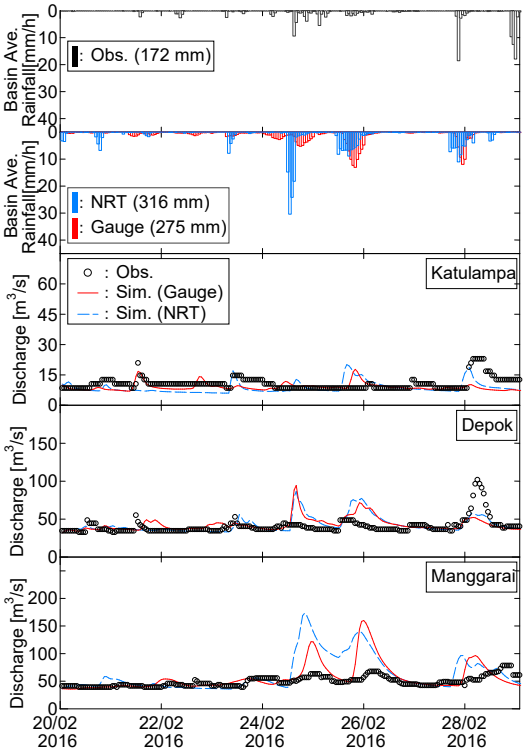

Fig.7.6. Hydrograph comparisons for flood event of 2016

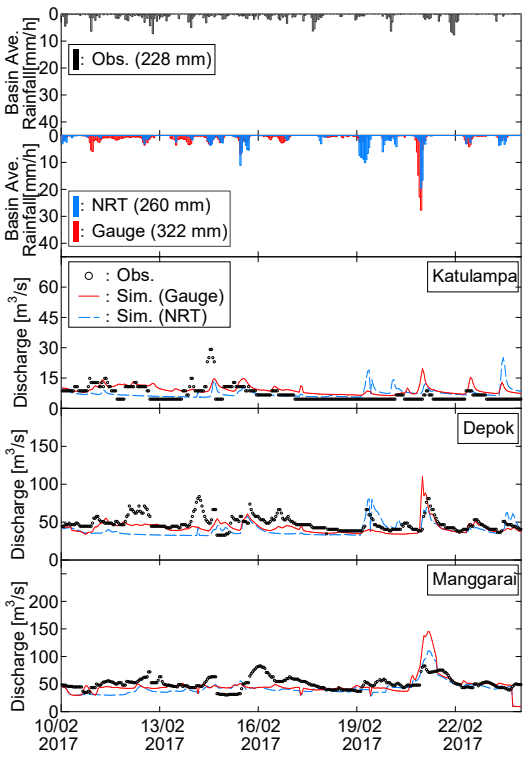

Fig.7.7. Hydrograph comparisons for flood event of 2017

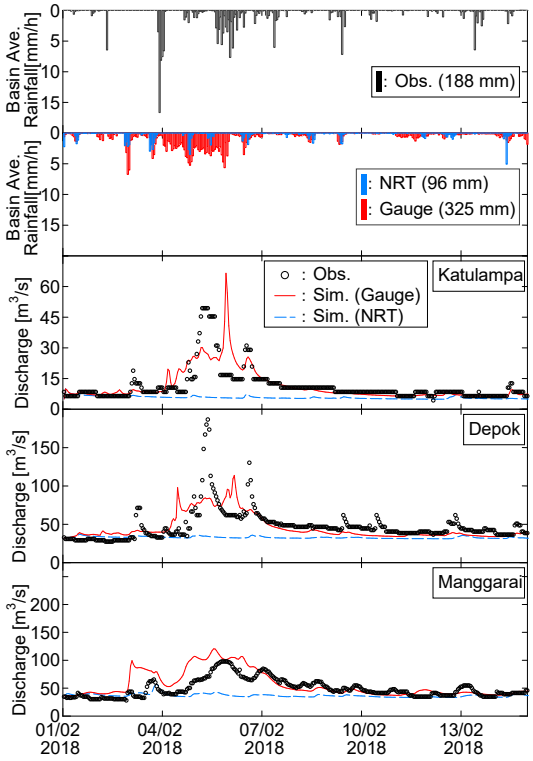

Fig.7.8. Hydrograph comparisons for flood event of 2018

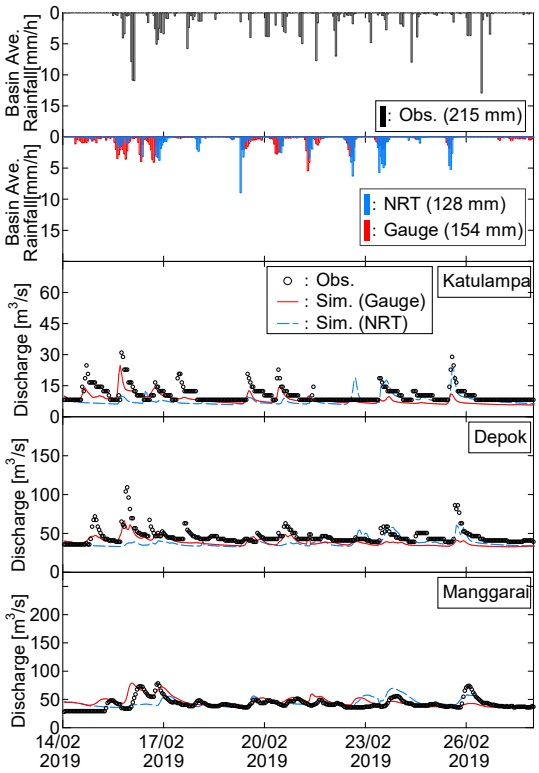

Fig.7.9. Hydrograph comparisons for flood event of 2019

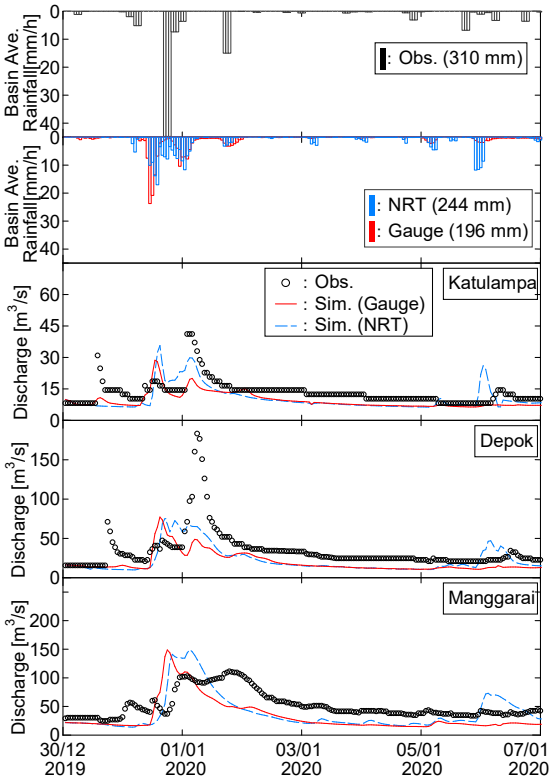

Fig.7.10. Hydrograph comparisons for flood event of

2020

Table 7.3. Summary of discharge hydrograph comparisons

Period	Water Level station	GSMaP NRT				GSMaP Gauge			
		Peak Discharge Bias (%)	Correlation coefficients (CCs)	Nash Index	RMSE (m^3/s)	Peak Discharge Bias (%)	Correlation coefficients (CCs)	Nash Index	RMSE (m^3/s)
Event 2015	Katulampa	-46	0.03	-0.36	3.15	0	0.52	-1.15	3.97
	Depok	-41	0.50	0.20	10.02	13	0.63	-0.80	15.02
	Manggarai	-19	0.53	-0.31	17.99	134	0.72	-2.39	28.92
Event 2016	Katulampa	-13	0.14	0.31	4.30	-23	0.03	0.44	3.86
	Depok	-15	0.35	-0.36	11.74	-7	0.24	-0.40	11.92
	Manggarai	122	0.49	-10.39	30.31	104	0.52	-5.18	22.32
Event 2017	Katulampa	190	-0.03	0.59	4.52	128	0.42	0.67	4.04
	Depok	0	0.16	-1.35	14.65	36	0.39	-0.44	11.48
	Manggarai	33	0.38	-0.78	16.85	76	0.39	-0.94	17.61
Event 2018	Katulampa	-80	0.13	-0.45	9.83	35	0.69	0.39	6.41
	Depok	-80	0.21	-0.46	25.75	-39	0.64	0.38	16.75
	Manggarai	-42	0.20	-0.53	20.19	24	0.73	-0.18	17.76
Event 2019	Katulampa	-19	0.35	0.57	4.71	-62	0.60	0.69	3.96
	Depok	-30	0.25	0.19	12.48	-52	0.60	0.43	10.49
	Manggarai	-5	0.36	-0.08	9.75	-28	0.49	-0.06	9.67
Event 2020	Katulampa	80	0.60	0.51	5.65	2	0.68	0.54	4.37
	Depok	22	0.64	0.32	17.22	-19	0.60	0.15	19.25
	Manggarai	-25	0.64	-0.43	21.77	-50	0.62	-0.61	23.11

7.3.2. Flood Inundation

The flood inundation conditions were also compared. **Figures 7.11**, **7.12**, **7.13**, **7.14**, **7.15**, and **7.16** show flood inundation maps based on the simulation and observation data for 2015– 2020 flood events. The observed flood inundation maps were provided by the National Disaster Management Agency. These observation maps were based on eyewitness reports of government officers during the flood events and interviews with residents after the event. The observation maps tended to overestimate the inundation area because the entire district in the map was treated as the entire inundation when the flooding of a part of a district was reported. The simulation of the flood inundation results using the GSMaP Gauge showed relatively good consistency with the observations, particularly for 2017, 2018, 2019, and 2020. A slight overestimation of the flood inundation in some districts can be confirmed in 2015 and 2016 due to overestimation of the flood hydrograph at some stations. The GSMaP NRT captured the flood inundation for 2015, 2016, and 2020 events but could not capture the inundation for 2018 due to significant underestimations of the rainfall during the event. It is noted that these comparisons were made by visual-graph comparisons because the observation maps were not appropriate for use as a statistical test because of the overestimation of the inundation area, as explained in the above sentences.

From these results, we concluded that the GSMaP Gauge data could be used to reproduce previous flood inundation events in Jakarta. However, it is challenging to use GSMaP NRT data as the input in a real-time

flood-forecasting system owing to its low accuracy. So, a good bias correction or data assimilation methods to adjust the GSMaP NRT data for the flood prediction would be required.

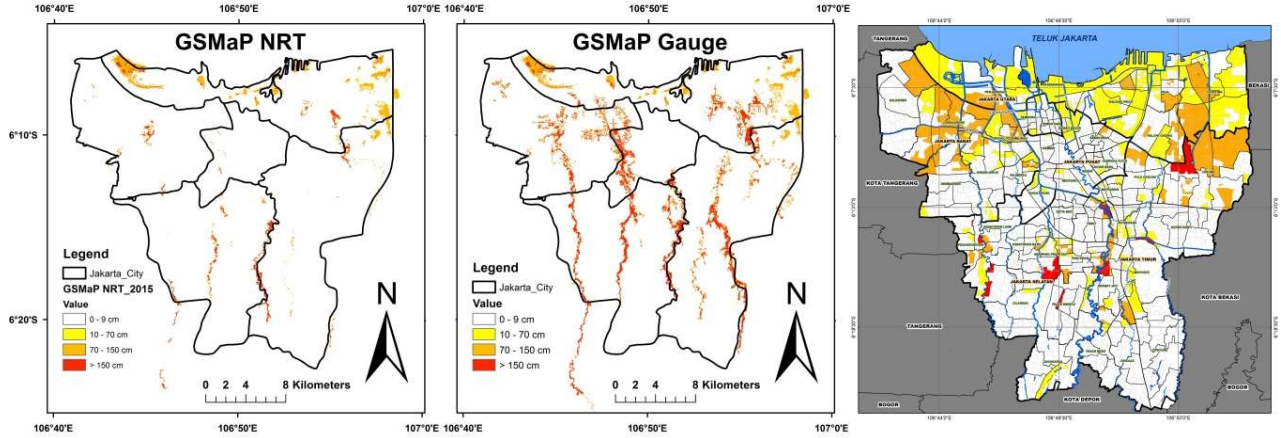

Fig. 7.11. Flood Inundation comparisons for flood event of 2015

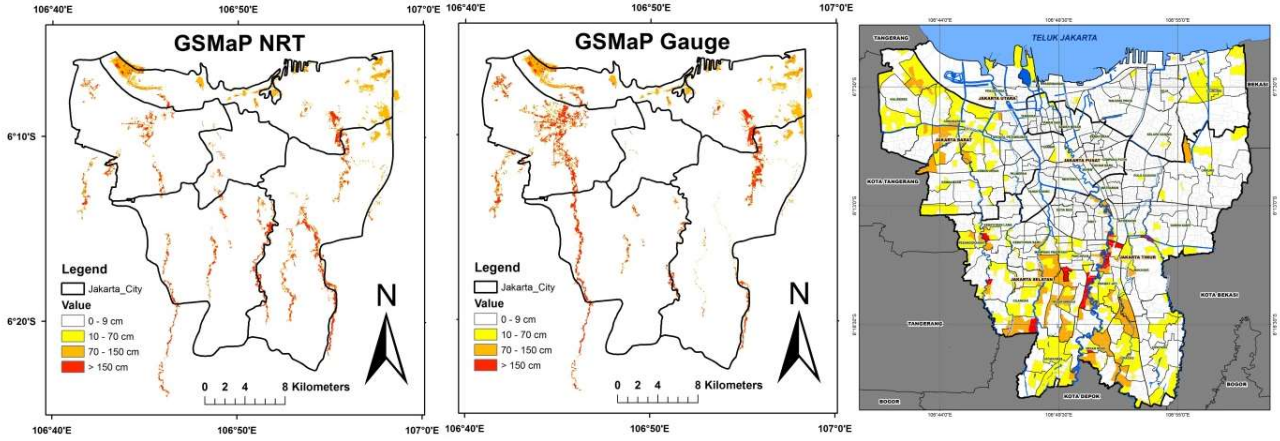

Fig. 7.12. Flood Inundation comparisons for flood event of 2016

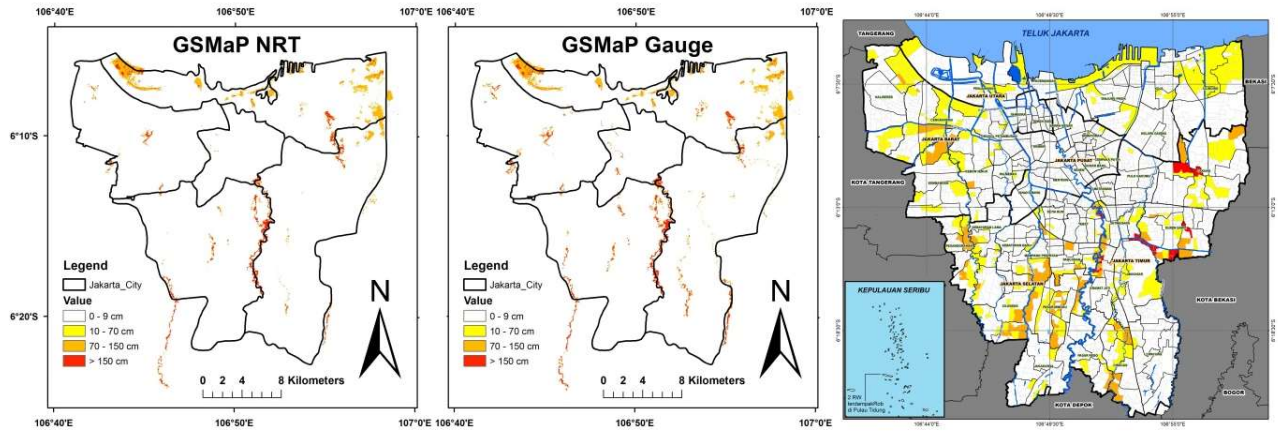

Fig. 7.13. Flood Inundation comparisons for flood event of 2017

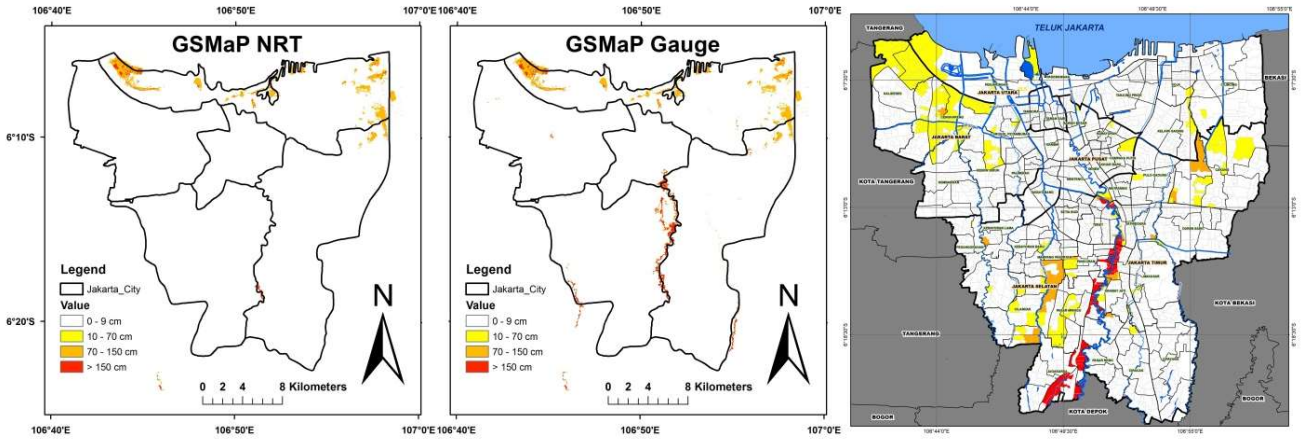

Fig. 7.14. Flood Inundation comparisons for flood event of 2018

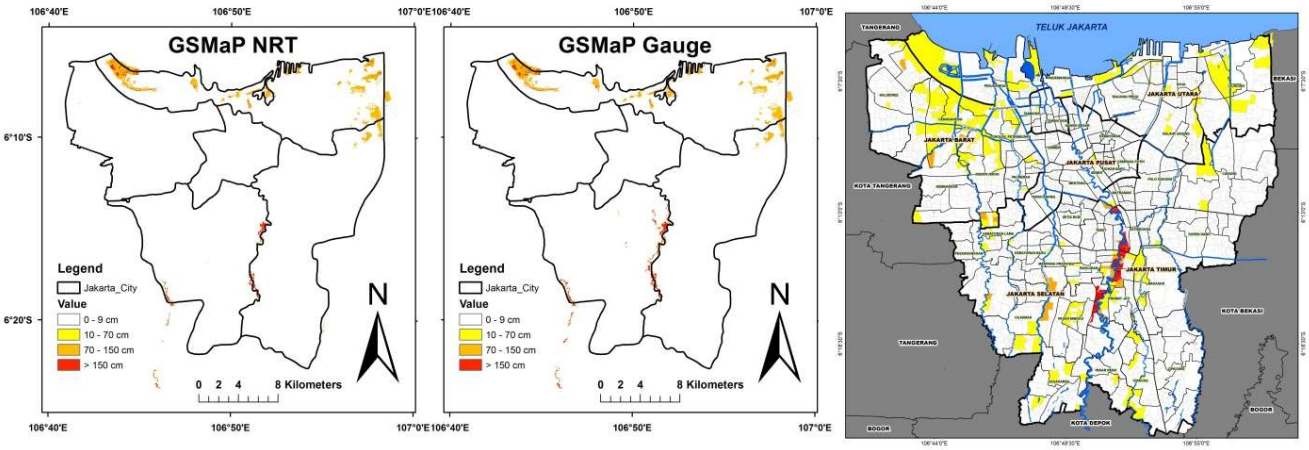

Fig. 7.15. Flood Inundation comparisons for flood event of 2019

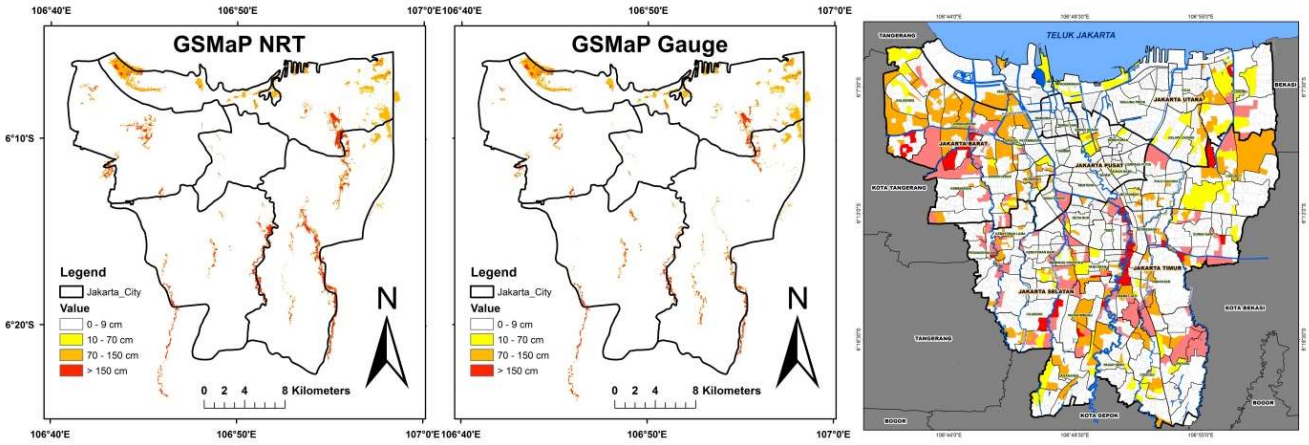

Fig. 7.16. Flood Inundation comparisons for flood event of 2020

7.4 Discussions

Based on the comparison between gauge-based observations and satellite-based GSMaP rainfall data, we found that the GSMaP NRT is not useful as an input for the real-time flood-forecasting system in Jakarta. Several previous studies have shown that the GSMaP products can capture the overall rainfall pattern (Kubota et al. 2009; Pakoksung and Takagi 2016) and could be useful as inputs to hydrologic models to reproduce past flood events (Sayama et al. 2012). However, several studies (Fu et al. 2011; Admojo et al. 2018; Pakoksung and Takagi 2016) have pointed out that the GSMaP products tended to be underestimated, and this underestimation was due to orographic effects (Kubota et al. 2009, 2020). Over coastal mountain ranges, heavy rainfall can be caused by shallow orographic rainfall, which is inconsistent with the assumption in the PMW algorithm that heavy rainfall results from deep clouds with significant ice (Kubota et al. 2020). Therefore, a new orographic/non-orographic rainfall classification scheme was installed in the PMW algorithm in V6 for the TMI and V7 for all sensors (Kubota et al. 2020). From the analysis of the paper in Jakarta, we observed both the underestimation and over- estimation of the GSMaP rainfall, and only the 2018 rainfall event showed difficulty in capturing the rainfall in the high-altitude zones. Therefore, it might be inferred that the orographic effects on the quality of the GSMaP products in Jakarta are negligible. It should be noted that it is difficult to capture the 2018 rainfall event that showed clear orographic effects even after the new scheme was installed. However, it is difficult to draw any conclusions from only one case, and other atmospheric conditions, such as wind fields, should be analyzed to understand the orographic rainfall effects in Jakarta.

Many reasons are attributed to the general difficulties in capturing heavy rainfall in Jakarta. First, Jakarta and its surroundings are highly urbanized areas, and convectional rainfall typically occurs in urban areas of humid tropical regions. Additionally, the heat island phenomenon is significantly progressing in Jakarta, and there exists the urban thermal influence on the background environment of convective rainfall (Sugawara et al. 2018). The rain retrieval algorithms may have errors when applied to “warm rain” processes that are typical of convectional rainfall in tropical regions (Chang et al. 2013). Thus, it might be difficult to predict and capture convectional rainfall in urban areas using satellite information. This convection type rainfall in an urban area may be a challenge for the accurate prediction of rainfall in Jakarta. Furthermore, the timing of microwave observation from the satellite might be related to the low quality of GSMaP because the local heavy rains regularly fall for short periods in Jakarta.

Second, the flood travel time in Jakarta is short. Jakarta and its surrounding areas are highly urbanized, and the flood travel time in rivers and canals is approximately 12–16 h. Local heavy rainfall should be captured hourly using the satellite to predict rapid floods. In previous studies, the GSMaP was evaluated at large-scale basins daily and monthly. This rapid flood response to rainfall is another challenge for GSMaP prediction in Jakarta.

Some researchers applied a bias correction method for rainfall simulation using the GSMaP algorithm to reduce the underestimation of rainfall intensity and amount (e.g. Sayama et al. 2012). However, for Jakarta, the difficulties mentioned above complicate the application of bias correction because GSMaP simulations occasionally overestimated and/or underestimated the flood-flow discharge of the 2016 and 2017 flood events. Moreover, the GSMaP NRT simulations did not show any flood responses for the 2018 event. In these situations, it is difficult

to apply bias correction to the GSMaP NRT data. If we could find any clear underestimation or overestimation trend of the GSMaP against the ground observation, a bias correction method would work well to improve the simulation results (Saber and Yilmaz 2018).

Multi-ensemble forecasting using several satellite rainfall products has been performed in previous studies (Jiang et al. 2014). Other satellite rainfall products such as TRMM (3B42RT) might be used as the input for flood modeling in Jakarta as a multi- ensemble forecasting. However, the temporal and spatial resolutions of other satellite products are in- adequate for capturing local heavy rainfall in Jakarta. Therefore, it is currently challenging to use GSMaP as the input for real-time forecasting systems. Radar information adjusted with ground gauge-based rainfall data is a more viable option for forecasting systems. It should be noted that the five rain gauge stations might be insufficient for capturing rainfall fields in Jakarta. Hence, radar observation systems should be installed and operated properly to predict rainfall and flood events in Jakarta in real time, and denser rain gauge station networks would be required to calibrate and assimilate the radar rainfall values based on the ground true observation rainfall data.

GSMaP Gauge data might be useful for reconstructing and simulating historical flood events to evaluate and compare past floods in poorly gauged basins. This is because the GSMaP Gauge can be used to observe the heavy rainfall that occurred in the past. However, in other words, GSMaP NRT could be used as the input for the flood prediction if a good bias correction or data assimilation method to correct the NRT data was developed.

7.5 Conclusions

This study was conducted to examine the possibility of using GSMaP rainfall data as the input for real-time flood forecasting in Jakarta, Indonesia. The NRT and Gauge V7 products of the GSMaP were compared with ground observation rainfall data at several stations and basin averages formed around Jakarta. The results indicated that the GSMaP Gauge data showed acceptable agreement in simulating the flood hydrograph and inundation of Jakarta. However, the gauge data were unavailable in real time and thus could not be used for real-time forecasting. The gauge data are suitable for replicating historical flood events that occur even in highly urbanized areas.

The GSMaP NRT product, which provided near real- time rainfall data, was suitable for real-time flood forecasting. However, it is necessary to develop a significant bias correction or data assimilation method or change the algorithm of the NRT data set adjusted for urban areas to improve the accuracy of the simulation results.

Also, other real time flood forecasting method such as the ensemble forecasting based on multi models should be checked. It is also emphasized that not only flood predictions but also other nonstructural counter measures should be checked in Jakarta to reduce the future flood damages.

7.6 References

Aonashi, K., Liu. G.,(2000). Passive Microwave Precipitation Retrievals Using TMI during the Baiu Period of 1998. Part I: Algorithm Description and Validation. 2024-2037.

Admojo, D.D., Tebakari, T., Miyamoto, M. (2018). Evaluation of a satellite-based rainfall product for a runoff simulation of flood event: a case study. Journal Japan Society Civil Eng. Ser B1. 74(4).I_73–I_78.

Berlinger, J., Yee, I. (2020). 66 people now killed by flooding in Jakarta, and more rain appears to be on the way. CNN World News https://edition.cnn.com/202 0/01/06/asia/jakarta-floods-intl-hnk/index.html. Accessed 1 Apr 2021.

Chang, L., Cheung, K., Mcaneney, J. (2013). Case study of TRMM satellite rainfall estimation for landfalling tropical cyclones: issues and challenges. Trop Cyclone Res Rev 2.(2). 109

Fu, Q., Ruan, R., Liu Y. (2011). Accuracy assessment of Global Satellite Mapping of Precipitation (GSMaP) product over Poyang Lake Basin, China. Procedia Environ Sci .10. 2265–2271. https://doi.org/10.1016/j.proenv.2011.09.354

Jiang, S., Ren, L., Hong, Y., Yang, X., Ma, M., Zhang, Y., Yuan, F. (2014). Improvement of multi-satellite real-time precipitation products for ensemble streamflow simulation in a middle latitude basin in South China. Water Resources Management 28(8). 2259–2278. https://doi.org/10.1007/s11269-014-0612-4

Kubota, T., Ushio, T., Shige, S., Kida, S., Kachi, M., Okamoto, K. (2009). Verification of high-resolution satellite-based rainfall estimates around Japan using a gauge- calibrated ground-radar dataset. Journal Meteorology Soccial Japan .87A:203–222. https://doi. org/10.2151/jmsj.87A.203

Kubota, T., Aonashi, K., Ushio, T., Shige, S., Takayabu, Y.N., Kachi, M., Arai, Y., Tashima, T., Masaki, T., Kawamoto, N., Mega, T., Yamamoto, MK., Hamada, A., Yamaji, M., Liu, G., Oki, R. (2020). Global satellite mapping of precipitation (GSMaP) products in the GPM era. In: Levizzani, V., Kidd, C., Kirschbaum, D., Kummerow, C., Nakamura, K., Turk, F. (Eds) Satellite precipitation measurement. Advances in global change research. vol 67. Springer, Cham. https://doi.org/10.1007/978-3-030-24568-9_20

Kure, S., Jang, S., Ohara, N., Kavvas, M.L., Chen, Z.Q. (2013). WEHY-HCM for Modeling interactive atmospheric-hydrologic processes at watershed scale: II. Model application to ungauged and sparsely gauged watersheds. Journal Hydrology Engineering 18(10). 1272–1281. https://doi.org/10.1061/(ASCE)HE.1943-5584.0000701.

Miyamoto, M., Sugiura, A., Okazumi, T., Tanaka, S., Nabesaka S., Fukami K. (2012). Suggestion for an advanced early warning system based on flood forecasting in Bengawan Solo River basin, Indonesia. In: Proceedings of 10th International Conference on Hydroinformatics, IWA IAHR. No.394

Moriasi, D., Arnold, J., Van Liew, M.W., Bingner, R., Harmel, RD., Veith, T.L. (2007). Model evaluation guidelines for systematic quantification of accuracy in watershed simulations. Trans ASABE 50(3).885–900. https://doi.org/10.13031/2013.23153.

Pakoksung, K., Takagi, M. (2016). Effect of satellite based rainfall products on river basin responses of runoff simulation on flood event. Model Earth System Environment 2(3). 143. https://doi.org/10.1007/s40808-016-0200-0

Saber, M., Yilmaz, K.K. (2018). Evaluation and bias correction of satellite-based rainfall estimates for modelling flash floods over the Mediterranean region: application to Karpuz River basin, Turkey. Water 10(5). 657. https://doi.org/1 0.3390/w100506,57

Sayama, T., Ozawa, G., Kawakami, T., Nabesaka, S., Fukami, K. (2012). Rainfall-runoff- inundation analysis of the 2010 Pakistan flood in the Kabul River basin. Hydrology Science Journal 57(2). 298–312. https://doi.org/10.1080/02626667.2011.644245

Setiawati, M.D., Miura, F. (2016). Evaluation of GSMaP daily rainfall satellite data for flood monitoring: case study–Kyushu Japan. Journal of Geoscience Environment Protection 4(12). 101– 117. https://doi.org/10.4236/gep.2016.412008

Sugawara, H., Oda, R., Seino, N. (2018). Urban thermal influence on the background environment of convective precipitation. Journal Meteorological Science Japan 96A. 67–76. https://doi.org/10.2151/jmsj.2018-010

Tian, Y., Peters-Lidard, C.D., Adler, R.F., Kubota, T., Ushio, T. (2010). Evaluation of GSMaP precipitation estimates over the contiguous United States. Journal Hydrometeorolgical 11(2):566–574. https://doi.org/10.1175/2009JHM1190.1

Ushio, T., Sasashige, K., Kubota, T., Shige, S., Okamoto, K.I., Aonashi, K., Inoue, T., Takahashi, N., Iguchi, T., Kachi, M., Oki, R., Morimoto, T., Kawasaki, Z.I. (2009). A Kalman filter approach to the global satellite mapping of precipitation (GSMaP) from combined passive microwave and infrared radiometric data. Journal Meteorological Social Japan Ser. II .87A. 137–151. https://doi.org/10.2151/jmsj. 87A.

Chapter 8

Summary and Recommendations

8.1. Summary

In this section, summaries of each chapter are presented as follows;

Floods in Indonesia are considered to be one of the major natural disasters. Jakarta City in Indonesia has experienced many floods in the past. The flood in February 2007 resulted in more than 80 deaths, and 40% of the area in Jakarta was inundated. Also, electrical system shutdowns in several districts in the city were reported. The flood event in 2013 caused the similar situation, which resulted in more than 40 deaths, 45,000 refugees, and terrible economic damage. According to the literature review, the factors contributing to floods in Jakarta are so complicated. In these factors, urban development and climate change could be main factors in the near future. Several previous studies had conducted climate change impact analyses in Jakarta, considering future climate and land use changes, land subsidence, and sea level rise. However, effects of urban development on the atmospheric environments of cities had not been taken into account in many previous climate change researches conducted in Jakarta or in urban cities across the world. Local urbanization is expected to affect the atmospheric environments of mega cities owing to the changing urban thermal environments, such as the heat island phenomena. In general, local urbanization was considered only for land use changes in runoff and flood inundation simulations. Also, previous studies only considered a land use change scenario (the worst case) toward the future. However, several land use change scenarios should be considered in the climate and land use change study in Jakart in order to show how much CO_2 mitigation plans may work to reduce the flooding. The main objective of this study is to quantify the effects of both land use and climate change on future rainfall and flood inundation in Jakarta based on future urban growth and urban climate change scenarios including the heat island effects. Also, several counter measures not only structural but also non structural types such as a flood forecasting are proposed and evaluated in this study.

Chapter 1: Introduction

The objectives in this study are explained. The results of the literature review, it was found that there are many studies related to the flood in Jakarta. However, there is no study that quantitatively evaluate the effects of the urban development with the several scenarios including the urban climate change such as heat island effects. So, the research framework and outline of the research are defined to achieve the research purpose.

Chapter 2: Study Area

The situations of study are and datasets explained. DEM and land use/cover maps and photos of the target areas were presented. Also, available dataset and sources used in this study are explained in this chapter. In addition, the historical flood events were explained and characteristics of Jakarta’s flood and damage were discussed.

Chapter 3: Flood Simulation Model

The flood simulation model used in this study was explained. The model consisted of modules representing the rainfall-runoff in each sub-basin, a hydrodynamic module representing the river and canal networks, and a flood inundation module for predicting the status of the flood plains. The model parameters were calibrated through the application to the 2013 flood event. The validation results in the hydrograph and flood inundation map comparisons show good agreement against the observations. The explained model was used to project the future flood inundation situations based on several scenarios in this study.

Chapter 4: Effects of Land Use/cover Change and Land Subsidence

First, the four scenarios of future changes in land use in Jakarta based on the SLEUTH model: the worst-case (RCP8.5-SSP3), compact-growth (RCP2.6-SSP1), and controlled-growth-I and -II scenarios were evaluated based on the flood inundation simulations. The controlled-growth is a scenario to decrease the growth rate and delay the progress of urbanization compared to the compact-growth scenario. This scenario may be derived from the efforts for the 1.5 degree-Celsius increase target. The future land subsidence was projected by the linear interpolation of the historical trend of the elevation changes in Jakarta.

According to the analyses, the predicted changes in land use with the land subsidence in the worst-case and controlled-growth-II scenarios would cause flood inundation volumes in 2050 to be 35% and 25% larger than in 2013, respectively. Thus, even under the controlled-growth-II scenario, the modeled changes in land use with the land subsidence would significantly increase flood inundation. Based on these results, I strongly recommend that the Jakarta government specify regulations for changes in land use in the forested upper regions and land subsidence in the lower regions as soon as possible to reduce future flood damage in the city.

However, in this chapter, climate change impact was not considered for the future projections. Next chapter will focus on the climate change and heat island effects associated with the urban development.

Chapter 5: Effects of Climate Change

In this chapter projected rainfall data of RCP2.6-SSP1 and RCP8.5-SSP3, based on the WRF simulation, were used as inputs for rainfall-runoff and flood inundation simulations in Jakarta. In addition, RCP2.6 and RCP8.5, without urban development scenarios, were investigated to specifically determine the effects of urbanization in Jakarta. At the same time, future land use/cover changes were considered based on the scenarios (SSP1 and SSP3).

Results showed that the rainfall intensity, peak discharge and flood inundation generally increased toward high RCP and SSP future scenarios. Significantly, the RCP2.6-SSP1 scenario showed a higher peak discharge value than RCP8.5 owing to the combination of land use change and increased rainfall. Based on the results of this analysis, urban development was clearly seen to increase not only the rainfall intensity and volume in future but also the runoff from the basin, river flow discharges, and flood inundations in Jakarta, due to the combination of land use change and increased rainfall. It should be emphasized that the urban development effects on the increases in

rainfall will contribute to an increase of the flood inundation volume by approximately 5–7% in a target area. I conclude that the effects of urban development on atmospheric and runoff processes should be considered for climate change studies in urban areas.

Chapter 6: Evaluation of Counter Measures

Finally, in order to reduce the flood damages in Jakarta, structural counter measures were evaluated based on the Expected Annual Damage Cost (EADC). Also, B/Cs were computed and compared with other counter measures proposed in previous studies. The counter measure discussed is to increase the flood flow capacity in the whole rivers in Jakarta. The scenarios for the counter measures are Case 1: increase bank height (1 m) and Case 2: increase bank height (1 m) and dredging bed level (1 m). The flood inundation simulations were conducted with and without the counter measures and the flood inundation area, flood damage cost and cost benefit analysis results are obtained and discussed.

From the results of analysis, it was found that the structural counter measures will reduce the flood damage effectively but the implementation cost is too expensive, so that these counter measures are difficult to be implemented in Jakarta. So, nonstructural measures such as flood forecasting with the evacuation plans should be developed.

Chapter 7: Flood Predictions as a Nonstructural Counter Measures

As a nonstructural measure, the flood prediction based on the satellite rainfall data was evaluated. The NRT and Gauge V7 products of the GSMaP were compared with ground observation rainfall data at several stations and basin averages formed around Jakarta. The results indicated that the GSMaP Gauge data showed acceptable agreement in simulating the flood hydrograph and inundation of Jakarta. However, the gauge data were unavailable in real time and thus could not be used for realtime forecasting. The gauge data are suitable for replicating historical flood events that occur even in highly urbanized areas. The GSMaP NRT product, which provided near real- time rainfall data, was suitable for real-time flood forecasting. However, it is necessary to develop a significant bias correction method or change the algorithm of the NRT data set adjusted for urban areas to improve the accuracy of the simulation results.

Based on the analysis and conclusions of the study, the recommendations for Jakarta were made and explained in the following sentences.

8.2 Recommendations

According to the analysis conducted in this study, the following recommendations for Jakarta were made;

1. the Jakarta government specify regulations for changes in land use in the forested upper regions and land subsidence in the lower regions as soon as possible to reduce future flood damage in the city. Also, monitoring and evaluation of the land subsidence and land use change should be continued.

2. Not only the climate change, but also heat island effects are contributed to increase the rainfall intensity in Jakarta, so that the efforts to reduce the urban heat environment should be considered in Jakarta as soon as possible. Counter measures such as a green infrastructure, updating the air conditioner as high energy efficiency, etc. should be evaluated how much the heat island effects would be reduced.

3. Several nonstructural counter measures must be prepared, evaluated and implemented in Jakarta as soon as possible because the structural counter measures are too expensive to be implemented.

4. Continuous research related to Jakarta's flood problem would be strongly requested. Jakarta and Indonesia government should support further researches to continue for mitigation and adaptation for the climate crisis and urban development in Jakarta.

Appendix Evaluation of Future Sea Level Rise

Future sea level projection was provided from Takagi et al. (2016) who concluded that land subsidence would be the main driver of coastal floods in the north coastal area of Jakarta by projecting the sea level rise under future climate change and land subsidence conditions. However, their study did not consider river flooding due to heavy rainfall, so we considered flood events from the ocean and the river, including the possibility of these occurring at the same time.

Figure A1 presents the change in the EADC due to only climate change without the sea level rise, and **Figure A2** presents the change in the EADC due to both climate change without the sea level rise and urban development. Climate change alone increases the mean of the EADC for the near future by 54–100%. The far future has a more severe flood risk and higher uncertainty compared to the near future, as indicated by the significant increase in the mean value of the EADC by 72–127%. Furthermore, the combination of urban development and climate change significantly increases the future flood risk as shown in **Figure A2**. Results for the near future indicate that the mean value of the EADC increases by 322% to 402%. Similarly, results for the far future indicate the mean value of the EADC significantly increases by 353% to 445%. These results indicate that the combination of urban development and climate change could increase future flood risks.

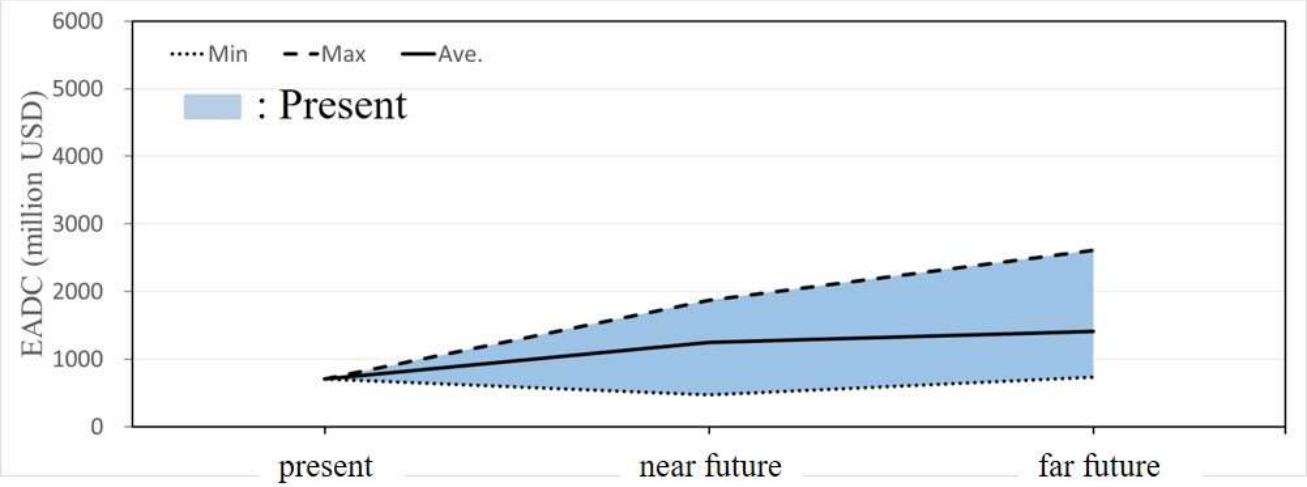

Figure A1. Projection of expected annual damage costs (EADC) in the near future (2011–2050) and far future (2051–2100) considering only climate change (Januriyadi et al., HRL, 2018).

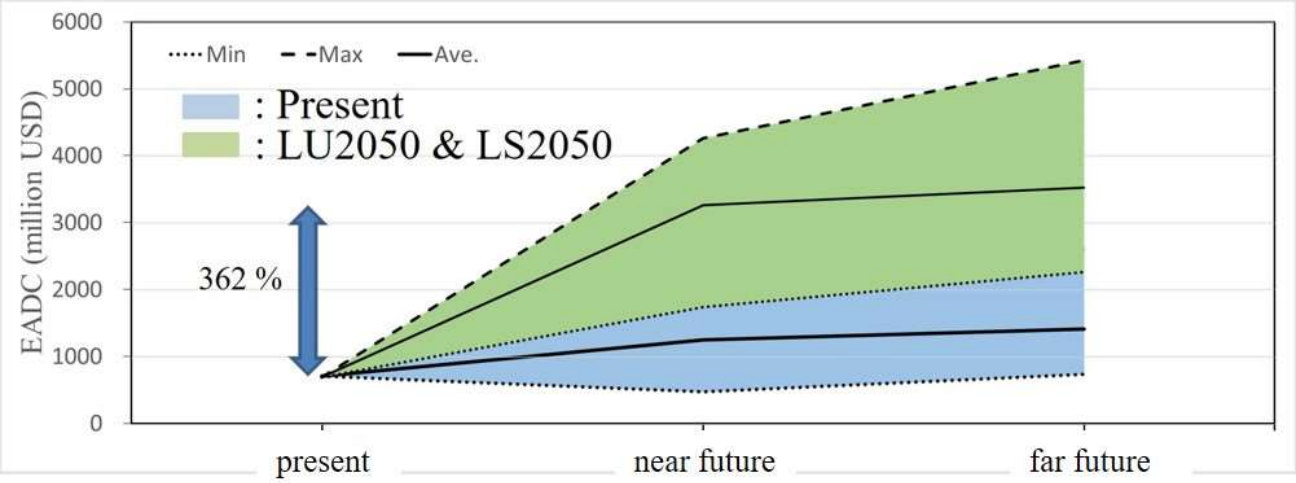

Figure A2. Projection of expected annual damage costs (EADC) in the near future (2011–2050) and far future (2051–2100) considering climate change, land use change, and land subsidence (Januriyadi et al. HRL, 2018).

Figure A3 shows the change in the EADC due to climate change including the sea level rise in the near future. Here, land use change and land subsidence were not considered in this simulation. It was found that the sea level rise will also increases the future flood risk. However, the effects are small compared to the land use change and land subsidence as shown in **Figure A2**. So, in the main contents of the thesis, we did not consider the effects of the sea level rise in this study.

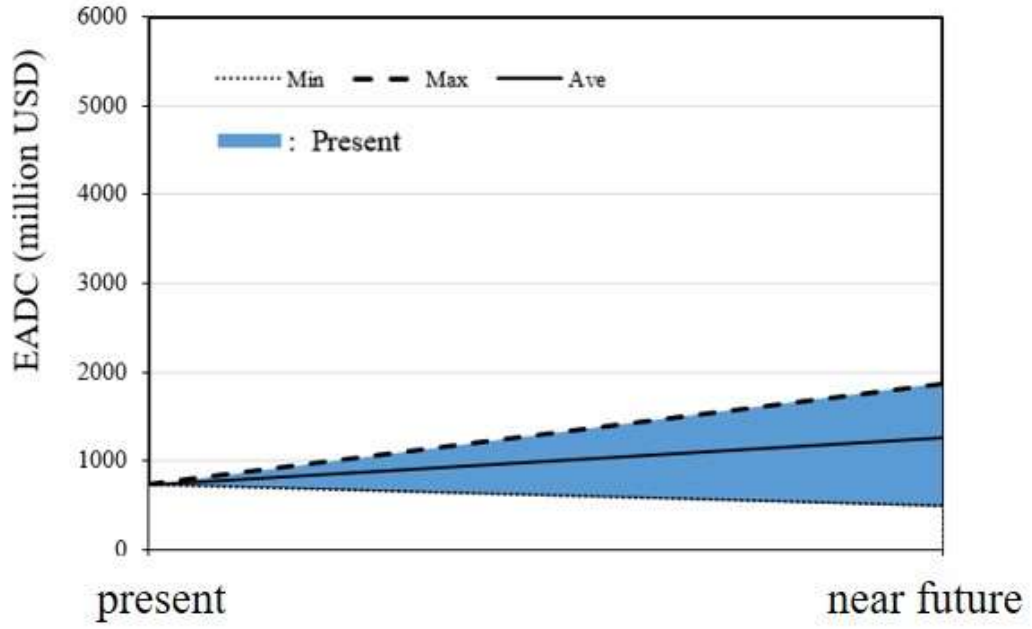

Figure A3. Projection of expected annual damage costs (EADC) in the near future (2011–2050) considering only climate change with sea level rise

ACKNOWLEDGEMENTS

I would like to express my sincere gratitude to my advisor Associate Professor Shuichi Kure for his support, advice, and guidance during the course of my study. He has been a source of inspiration and encouragement for me, and his remarkable patience in waiting for appearance of my research.

I had a remarkable benefit from the knowledge and advice of some prominent professors of the Departement of Environment and Civil Engineering, Toyama Prefectural University, such as: Professor Keisuke Hoshikawa, Professor Koichi Watanabe and Associate Professor Tomoko Kyuka for their support during my study.

Also, I would like to thank Prof. So Kazama, Tohoku University, for his insightful comments and supports to improve my thesis and presentations.

I owe special gratitude to the late Prof. Akira Mano, Tohoku University. Prof. Mano made me to come to Japan and his support made this work possible. His kindness and passion were a gift to the scientific community of Indonesia and Japan, and he will be sorely missed.

List of Publications (As of February 17, 2022)

Peer-Reviewed Papers

1) **Priyambodho, B.A.**, Kure, S., Januriyadi, N.F., Farid, M., Varquez, A.C., Kanda, M., and Kazama, S. "Effects of Urban Development on Regional Climate Change and Flood Inundation in Jakarta, Indonesia" J*ournal of Disaster Research*, Accepted.
2) **Priyambodho, B.A.**, Kure, S., Yagi, R. (2021) "Flood inundation simulations based on GSMaP satellite rainfall data in Jakarta, Indonesia" *Prog Earth Planet Sci* **8**, 34, https://doi.org/10.1186/s40645-021-00425-8
3) **Priyambodho, B.A.**, Yagi, R., Kidou, A., Ishikawa, S., and Kure, S. (2020) "Relationship between Flood Inundation Flow and Building Damage Due to Flood Disaster at Chikuma River in Nagano Prefecture in 2019, *Journal of Japan Society of Civil Engineers*, Ser. B1 (Hydraulics), Vol.76, No.2, pp.I_619-I_624, 2020.
4) Ojima, Y., Kure, S., Ishikawa, S., **B.A. Priyambodho**, Maruya, Y. (2019) "Rainfall Runoff and Flood Inundation Analysis in Shogawa River and Evaluation of Flood Control by TOGA dam" *Journal of Japan Society of Civil Engineers*, Ser. G (Environment), Vol.75, No.5, pp.I_281-I_287, 2019.
5) **Priyambodho, B.A.**, S. Kure, I.R. Moe, and S. Kazama (2018) "Numerical Experiments of Future Land Use Change for Flood Inundation in Jakarta, Indonesia" *Journal of Japan Society of Civil Engineers*, Ser. G (Environment), Vol.74, No.5, I_265-I_271.

Proceedings of the Academic Conferences

International Conferences

1) S. Ishikawa, S. Kure, R. Yagi, **B.A. Priyambodho** (2020). "FLOOD HAZARD EVALUATION FOR RIVERS IN TOYAMA PREFECTURE, JAPAN" Proceedings of 22th IAHR-APD congress 2020, 5-5 (4-5-6), 査読有.
2) R. Yagi, S. Kure, S. Ishikawa, **B.A. Priyambodho** (2020). "Development of User-Friendly Hazard Ma ps and Information Based on Maximum Flood Inundation" ASCE, Proceedings of Watershed Managem ent 2020, pp.124-130, 査読有.
3) S. Ishikawa, S. Kure, R. Yagi, **B.A. Priyambodho** (2020). "Development of a Real Time Flood Predi ction Model for Rivers in Toyama Prefecture, Japan" ASCE, Proceedings of World Environmental and Water Resources congress 2020, pp.201-206, 査読有.

Japanese Conferences

4) **B.A. Priyambodho**, S. Kure, I.R. Moe, N.F. Januriyadi, M. Farid and S. Kazama : Impact of Land Use Change, Land Subsidence and Climate Change on Flood Inundation in Jakarta, Indonesia, 第27回土木学会地球環境シンポジウム講演集, pp.55-60, 2019.
5) **B.A. Priyambodho**, S. Kure, I. R. Moe, and S. Kazama: Sensitivity Analysis of DEM resolutions on Fl

ood Inundation Simulations in Jakarta, Indonesia, 第25回土木学会地球環境シンポジウム講演集, pp.45-49, 2017.

Abstracts of the Academic Conferences and Presentations

International Conferences

1) **B.A. Priyambodho**, S. Kure, I.R. Moe, N.F. Januriyadi, M. Farid and S. Kazama, 10th International Conference on Asian and Pacific Coasts (APAC 2019) Hanoi, Vietnam, 2019. "Regional Climate Change Impacts on Flood Inundation in Jakarta, Indonesia"
2) **B.A. Priyambodho**, S. Kure, and S. Kazama (2018). "Impacts of land-use/cover change at upstream region on flood inundation in Jakarta, Indonesia" 15th Annual Meeting AOGS, 2018, Honolulu, USA.
3) S. Kure, I.R. Moe, **B.A. Priyambodho**, N.F. Januriyadi, and S.Kazama (2017). "Land use change and land subsidence impacts on flood inundation in Jakarta, Indonesia", ASCE, World Environmental & Water Resources Congress 2018, 2017.5.24, Sacramento, USA.

Japanese Conferences

4) R. Zhang, S. Kure, **B.A. Priyambodho**, 土木学会中部支部2019年度研究発表会, 長野高専, 長野市, 2020. "Application of rainfall runoff model to rivers in Himi city toward habitat evaluation of Itasenpar"
5) **B. A. Priyambodho**, S. Kure, N.F. Januriyadi and S. Kazama, 土木学会中部支部2019年度研究発表会, 長野高専, 長野市, 2020. "Climate change impact study for flood inundation in Jakarta, Indonesia based on dynamical downscaling of future scenarios"
6) **B.A. Priyambodho** and S. Kure, 土木学会中部支部2019年度研究発表会, 長野高専, 長野市, 2020. "Evaluation of GSMaP-NRT for Flood Inundation Modeling in Jakarta, Indonesia"
7) **B.A. Priyambodho**, S. Kure, N.F. Januriyadi and S. Kazama, 水文・水資源学会2019年度研究発表会, 千葉工業大学, 習志野市, 2019. "Effects of Regional Climate Change on Flood Inundation in Jakarta, Indonesia"
8) **B.A. Priyambodho** and S. Kure : Evaluation of GSMaP Satellite Rainfall Dataset in Jakarta, Indonesia, 水文・水資源学会2019年度研究発表会, 千葉工業大学, 習志野市, 2019.
9) **B.A. Priyambodho** and S. Kure : Evaluation of a GSMaP NRT data for Flood Inundation Model in Jakarta, Indonesia, 平成30年度土木学会中部支部技術研究発表会, 愛知工業大学, 豊田市, 3月1日, 2019.
10) **B.A. Priyambodho**, S. Kure and S. Kazama : Future Projections of Flood Inundation at Ciliwung River Basin in Jakarta, Indonesia, 水文・水資源学会2018年度研究発表会, pp.282-283, 三重大学, 津市, 9月12日-14日, 2018.
11) **B.A. Priyambodho** and S. Kure : Evaluation of GSMaP rainfall for flood inundation simulation in Jakarta, Indonesia, 水文・水資源学会2018年度研究発表会, pp.272-273, 津市, 9月12日-14日, 2018.
12) **B.A. Priyambodho** and S. Kure : EFFECTS of LAND USE/COVER CHANGE on FLOOD INUNDATION at CILIWUNG RIVER BASIN in Jakarta, Indonesia, 平成29年度土木学会中部支部技術研究発表会, 名古屋大学, 名古屋, 3月2日, 2018.